



February 4, 2011

Mr. Thomas Simmons  
USACE, Kansas City District  
CENWK-PM-ES  
601 East 12<sup>th</sup> Street  
Kansas City, MO 64106-2896

Re: Response to Comments on Updated Groundwater  
Modeling Report  
Claremont Polychemical Superfund Site  
SAIC Project 01-1633-04-5386-552

Dear Mr. Simmons:

Science Applications International Corporation (SAIC) has evaluated the review comments received from US Army Corps of Engineers, Kansas City District (CENWK) and United States Environmental Protection Agency (USEPA) Region II on the first draft version of the Updated Groundwater Modeling Report prepared by SAIC for the Claremont Polychemical Superfund Site. The comments received and SAIC's responses to the comments (shown in bold type) are provided below.

**Response to Comments From Reviewer – Ed Modica, Hydrogeologist, Program Support  
Branch, Technical Support Team, USEPA**

1. In general, the groundwater flow model for Claremont Polychemical Site is well designed. Based on data presented in the subject report, the aquifer structure and water transmitting properties near the site are well represented. The reformulation of the model based on additional data since the previous version appear to have improved on the model's representativeness. The ability to employ solute transport modeling and particle tracking allow for more in depth characterization of contaminant plumes and their relation to potential source zones and discharge locations.

**Concur. No change to the report is necessary.**

2. *Page 5, ¶ under 2.2.3 Constant Head Boundary:* There is some concern that the specification of a constant head boundary close to simulated pumping wells can create the potential for an unrestrained quantity of flow to enter the system; i.e., the model can generate whatever quantity of flow is necessary from the constant head boundary to satisfy the sink term. This can lead to simulated flow conditions that are not representative of actual conditions. From the model input files, it appears that two wells (located at layer 5, row 63, column 62; and at layer 5, row 67, column 54) may be close enough to the upper constant head boundary and may have a sufficient withdrawal rate so as to induce flow from constant head. Please discuss further whether the

discharge affects on the specified head boundary have been considered.

**Concur. Evaluation of the interaction between these two wells and the upgradient constant head boundary (~1500ft away) suggests that the proximity of the two limits the predictive capabilities of the model in the immediate area around the wells. However, that evaluation also indicates that the predictive capabilities of the model are not compromised at Claremont and nearby areas. Discussion has been added to Section 2.2.5 to clarify this.**

3. *Page 8, ¶ under 2.2.10 Model Validation:* Note that the validity of a steady state model, calibrated to a set of water level data representative of long-term, average conditions, is neither confirmed nor negated by comparing to a data set not used in model development, such as the July 2006 water level set, unless these data are also representative of long-term, average conditions. For example, if the water level data used to validate the model reflected draught or unusually wet conditions, model results would not agree. But the model would not necessarily be invalidated.

**Concur. Section has been revised to reflect that the comparison is not model validation, but simply a test of the model on data not used in model development. Additionally, a section entitled “Model Verification” has been added, wherein a recommendation is made to perform model verification prior to using the model to support final treatment system configuration/construction recommendations.**

4a. *Page 9, 3<sup>rd</sup> ¶ under 3.1 Conceptual Solute Transport Model; figure 3-2:* a. The paragraph indicates that there is a possibility of an up-gradient contribution to the groundwater TCE plume thought previously to originate entirely from the Claremont site. However, it is not clear what evidence there is for this supposition. Figure 3-2 shows the 5 ppb iso-concentration line for the TCE plume as solid along the northern extent of the site. This representation indicates that the plume’s extent is constrained by data points north of the plume. If this is the case, then there appears to be no contaminated groundwater in the area immediately up-gradient of the site. Please discuss further what the evidence is for an up-gradient contribution to TCE contamination.

**Concur. Text has been edited to indicate that additional ongoing investigations corroborate the existence of an upgradient source (in addition to the existing statement that the highest TCE concentrations are detected near monitoring wells EW-7C and EW-10C, which are located at the upgradient and eastern side of the Claremont site). The iso-concentration lines on the TCE plume map (Figure 3-2) have been changed from solid lines which close north of the Claremont property to dashed lines projecting an open, undefined extent of groundwater contamination north of the site.**

4b. The paragraph states that the area near wells EW-7C/EW10C is considered to represent a continuing source of TCE. The highest TCE concentration reported for well EW10C is 1,400 µg/L. Note, however, that according to OSWER publication 9355.4-07FS (Estimating Potential for Occurrence of DNAPL at Superfund Sites) concentrations of DNAPL related chemicals in groundwater that are greater than 1% of pure-phase or effective solubility, indicate proximity to source. For TCE a concentration of 11,000 ppb would indicate a potential source in the aquifer.

Hence, concentration at the well is somewhat low to indicate a potential source.

**Concur in part:** It was assumed in the model that in the area of wells EW-7C/EW-10C, there is a constant flux of TCE from a source up-gradient of the site resulting in a steady state concentration in this area. Therefore, the EW-7C/EW-10C area was assumed to be constantly receiving TCE from an up-gradient source, causing this area to act as a constant source for the further down-gradient portions of the plume.

Statement in question (i.e., “For modeling purposes, this area is considered to represent a continuing source of TCE.”) has been eliminated from Section 3.1 (as Section 3.1 is conceptual model and not numerical model discussion). This issue has been clarified in appropriate location in Section 3.2.3.2.

5. *Page 9, last ¶; figures 3-1 to 3-3; tables 3-1 to 3-3:* It is recommended that the vertical stratification of plumes be considered when characterizing plume distribution in the aquifer. The tables containing TCE, PCE, and 1,1-DCE data should list the screening intervals for wells in which detections were reported. Additional plots can be made that show concentrations relative to model layers or to horizontal planes representing highest intersection of well screens. Select cross sections could also be useful to help envision plume distribution with depth.

**Concur in part.** The screened intervals for all wells have been inserted in Tables 3-1, 3-2, and 3-3. There are an insufficient number of data points within any one layer of the aquifer to develop a plume map for an individual aquifer layer. Since there is insufficient data to support development of per layer plume maps, cross-sections have been developed to illustrate concentrations at various depths along one transect through the axis of the northern end of the plume (well EW-7D to well EW-14-D), one transect perpendicular to the axis of the northern end of the plume (well EW-8D to well EW-13D), one transect along the axis of the southern end of the plume (well EW-14D to well BP-12A,B,C), and one transect perpendicular to the axis of the southern end of the plume (well OBS-1 to BP-10,B,C).

6. *Page 10; 1<sup>st</sup> ¶; table 3-1:* The paragraph indicates that the highest concentration of PCE were located in monitoring well BP-14C. Tables 3-1 show well BP-14B to have the highest. Please resolve.

**Concur.** This is a typographical error. The paragraph has been corrected to state that *highest concentration of PCE were located in monitoring well BP-14B.*

7. *Page 13, under 3.2.4 Particle Tracking Analysis:* It is not clear why well EW-9 is the subject of a particle tracking analysis; tables 3-1 to 3-3 indicate that concentrations of TCE, PCE, and 1,1-DCE are relatively low for this well group. Please explain.

**Concur in part.** EW-9 is located at the west side of the Claremont site and roughly defines the western extent of the plume coming onto the site. Reverse particle tracking originating from EW-9 helps to identify possible upgradient source areas; areas to the northeast of this particle track may contribute to the plume moving onto the Claremont site, while areas to

**the southwest may not. The text has been edited to provide this reasoning for the particle tracking analysis.**

8. Page 14, ¶beginning with “Particle tracking analysis...”: It is not apparent what the capture zone analysis intends to demonstrate. In the analysis described in the report, a line of particles is located along a model row just down-gradient of the Claremont site, presumably to determine capture zone width for various supply wells located down-gradient of the site. Because the particles describe a limited recharge area (a model row), a full mapping of recharge locations to discharge locations (wells) is not realized. Consider performing an analysis that maps the full recharge areas to wells. Consider also mapping capture areas in sections perpendicular to flow that coincide with plume boundaries to wells. The particle tracking software used in this analysis (Modpath) allows for such an analysis (referred to as an end-point analysis).

**Concur. A capture zone analysis (using endpoint analysis as appropriate) has been preformed for Claremont, TOB, and FTC recovery wells, and selected municipal water supply wells within the model domain. The results of the capture zone analysis are illustrated on Figure 3-6.**

9. Page 15, 2<sup>nd</sup> ¶ under section 3.2.5.1: The paragraph states that the migrating PCE plume will impact the village of Farmingdale municipal supply well in ten years. Please confirm whether or not the well referred to is the well designated as N7852 in figures 3-8 to 3-11.

**Concur. Yes, the well referred to is N-7852. Text will be clarified.**

10. Typos:

- Page 13, 8 lines from top of page: “Table 3-2” should be “Table 3-4”
- Page 13, section 3.2.3.7, 3<sup>rd</sup> line: “Table A-2” should be “Table A-1”
- Page 14, ¶beginning with “Particle tracking analysis”, 10<sup>th</sup> line: “1,1-DCA” should be “1,1-DCE”
- Page 15, 2<sup>nd</sup> ¶ under section 3.2.5.1, 1<sup>st</sup> line: “Figures 3-6, 3-7, 3-8, and 3-11” should be changed to “Figures 3-8, 3-9, 3-10, and 3-11”
- 3<sup>rd</sup> line: “TCE” should be “PCE”

**Concur. All the above typos have been fixed in the report.**

**Response to Comments from Reviewer – James Lyons, Hydrogeologist,**  
**USACE, Kansas City District**

1. Page 13, Line 8, 3.2.3.6 Sorption. Please correct the line referencing Table 3-2, it should be Table 3-4.

**Concur. Table 3-2 has been changed to Table 3-4.**

2. Page 13, Line 13, 3.2.3.6 Sorption. Retardation factors are listed in Table 3-4, not Table 3-2, please correct.

**Concur. Table 3-2 has been changed to Table 3-4.**

3. Page 15, paragraph 2, 3.2.5.1. The results of the solute transport modeling of the PCE Plumes are presented in **Figures 3-8, 3-9, 3-10, and 3-11**; the text reads Figures 3-6, 3-7, 3-8, and 3-11, please correct.

**Concur. Figures 3-6, 3-7, 3-8, and 3-11 have been changed to Figures 3-8, 3-9, 3-10, and 3-11.**

4. Page 15, paragraphs 2 and 3, 3.2.5.1. Please add the Village of Farmington well number to the text that may be impacted by the PCE and TCE plumes.

**Concur. The text in paragraphs 2 and 3 of section 3.2.5.1 has been edited to ...Village of Farmingdale municipal water supply well (N-7852).**

5. Page 17, Summary and Conclusions. Please correct, the following statement is written twice: "the flow field was modeled as steady-state".

**Concur. The third sentence of the paragraph, i.e *The flow field was modeled as steady state.*, has been deleted.**

6. Figures 3-7a and 3-7b. Please change the backward particle track color to green to be consistent with Figure 3-4.

**Concur. The color of the backward particle track color has been changed from red to green to be consistent with Figure 3-4.**

We trust that you will agree that the above responses to the comments are appropriate. Please contact the undersigned if you have any questions or comments on this matter. We look forward to any discussions required regarding these responses and to preparing the final versions of the Updated Groundwater Modeling report.

Sincerely,



Richard C. Cronce, Ph.D., CCA  
Project Manager

Mr. Thomas Simmons

- 6 -

February 4, 2011

Cc: Nat Voorhies, SAIC

---

---

# **UPDATED GROUNDWATER MODELING REPORT FOR THE CLAREMONT POLYCHEMICAL SUPERFUND SITE**

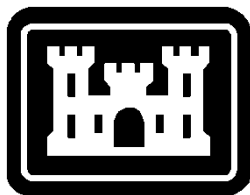
## **FINAL**

### **OLD BETHPAGE, NEW YORK**

**February 2011**

---

---



Prepared for:

United States Army Corps of Engineers, Kansas City District

Prepared by:

Science Applications International Corporation

Under Contract No. DACW41-02-D-0005, Task Order No. 0002

# TABLE OF CONTENTS

	<i>Page</i>
<b>ABBREVIATIONS/ACRONYMS</b> .....	Preceding Text
<b>1.0 INTRODUCTION AND OBJECTIVES</b> .....	1
<b>2.0 GROUNDWATER FLOW MODEL</b> .....	2
2.1 Conceptual Model.....	2
2.1.1 Conceptual Hydrogeologic Layers .....	2
2.1.2 Justification for Hydraulic Conductivity Values .....	3
2.2 Numerical Model Development.....	4
2.2.1 Model Selection and Description.....	4
2.2.2 Finite-Difference Grid .....	4
2.2.3 Constant Head Boundaries.....	5
2.2.4 No-Flow Boundaries.....	5
2.2.5 Pumping and Injection Systems within the Model Domain .....	5
2.2.6 Aquifer Properties.....	6
2.2.6.1 Layer Elevations .....	6
2.2.6.2 Hydraulic Conductivity (K) .....	6
2.2.6.3 Recharge (R) .....	7
2.2.6.4 Porosity (N).....	7
2.2.7 Calibration.....	7
2.2.8 Mass Balance .....	8
2.2.9 Sensitivity Analysis .....	8
2.2.10 Testing of Model on Blind Data .....	9
2.2.11 Verification .....	10
2.3 Flow Model Summary .....	10
<b>3.0 SOLUTE TRANSPORT MODEL</b> .....	11
3.1 Conceptual Solute Transport Model .....	11
3.2 Numerical Model Development.....	13
3.2.1 Model Selection and Description.....	13
3.2.2 Finite Difference Grid.....	14
3.2.3 Solute Transport Specific Properties .....	15
3.2.3.1 Initial Conditions .....	15
3.2.3.2 Specified Concentration Boundary Conditions .....	15



3.2.3.3	Dispersivity .....	15
3.2.3.4	Porosity .....	15
3.2.3.5	Bulk Density .....	15
3.2.3.6	Sorption.....	15
3.2.3.7	Degradation.....	16
3.2.4	Particle Tracking Analysis .....	16
3.2.5	Predictive PCE, TCE, and 1,1-DCE Simulations .....	18
3.3	Transport Model Summary .....	19
<b>4.0</b>	<b>SUMMARY AND CONCLUSIONS.....</b>	<b>19</b>
<b>5.0</b>	<b>REFERENCES.....</b>	<b>21</b>

## List of Figures

Figure 2-1	Groundwater Model Domain.....	Following Text
Figure 2-2	Vertical Discretization of the Model .....	Following Text
Figure 2-3	Groundwater Counter Map and Principal Flow Direction .....	Following Text
Figure 2-4	Injection Wells, Pumping Wells, and Infiltration Basins .....	Following Text
Figure 2-5	Observed Versus Model Predicted Head.....	Following Text
Figure 2-6	Model Calibration Target Locations .....	Following Text
Figure 2-7	Model Predicted Groundwater Head at Zone A.....	Following Text
Figure 2-8	Model Predicted Groundwater Head at Zone B .....	Following Text
Figure 2-9	Model Predicted Groundwater Head at Zone C-Upper.....	Following Text
Figure 2-10	Model Predicted Groundwater Head at Zone C-Middle .....	Following Text
Figure 2-11	Model Predicted Groundwater Head at Zone C-Lower .....	Following Text
Figure 2-12	Sensitivity Analysis for Zone “A” Kh.....	Following Text
Figure 2-13	Sensitivity Analysis for Zone “B” Kh.....	Following Text
Figure 2-14	Sensitivity Analysis for Zone “C” Kh.....	Following Text
Figure 2-15	Sensitivity Analysis for Zone “C-Middle” Kh.....	Following Text
Figure 2-16	Sensitivity Analysis for Zone “C-Lower” Kh .....	Following Text
Figure 2-17	Sensitivity Analysis for Zone “A” Kz.....	Following Text
Figure 2-18	Sensitivity Analysis for Zone “B” Kz .....	Following Text
Figure 2-19	Sensitivity Analysis for Zone “C-Upper” Kz.....	Following Text
Figure 2-20	Sensitivity Analysis for Zone “C-Middle” Kz .....	Following Text
Figure 2-21	Sensitivity Analysis for Zone “C-Lower” Kz .....	Following Text
Figure 2-22	Sensitivity Analysis for Recharge .....	Following Text
Figure 2-23	Well Locations for Blind Test Data .....	Following Text
Figure 2-24	Simulated Head versus Observed Head for Blind Test Data .....	Following Text
Figure 3-1	PCE Plume Map .....	Following Text
Figure 3-2	TCE Plume Map.....	Following Text
Figure 3-3	1,1-DCE Plume Map .....	Following Text
Figure 3-4a	Stratigraphic and Contaminant Cross-Section A-A’ .....	Following Text
Figure 3-4b	Stratigraphic and Contaminant Cross-Section B-B’ .....	Following Text
Figure 3-4c	Stratigraphic and Contaminant Cross-Section A’-A’’ .....	Following Text
Figure 3-4d	Stratigraphic and Contaminant Cross-Section C-C’ .....	Following Text
Figure 3-5	Particle Tracking in Zone B from Wells EW-9, EW-7 and MW-10..	Following Text
Figure 3-6	Starting Locations for Particles Discharging to Selected Wells.....	Following Text
Figure 3-7	Backward Particle Tracking from Village of Farmingdale Municipal Supply Wells and Suffolk County Water Supply Wells...	Following Text
Figure 3-8	USGS/MODFLOW/MT3D Predicted PCE Plumes in 5 Years for Zone A and Zone B.....	Following Text
Figure 3-9	USGS/MODFLOW/MT3D Predicted PCE Plumes in 5 Years for Zone C-Upper and Zone C-Middle.....	Following Text
Figure 3-10	USGS/MODFLOW/MT3D Predicted PCE Plumes in 10 Years for Zone A and Zone B.....	Following Text
Figure 3-11	USGS/MODFLOW/MT3D Predicted PCE Plumes in 10 Years for Zone C-Upper and Zone C-Middle.....	Following Text
Figure 3-12	USGS/MODFLOW/MT3D Predicted TCE Plumes in 5 Years	

	for Zone A and Zone B.....	Following Text
Figure 3-13	USGS/MODFLOW/MT3D Predicted TCE Plumes in 5 Years for Zone C-Upper and Zone C-Middle.....	Following Text
Figure 3-14	USGS/MODFLOW/MT3D Predicted TCE Plumes in 10 Years for Zone A and Zone B.....	Following Text
Figure 3-15	USGS/MODFLOW/MT3D Predicted PCE Plumes in 10 Years for Zone C-Upper and Zone C-Middle.....	Following Text
Figure 3-16	USGS/MODFLOW/MT3D Predicted 1,1-DCE Plumes in 5 Years for Zone A, Zone B, and Zone C-Upper .....	Following Text
Figure 3-17	USGS/MODFLOW/MT3D Predicted 1,1-DCE Plumes in 10 Years for Zone A, Zone B, and Zone C-Upper .....	Following Text

## List of Tables

Table 2-1	Borehole Data Used to Interpret the Conceptual Model .....	Following Text
Table 2-2	Hydraulic Conductivities of the Aquifer .....	Following Text
Table 2-3	Modeled Aquifer Parameters.....	Following Text
Table 2-4	Model Calibration Result .....	Following Text
Table 2-5	Steady State Calibration Statistics.....	Following Text
Table 2-6	Mass Balance.....	Following Text
Table 2-7	Blind Test Result (July 2006 Water Level Data) .....	Following Text
Table 3-1	PCE Data Used to Develop Current PCE Plume .....	Following Text
Table 3-2	TCE Data Used to Develop Current TCE Plume .....	Following Text
Table 3-3	1,1-DCE Data Used to Develop Current 1,1-DCE Plume .....	Following Text
Table 3-4	Sorption Parameters .....	Following Text

## List of Appendices

Appendix A	Chemical Data Summary and Transmissivity Calculations.....	Following Text
Appendix B	Claremont Calibrated Groundwater Model (on CD) .....	Following Text

## ABBREVIATIONS/ACRONYMS

amsl	Above Mean Sea Level
ASTM	American Society for Testing Materials
bgs	Below Ground Surface
Claremont	Claremont Polychemical Corporation
CUGIR	Cornell University Geospatial Information Repository
K	Conductivity
DCE	Dichloroethene
DNAPL	Dense Nonaqueous Phase Liquids
Foc	Organic Carbon Fraction
FTC	Fireman's Training Center
g/cm <sup>3</sup>	Grams Per Cubic Meter
gpd/ft	Gallons Per Day Per Foot
K	Conductivity
Kd	Equilibrium Distribution Coefficient
Kh	Horizontal Hydraulic Conductivity
Kz	Vertical Hydraulic Conductivity
Koc	Organic Carbon Partition Coefficient
MCL	Maximum Contaminant Level
mg/L	Milligrams per Liter
ml/g	Milliliters Per Gram
MT3DMS <sup>®</sup>	Modular Three-Dimensional Multispecies Transport Model
N	Porosity
NCDPW	Nassau County Department of Public Works
NYSDEC	New York State Department of Environmental Conservation
OBL	Old Bethpage Landfill
PCE	Tetrachloroethylene or Perchloroethylene
R	Recharge
SAIC	Science Applications International Corporation
SSR	Squared Residuals
TCE	Trichloroethylene
T	Transmissivity
TOB	Town of Oyster Bay
µg/L	Micrograms Per Liter
USGS	U.S. Geological Survey

## 1.0 INTRODUCTION AND OBJECTIVES

Science Applications International Corporation (SAIC) has developed an updated groundwater flow and contaminant fate and transport model for the Claremont Polychemical site, located in Old Bethpage, Nassau County, New York (see Figure 2-1). This work was completed in accordance with SAIC's proposal for Completion of Additional Groundwater Modeling, dated December 22, 2006. Recommendations made in the previous groundwater modeling report included the following:

- The groundwater model should be refined and recalibrated using additional groundwater elevation data. This should be particularly useful in increasing the accuracy of the model in the southern portion of the model domain where very little information was available for the current modeling effort.
- Any available updated or more precise pumping and infiltration data from any regional facilities should be provided and used to refine and update the current model.
- Further analysis of tetrachloroethene (PCE) breakdown products, including dichloroethene (DCE), should be performed to further the understanding of the contaminant plume fate and transport principles.
- Additional aquifer characterization data should be collected from the southern portion of the plume to increase the accuracy of the model.
- The current model should be recalibrated using additional groundwater elevation data to improve model accuracy.
- Additional information should be collected on surrounding municipal water supply wells, and the risk to these wells from the existing groundwater contaminant plume should be further evaluated.

This current work constitutes a continuation of the previous groundwater modeling work for this site and addresses several of the recommendations made in the first report. The objectives of the present work were to:

- Reevaluate the orientation of the model boundary and evaluate the potential impact of the delineated groundwater contaminant plume to additional off-site groundwater supply wells. During the review of the initial model, it was postulated that the conceptualized model plume was oriented too far to the east in comparison to a reported historical United States Geological Survey (USGS) groundwater plume map. It was also thought that the model boundary may need to be extended to address reported additional off-site water supply wells that may be impacted by the groundwater plume. These issues are addressed in the following sections of this report.
- Revise the groundwater flow model using additional groundwater elevation and aquifer characterization acquired since development of the initial model. During the review of the initial model, it was determined that some relevant hydrogeologic and groundwater elevation data available from Nassau County and Town of Oyster Bay (TOB) had not been available for inclusion in the initial model. As a result, it was projected that revision of the model in consideration of the additional data would improve the model. An initial validation of the existing model using a comprehensive set of groundwater elevation data collected in March 2006 revealed that the current model and associated conclusions in the

initial modeling report were valid. This analysis, however, indicated that the overall goodness of fit of the model and the confidence in related projections of groundwater flow and chemical fate and transport could likely be improved over a much larger area of the groundwater plume by further calibration of the model using the additional available data. The revised groundwater flow model is the subject of this current report.

- Model additional contaminants, particularly 1,1-DCE which is one of the breakdown products of trichloroethene (TCE).
- Use the modeling results, if possible, to evaluate the general decomposition pathways and degradation rates for TCE, one of the primary groundwater contaminants.

## 2.0 GROUNDWATER FLOW MODEL

This section of this report describes the development of the groundwater flow model and evaluation of the transport of PCE, TCE, and 1,1-DCE in groundwater at and downgradient of the Claremont site. The conceptual groundwater model and numerical flow model are described in Section 2.0. The numerical model used to evaluate the PCE, TCE, and 1,1-DCE transport is described in Section 3.0. The model was developed in accordance to the American Society for Testing and Materials (ASTM) D5447 standard guideline for the application of a groundwater model to a site-specific problem (ASTM 2004).

### 2.1 Conceptual Model

A conceptual model is a qualitative understanding of the site groundwater flow system and is a prerequisite to constructing a numerical flow model. The conceptual model is a summary of the hydrogeologic features that control groundwater flow at the site. A sound conceptual model minimizes the potential for errors to enter into the modeling process and increases the chance of constructing a numerical model that is consistent with the actual hydrogeologic system. The same conceptual model was used for the current modeling effort as was used for the previous modeling effort. The reader is referred to Chapter 2 of the previous modeling report for a presentation of the literature review, as well as a full description of the resulting conceptual geologic and hydrogeologic conceptual model (SAIC, 2007).

#### 2.1.1 Conceptual Hydrogeologic Layers

One difference between the current and previous model involves the definition of the geologic layers. Based on an interpretation of the available data and past work performed for the site, the current hydrogeologic model has been divided into three hydrologic zones: A, B, and C. The borehole data used to interpret the conceptual model are listed in Table 2-1. The bottom elevations of Zone A and Zone B were calculated assuming that the thicknesses of Zone A and Zone B are 100 and 120 feet, respectively. The saturated thickness of the aquifer at EW-7C (area of highest TCE detected) was assumed to be 690 feet. The previous modeling effort had assumed the saturated thickness to be 650 to 700 feet (Department of Army, August 1994). The water level at EW-7C is approximately at 68 feet elevation. An elevation of -622 msl feet was provided as the bottom of the Zone C. The bottom of Zone C was calculated by subtracting 68 feet from the assumed saturated depth of 690 feet. Zone C was further divided into three sub-

layers as upper (130 feet thick), middle (130 feet thick), and lower layer (as shown in Figure 2-2). Ground surface elevation data for the entire model domain were obtained from the Cornell University Geospatial Information Repository (CUGIR) data base (data provider: New York State Department of Environmental Conservation [NYSDEC]).

**Zone A** - The upper unit ranges from the ground surface to 100 feet below ground surface (bgs). The unit is mostly comprised of glacial sediments but also includes sands of the very upper portion of the Magothy Formation. The average groundwater potentiometric surface derived from measurements in October 2003 and July 2004 was 61.9 feet above mean sea level (amsl). The average saturated thickness for this unit is estimated to be 31 feet based on available information. Some wells in Zone A were dry or were very close to the top of Zone B. Transmissivity (T) value of well DW-2 is 162,600 gallons per day per foot (gpd/ft) (SAIC, 2003). DW-2 is screened at the bottom of Zone A, and the screen is entirely within Zone A. As shown in Table 2-2, the estimated hydraulic conductivity (K) for Zone A, assuming a saturated thickness of the aquifer of 690 feet, is 31.5 ft/day.

**Zone B** - This is the middle hydrologic zone for the site. Most of the water produced from wells in the area appears to be from this zone. This zone is interpreted to range from 100 feet bgs to 220 feet bgs. It is entirely within the Magothy Formation. The transmissivity for Zone B is estimated using SAIC values derived in 2003 from Zone B. The K value for Zone B is based upon the average of the T values obtained by SAIC from short-term pumping tests of extraction wells EX-2 and EX-3. Both are screened in Zone B, and as shown on Table 2-2, a saturated thickness of 690 feet is used to derive a K value of 52.3 ft/day.

**Zone C** - This is the lowermost zone. This zone ranges from a depth of 220 feet bgs to an elevation of -622 feet msl (this elevation corresponds to the bottom of the model) and lies within the Magothy Formation. The Fireman's Training Center (FTC) report (Firemen's Training Center, 2004) defined the bottom of Zone C as 300 feet bgs; however, because of the lateral variability of the clays, it is interpreted that the zone could be deeper, and for this modeling purpose, the bottom of Zone C was assumed at -622 feet msl with a no-flow boundary at the bottom of the model.

Well MW-8C had a T value calculated to be 190,700 gpd/ft (SAIC, 2003) which corresponds to a K value of 36.9 ft/day (assuming 690 feet saturated thickness) (see Table 2-2). Further, the geometric average transmissivity of 17 wells in Zone C was calculated as 58,613.8 gpd/ft, which corresponds to a K value of 11.35 ft/day (see Table A-1, Appendix A). The transmissivity ranged from 14,260 gpd/ft (K = 2.76 ft/day) at well N-5890 to 153,985 gpd/ft (K = 29.83 ft/day) at well S-20041 as listed in Appendix A.

### 2.1.2 Justification for Hydraulic Conductivity Values

The K values used as the initial estimate values for the modeling were based on recent pump test data performed by SAIC in 2003. The wells used for this test were closer to the Claremont site and may reflect local hydraulic conductivity in an aquifer that has a heterogeneous stratigraphy. The values are not as high as those calculated by the 1987 Geraghty & Miller pump test (see Table 2-2).



Slug tests performed by Ebasco in 1990 were very low. The extent to which slug tests are used to estimate the K for an aquifer is dependent on the homogeneity of the aquifer and the amount of the aquifer this method actually tests. Pump tests utilize a much larger portion of the aquifer and are considered to be more reliable than a slug test for K in an aquifer such as at Claremont. Therefore, these slug test results were not included in the calculation of K for this site.

## 2.2 Numerical Model Development

The development of the numerical model was as follows. Once the conceptual model had been formulated, it was translated into a numerical representation of the groundwater flow system. In general, a modeling code was first selected that was appropriate to the hydrogeologic features represented in the conceptual model. Next, a grid or mesh was geographically superimposed over the system. Aquifer properties, stresses, and boundary conditions were assigned to discrete points or volumes within the grid or mesh. Based on these parameters, the modeling code was then used to calculate head and flux at each discrete point within the grid or mesh. Parameter values were then adjusted until acceptable agreement was reached between the simulated and observed values for a given parameter, such as hydraulic head. The following sections describe this process in detail.

### 2.2.1 Model Selection and Description

The USGS computer program, MODFLOW<sup>®</sup>, was used to simulate groundwater flow at the site. MODFLOW<sup>®</sup> is a well-documented and verified industry-standard numerical code for simulating groundwater flow (Harbaugh and McDonald, 1996; McDonald and Harbaugh, 1988). MODFLOW<sup>®</sup> is a three-dimensional finite-difference groundwater flow modeling package that simulates steady and nonsteady flow in an irregularly shaped flow system. MODFLOW<sup>®</sup> can simulate aquifer materials as confined, unconfined, or a combination of confined and unconfined. External flow stresses such as wells, areal recharge, and flow through riverbeds can be simulated. Aquifer properties, such as K, may differ spatially and be anisotropic for any given layer within a MODFLOW<sup>®</sup> model. The versatility of the MODFLOW<sup>®</sup> code is well-suited to the heterogeneous nature of the hydrogeologic units represented in the Claremont model.

### 2.2.2 Finite-Difference Grid

To translate the conceptual model discussed above into a numerical representation within MODFLOW<sup>®</sup>, a grid was geographically superimposed over the system. Areally, the finite difference grid is a regular grid of cells measuring 25 feet by 25 feet which covers the model area, a 17,700-foot by 15,400-foot area shown in Figure 2-1. The 25-foot by 25-foot dimensions of the cells are capable of modeling the groundwater flow at sufficient resolution for this study. Within each of the aquifers (Zone A, Zone B, and Zone C), the lateral extent of the grid was established, considering that the grid must encompass the region of interest for simulating groundwater flow (and solute transport).



Vertical discretization is based on the hydrogeology in the study area as presented in Section 2.1.2 of the previous modeling report (SAIC, 2007). A total of five layers were simulated in the model representing Zone A, Zone B, Zone C-upper, Zone C-middle, and Zone C-lower. The top and bottom elevations of each of the layers are specified based on the elevations of the top and bottom of Zone A, Zone B, and Zone C. Vertical discretization of the model domain is shown in Figure 2-2. The model is relatively thin, with a horizontal to vertical dimension ratio of approximately 23:5.

The finite difference grid superimposed over the study area is oriented at 29° from the north, aligning with the principal direction of the regional groundwater flow as shown in Figure 2-3. The regional principal groundwater flow direction was determined based on comprehensive March 2006 groundwater elevation data. Note that different interpolation methods provide different inferred groundwater flow directions locally within the flow field. This—along with the approximations the model makes—introduces uncertainty into the solutions of both the flow and transport and particle tracking.

### **2.2.3 Constant Head Boundaries**

In general, it is desirable that model boundaries correspond to natural hydrogeologic boundaries (rivers, lakes, etc.). However, when natural hydrogeologic boundaries are far removed from the study area, it is numerically impractical to make lateral model boundaries correspond with natural hydrogeologic boundaries. In this case, the model boundary is an artificial hydrogeologic boundary. In this model, constant head boundaries are specified along the northwestern and southeastern sides of the model domain. These constant head boundaries permit groundwater flow to cross (enter or exit) the model boundaries. A constant head of 80.16 feet on the northwestern boundary and 48.45 feet on the southeastern boundary was specified.

### **2.2.4 No-Flow Boundaries**

The historic (1990-1992) potentiometric map (Nassau County Department of Public Works [NCDPW], 2004) and groundwater contour map based on March 2006 water level data (Figure 2-3) show that the regional direction of groundwater flow is northwest to southeast. Therefore, a no-flow boundary was selected on the boundaries parallel to the direction of groundwater flow (i.e., the northeastern and southwestern sides of the model domain). The base of the model was also assumed as a no-flow boundary as described in the discussion of Zone C in Section 2.1.1.

### **2.2.5 Pumping and Injection Systems within the Model Domain**

Multiple water pumping and injection systems occur within the modeled domain as shown in Figure 2-4. A significant improvement of the current model in comparison to the previous model is the inclusion of seven additional pumping municipal water supply wells into the model. Information on public, state, and USGS wells located within and near the model domain was acquired from the files and electronic data base of the USGS in Coram, New York. This information was then used to calculate additional aquifer transmissivities as presented in Section 2.1.1. A summary of the recent data added to the model data base is provided in

Appendix A. These injection and pumping systems were simulated in the model as injection and extraction wells. These fluxes provide stresses on the aquifer which give excellent information for which to calibrate the hydraulic conductivity fields.

Late in the course of updating the groundwater model, information was obtained on two municipal water supply wells (N-8767 and N-8768; Figure 2-4) located in the extreme northwestern corner of the model domain. Given the relative proximity of these wells to the northwestern constant head boundary (~1500 feet separation), the potential exists for unrestricted flow from the constant head boundaries to the wells to satisfy the specified pumping rate. Consequently, the interaction between these wells and the upgradient constant head boundaries was evaluated by comparing the calibrated flow model discussed subsequently to the same model with these two wells removed.

Adding these two wells to the model increased the flux in from the constant head boundaries in this area by about 15%. The absolute value of the increase was about 125,000 ft<sup>3</sup>/day, corresponding to about 65% of the 190,000 ft<sup>3</sup>/day specified combined pumping rate for the two wells. Thus, there is significant interaction between the constant head boundaries and these wells that may limit the predictive capabilities of the present model in the immediate area.

However, the impacts on Claremont and surrounding areas are negligible. Within about 4,000 feet upgradient and sidegradient of Claremont, and extending to the downgradient model boundary, heads differences between the flow fields with and without the two wells are less than 0.1 feet. Particle tracking simulations from upgradient of Claremont accordingly were virtually identical for the two cases. Thus, the proximity of these wells to the upgradient constant head boundary does not compromise the usefulness of the model as a decision-support tool for Claremont and nearby sites.

## 2.2.6 Aquifer Properties

Aquifer properties such as aquifer elevation, hydraulic conductivity (K), recharge (R), and porosity (N) are assigned to model grid cells based on a combination of site-specific measurements, values reported for the region in the literature, and model calibration. The following sections discuss assignment of these properties.

**2.2.6.1 Layer Elevations** - The top and bottom elevations of each of the layers are specified based on the elevations of the top and bottom of the Zone A, Zone B, and Zone C as described in Section 2.1.1.

**2.2.6.2 Hydraulic Conductivity (K)** - Horizontal hydraulic conductivity values estimated in Section 2.1.1 were used as starting conductivity values for the model. The initial conductivity values used were 31.5, 52.3, and 36.9 ft/day for Zones A, B, and C, respectively. The model was further calibrated (see Section 2.2.7) resulting in the values as shown in Table 2-3. A conventional ratio for Kh (horizontal hydraulic conductivity) to Kz (vertical hydraulic conductivity) of 10 was used. This is an assumption and is not able to be further refined from calibration efforts at this time.

**2.2.6.3 Recharge (R)** - The average annual recharge rate for the Claremont area is on the order of 21 inches (Isbister, 1966). The model was calibrated to fit the measured water level data with the given recharge, and a recharge rate of 20.58 inches per year gave the best fit (see Section 2.2.9).

**2.2.6.4 Porosity (N)** - The flow calibration efforts with this model are under steady-state conditions. Porosity is important when evaluating the particle tracking and contaminant transport analysis. An effective porosity value of 0.30 was used.

## 2.2.7 Calibration

Calibration of the flow model is a necessary step to ensure that the model is accurately simulating the observed conditions and, therefore, can be reliably used for predictive assessment of groundwater flow and, ultimately, contaminant migration. Model calibration was performed for steady-state recharge, pumping, and injection conditions, as well as steady boundary conditions. The simulated water levels were compared to actual water levels measured in March 2006 at well locations in the three modeled aquifers (Zones A, B, and C). The model was iteratively calibrated by adjusting the boundary condition, recharge rate, and hydraulic conductivities until observed heads matched closely with the model predicted heads. Approximately 20 iterative runs were performed to calibrate the model. Table 2-4 lists the model calibration results. Residuals (observed minus simulated water levels) were calculated for each target location. A residual of 0 feet indicates that the observed and simulated water levels are identical; values (either positive or negative) other than zero indicated a deviation of the model results from observed field data for a given point.

The results of the calibration showed that the simulated and observed water levels for March 2006 were in high agreement. All the head residuals (Table 2-4) are between -2.0 feet and +1.7 feet. The maximum absolute residual of 2.0 feet is less than 13.5% of the observed head data range of 14.88 feet (high of 70.90 feet at RB-1 and low of 56.02 feet at BP-10C).

Summary statistics for the calibration residuals are provided in Table 2-5. The residual mean error (-0.05 feet) for each of the three aquifers is near zero, indicating little overall bias in the simulated water levels. The residual standard deviation (0.68 feet) and the absolute residual mean (0.53 feet) are low, indicating that residuals are generally tightly clustered around the ideal value of 0. The residual standard deviation divided by the overall range in target head values is a critical measure of model calibration. The range for a well-calibrated model is 10% to 15% (Environmental Simulations, Inc., 2004). As shown in Table 2-4, this parameter is 4.58% for the current model, indicating excellent calibration. The observation (calibration) targets are located in all three major zones, and the flow system is calibrated as a fully three-dimensional flow system.

A useful visualization of model calibration is a plot of simulated vs. observed water levels as shown in Figure 2-5. For an ideal calibration, all points would lie on a 45-degree line. As shown in Figure 2-5, this is nearly the case. The correlation coefficient ( $R^2$ ) of the observed versus measured water levels is 0.96 (Figure 2-5), indicating excellent fit of the simulated to the observed heads. Model calibration target locations are shown in Figure 2-6. This figure

illustrates that there is a much larger number of more spatially distributed wells in the calibration of the current versus the previous model. The calibration is of high quality in general and is best in the area immediately surrounding the Claremont site due to a greater density of calibration wells in this area of the model domain. The model accuracy tends to decrease somewhat in the downgradient portions, where heads are less than 59 feet.

Simulated heads and calibration residuals for Zones “A”, “B”, “C-Upper”, “C-Middle”, and “C-Lower” are shown in Figures 2-7 through 2-11, respectively. Note that this solution is generated from a best-fit approach to the observed point data. This represents a model smoothed solution based on the groundwater flow equation and is accurate to the stated limits. The contour information shown on Figure 2-3 was not used in the modeling process; it is meant for understanding and comparison to the model results. Those contours are based on the data only and do not include the physics of the flow system. The true groundwater flow field is likely between these three representations. Hence, aspects like flow direction, transport, and particle tracking are understood within this range of the three flow direction estimates.

In summary, calibration evaluations indicate that the model is an excellent representation of groundwater flow conditions throughout the model study area.

### **2.2.8 Mass Balance**

A mass balance of the groundwater flow through the model was performed to evaluate the degree of agreement between water moving into versus out of the model domain. Table 2-6 presents the mass balance results of the steady-state model. Under the assumptions of the model, the total mass balance error is 1.7E-07%. For comparison, 1% is a typical maximum acceptable limit for total mass balance error.

### **2.2.9 Sensitivity Analysis**

A sensitivity analysis was conducted for the horizontal hydraulic conductivity ( $K_h$ ), the vertical hydraulic conductivity ( $K_z$ ), and the recharge rate. The provisionally calibrated values for each of these parameters were multiplied by 0.25, 0.50, 1.0, 1.25, and 1.50 to ascertain the effects on the model flow solution. For  $K_h$ , the value was varied on a per-layer basis, and the effects upon model calibration as a whole were assessed. The same approach was taken for  $K_z$ .

Results are presented in Figures 2-12 through 2-22 in the form of graphs of sum of squared residuals (a measure of the overall error in model calibration) versus parameter multiplier for each parameter. The most sensitive parameters are those with the greatest change in the sum of squared residuals (SSR) when the parameter value is adjusted away from the provisionally calibrated value (the latter is designated by a parameter multiplier of 1.0 on Figures 2-12 through 2-22).

Note that the sensitivity analysis was conducted prior to a final adjustment to the recharge distribution in the calibrated model. This adjustment involved applying recharge to the uppermost active layer (rather than layer 1 only), so that the extreme northern corner of the model (which is dry in layer 1) received recharge. This change had a negligible impact on

calibration and does not impact the findings in this sensitivity analysis. However, since this slight adjustment to the calibrated model was conducted after the sensitivity analysis, the calibrated SSR of 38.66 ft<sup>2</sup> shown in Table 2-5 differs slightly from the SSR of 38.99 ft<sup>2</sup> shown on the sensitivity figures discussion in this section.

Within the multiplier range considered, the sensitivity analysis reveals that model calibration is very sensitive to the recharge value (Figure 2-22). The model calibration is also sensitive to Kh for Zone “A” (Figure 2-12). The model is only slightly sensitive to Kh for Zones “B” (Figure 2-13) and “C-Lower” (Figure 2-16), and to Kz for Zone “B” (Figure 2-18). The model calibration is insensitive to the remaining parameters: Kh for Zones “C-Upper” (Figure 2-14) and “C-Middle” (Figure 2-15); and Kz for Zones “A” (Figure 2-17), “C-Upper” (Figure 2-19), “C-Middle” (Figure 2-20), and “C-Lower” (Figure 2-21). Neglecting insignificant gains from adjustment of Kz values (Figures 2-17 through 2-21), the parameter values used in the model provide the best possible fit to the March 2006 water level dataset.

A sensitivity analysis was also conducted on the pumping and extraction wells. In the base case, the SSR was 38.66 ft<sup>2</sup>. When the injection and extraction rates were doubled, the SSR increased to 123 ft<sup>2</sup>. When the injection and extraction rates were cut in half, the SSR increased to 58.8 ft<sup>2</sup>. Hence, the calibrated hydraulic conductivity field is sensitive to (and a strong function of) the pumping and injection rates provided. If the pumping and injection rate data used in the steady-state calibration are erroneous, then the hydraulic conductivity field in the calibrated model is unlikely to be representative of the actual physical system.

### 2.2.10 Testing of Model on Blind Data

The model was tested on July 2006 water level data that was unseen as far as the model development and calibration are concerned. The locations of the wells in this dataset are shown in Figure 2-23. Model simulated versus observed water levels are shown in Figure 2-24. The correlation coefficient ( $R^2$ ) is 0.92 (Figure 2-24), indicating excellent fit of the simulated to the observed heads. The July 2006 water level data are listed in Table 2-7. As discussed above, the model accuracy diminishes the further it is downgradient from the well-studied area of the model (the site area).

Although the observed and simulated heads correspond closely in this blind data test, the results are of limited value in increasing confidence that the model accurately represents the physical system. This is because the same model stresses were used as in the calibration simulation, and the blind data set is 1) spatially less comprehensive than the calibration dataset, 2) near in time to the calibration dataset (July 2006 vs. March 2006), and 3) very similar to the calibration data water levels. Of the 68 wells in the blind dataset, 67 also appeared in the 83 well calibration dataset. Thus, the blind dataset provides essentially no additional coverage of the model domain. Of the 67 wells appearing in both datasets, 52 (or 78%) had water level changes of less than 0.5 ft, and all had water level changes of less than 1.5 ft. Thus, the water levels in the two datasets are very similar; therefore, given that the same pumping stresses were modeled in both cases, it is not surprising that the simulated and observed water levels closely correspond in the test on blind data.

### 2.2.11 Verification

The confidence that the model accurately represents the physical system can best be increased by conducting a model verification simulation. A calibrated model uses selected values of hydrogeologic parameters, sources and sinks, and boundary conditions to match field conditions for selected calibration conditions. However, the choice of the parameter values and boundary conditions used in the calibrated model is not unique, and other combinations of parameter values and boundary conditions may give very similar model results. In model verification, the calibrated model is used to simulate a different set of aquifer stresses for which field measurements have been made. The model results are then compared to field measurements (collected under the distinct aquifer stress conditions) to assess the degree of correspondence. If the comparison is unfavorable, then additional calibration or data collection is required. If the comparison is favorable, then the degree of confidence in model predictions is increased.

The need for model verification is highlighted by the results of the sensitivity analysis. For example, model calibration was relatively insensitive or only slightly sensitive to the Kh values for Zones “B”, “C-Upper”, “C-Middle”, and “C-Lower”. Thus, there is significant uncertainty in the Kh values used for these zones. More accurate parameter values could be specified and uncertainty reduced by conducting a verification simulation wherein different aquifer stresses are simulated than were used in the calibration simulation.

Adequate data were not available during this phase to conduct model verification. Such data would include transient pumping rates for public water supply, irrigation, and treatment system wells within the model domain, and transient water levels for monitoring wells within the model domain. Based on reports of other hydrogeological analyses for the study area (Camp, Dresser and McKee [CDM], 2008), transient pumping rate data appears to be available 1) from the various water districts for the public water supply wells within the model domain, 2) from NCDPW and NYSDEC for irrigation wells at Bethpage State Park, and 3) from NCDPW for treatment system wells. Transient water level data also appears to be available for some pumping wells within the model domain (CDM, 2008); transient water level data for monitoring wells within the model domain is desirable for a verification simulation. Transient precipitation data available for area National Weather Service stations may also be utilized for a verification simulation.

The current model can be applied for screening level design and analysis of hypothetical scenarios. Model verification should be conducted prior to using the model to support final treatment system configuration/construction recommendations.

## 2.3 Flow Model Summary

The calibrated groundwater model accurately reproduces observed March 2006 heads within the model domain. Additionally, model-simulated heads closely match the blind July 2006 water level dataset (although the value of this comparison is limited, as discussed in Section 2.2.10). The current model can be applied for screening level design and analysis of hypothetical scenarios. As recommended in Section 2.2.11, model verification should be conducted prior to



using the model to support final treatment system configuration/construction recommendations. Groundwater model (MODFLOW<sup>®</sup>) input and output files are included in Appendix B.

### 3.0 SOLUTE TRANSPORT MODEL

This section describes the development of the solute transport model, which was performed using the groundwater flow model described in Section 2.0 above. The solute transport model evaluated the current and future contaminant fate and transport of PCE, 1,1-DCE, and TCE (the primary contaminant) in the study area. Using this model, PCE, TCE, and 1,1-DCE concentrations in the aquifer were predicted over time under the influence of site-specific hydrogeologic conditions and chemical and physical mechanisms including advection, dispersion, sorption, and degradation. The objective of the solute transport modeling was to predict future dissolved-phase concentrations of the PCE, TCE, and 1,1-DCE contaminant and to indicate, generally, the potential source area(s) of the contaminants in the groundwater plume and the potential risk of the contaminants to downgradient municipal water supplies. The solute transport model was developed in two phases: 1) conceptual model development; and 2) translation of the conceptual model to a numerical model. The model development process is discussed in the sections below.

#### 3.1 Conceptual Solute Transport Model

A conceptual solute transport model is a qualitative understanding of the site solute transport system and is a prerequisite to constructing a numerical transport model. The conceptual model is a summary of the geochemistry of the site. In addition to geochemical features, the conceptual solute transport model implicitly includes the conceptual groundwater flow model (Section 2.0), since advective transport of contaminants along with groundwater flow is a primary solute transport mechanism. A sound conceptual model minimizes the potential for errors to enter into the modeling process and increases the chance of constructing a numerical model that is consistent with the actual solute transport system.

PCE, TCE, and 1,1-DCE data collected in the year 2006 from all three zones were used to develop the current plume maps. Maximum PCE, TCE, and 1,1-DCE concentration values were used if more than one value was available for the same monitoring well. For those monitoring wells for which PCE, TCE, and 1,1-DCE data were not available for 2006, the most recent data from earlier years were used. Data used to develop the current PCE, TCE, and 1,1-DCE plumes are listed in Table 3-1, Table 3-2, and Table 3-3, respectively. The estimated PCE, TCE, and 1,1-DCE plume maps based on the most recent data are shown in Figure 3-1, Figure 3-2, and Figure 3-3, respectively. The dotted lines in Figure 3-1 and Figure 3-2 indicate that the concentration lines are estimated due to a lack of monitoring wells to contour contaminant concentrations in these areas.

The plume delineations indicate that both the TCE and PCE plumes extend from the Claremont site, southward to near the southern boundary of the Old Bethpage golf course. The highest concentration of TCE is located near monitoring wells EW-7C and EW-10C, which are located in the northeastern portion of the Claremont site, upgradient of known and suspected Claremont

source areas. This indicates the possibility of an upgradient contribution to the groundwater TCE plume thought previously to be originating entirely from the Claremont site. Additional ongoing investigations corroborate the existence of an upgradient source.

TCE concentrations generally decrease in a southerly direction. The noted restriction in the width of the TCE plume in the area of EW-3B and EW-3C may indicate that the bottom of these wells is not deep enough to monitor the maximum groundwater TCE concentrations in this area of the plume. Alternatively, this may indicate that other sources in addition to the Claremont site may be influencing the TCE concentrations in the southern area of the plume. Additional and deeper groundwater monitoring wells are required to better define the relationship between the northern and southern ends of the TCE plume.

In contrast, the highest concentrations of PCE were located at the southern end of the plume in the area of monitoring well BP-14B. The unusual distribution of PCE across the area may indicate that the PCE concentrations in the southern end of the plume are related to a PCE source other than one located in the area of the Claremont site. Again, for modeling purposes, the PCE concentrations in the area of BP-14B are considered to represent a continuing source of PCE.

The 1,1-DCE data show that four physically separate areas of 1,1-DCE occur throughout the plume. These areas are associated with areas of higher concentrations of both PCE and TCE and are therefore considered to be degradation products of these parent compounds.

The dotted lines in Figures 3-1 and 3-2 indicate that the PCE and TCE contour lines along the eastern edge and southern end of the plumes are estimated due to a lack of monitoring wells in these areas. The overall dimensions and apparent direction of migration of the conceptual TCE and PCE plumes agree generally with the model predicted groundwater flow directions (Figure 2-7 through Figure 2-11), with the exception of the most southern portions of the plumes centered on BP-14B. A source not located at the Claremont site is likely responsible for solvent contamination in this area, given the plume shapes relative to the groundwater flow direction. This is consistent with conclusions drawn in preceding paragraphs based on observation of the highest PCE concentrations at BP-14B. Note that PCE concentrations in this area are approximately an order of magnitude greater than TCE concentrations; TCE in this area may therefore result from degradation of PCE. Additional groundwater monitoring wells will be required to adequately define the relationship between the northern and the southern ends of the PCE plume.

The screened intervals for all wells are provided in Tables 3-1, 3-2, and 3-3. Since there were an insufficient number of data points within any one layer of the aquifer to develop a plume map for an individual aquifer layer, cross-sections were developed through the plume to display relationships in the vertical distribution of chlorinated solvent contamination. The cross-sections were developed subsequent to the plan view plume maps (Figures 3.1 through 3.3) and therefore use more recent contaminant sampling data.

Figure 3.4a illustrates TCE, DCE, TCA, and PCE concentrations at various depths along the axis of the northern end of the regional groundwater plume (well EW-7D to well EW-14-D). Contaminant concentrations are low to non-detect in the upper part of the aquifer and higher in



the deeper portions. For example, EW-7 (northern, upgradient side of Claremont site) and EW-4 (eastern edge of Claremont site) exhibit significant solvent contamination deeper in the aquifer (-10 to -40 ft msl) and lesser contamination moving upwards (50 ft msl) toward the water table (~65 ft msl at Claremont). This suggests that contamination in these wells originates upgradient of Claremont, rather than from Claremont itself.

Figure 3.4b illustrates TCE, DCE, TCA, and PCE concentrations at various depths perpendicular to the axis of the northern end of the plume, along the northern boundary of the Claremont site (well EW-8D to well EW-13D). The highest concentrations occur at the northeastern corner of the Claremont site at EW-7C, and decrease to the east and west. This indicates that the upgradient source of groundwater contamination lies north of well EW-7C.

Figure 3.4c illustrates TCE, DCE, TCE, and PCE concentrations at various depths along the axis of the southern portion of the regional groundwater plume (well EW-14D to well BP-12A,B,C). The chemical signature at well EW-14D (primarily TCE) differs from that at downgradient well BP-14B,C (primarily PCE with lesser TCE), and the intervening well (BP-3A,B,C) is relatively unimpacted. These observations indicate that contaminants at EW-14D and BP-14B,C originated from different sources.

Figure 3.4d illustrates TCE, DCE, TCE, and PCE concentrations at various depths through the southwestern lobe of the groundwater plume (well OBS-1 to BP-10,B,C). Groundwater contaminant concentrations are highest at well BP-14B, and decrease to both the north and south of this location.

## 3.2 Numerical Model Development

### 3.2.1 Model Selection and Description

The Modular Three-Dimensional Multispecies Transport Model (MT3DMS<sup>®</sup>) (Zheng and Wang, 1999) was selected to model the transport processes for the primary contaminants at the study area. MT3DMS<sup>®</sup> is a modular mass transport modeling system that can simulate contaminants in groundwater while considering advection, dispersion, diffusion, and decay. The MT3DMS<sup>®</sup> model was selected in part because it is configured to run in conjunction with the results of the MODFLOW<sup>®</sup> model that was developed to model groundwater flow.

MT3DMS<sup>®</sup> is a modular three-dimensional transport model that can simulate advection, dispersion, and basic chemical reactions of dissolved constituents. The MT3DMS<sup>®</sup> transport model is used in conjunction with MODFLOW<sup>®</sup> in a two-step flow and transport simulation. First, the heads and cell-by-cell flux terms are computed by MODFLOW<sup>®</sup> during the flow simulation and are written to a specially formatted file. This file is then read by MT3DMS<sup>®</sup> and utilized as the flow field for the transport portion of the simulation. MT3DMS<sup>®</sup> is a newer version of the MT3D<sup>®</sup> model. MT3DMS<sup>®</sup> differs from MT3D<sup>®</sup> in that it allows for multi-species transport, supports additional solvers, and allows for cell-by-cell input of all model parameters. The MT3DMS<sup>®</sup> model program includes the three major classes of transport solution techniques in a single code, i.e., the standard finite difference method; the particle

tracking based Eulerian-Lagrangian methods; and the higher order finite volume method. Since no single numerical technique has been shown to be effective for all transport conditions, the combination of these solution techniques, each having its own strengths and limitations, is believed to offer the best approach for solving the most wide-ranging transport problems with desired efficiency and accuracy. MT3DMS<sup>®</sup> is ideally suited for simulating the migration of simple contaminant plumes over time. Major input parameters for the MT3DMS<sup>®</sup> model are porosity, dispersivity, half-life of the contaminant, and adsorption coefficient.

MT3DMS<sup>®</sup> can accommodate very general spatial discretization schemes and transport boundary conditions, including:

- Confined, unconfined, or variably confined/unconfined aquifer layers.
- Inclined model layers and variable cell thickness within the same layer.
- Specified concentration or mass flux boundaries.
- Solute transport effects of external hydraulic sources and sinks such as wells, drains, rivers, areal recharge, and evapotranspiration.

MT3DMS<sup>®</sup> produces an array of dissolved concentrations in response to a source of known concentration within the groundwater flow field generated by the boundary conditions set up in the groundwater flow model.

In addition, for solute transport simulations of PCE, TCE, and 1,1-DCE, the particle tracking code (MODPATH<sup>®</sup>) was used. The USGS computer program, MODPATH<sup>®</sup>, is used for particle-tracking analysis to project the path and direction of movement of a water particle forward or backward through time. MODPATH<sup>®</sup> is a groundwater particle-tracking, post-processing package that computes three-dimensional flow paths using output from steady-state or transient groundwater flow simulations by MODFLOW<sup>®</sup> (Pollack, 1994). MODPATH<sup>®</sup> allows for the analysis of groundwater flow times and flow directions. For example, if a contaminant release is known to have occurred at a given location, particle-tracking simulations may be performed with groundwater particles starting at the source location and allowed to travel in the flow field for some user-specified amount of years, either forward or backward. The particle locations at some time (i.e., the past, present, or future) may then be compared to the current extent of the known contamination. This can provide a helpful gauge to determine if the flow directions/patterns and velocities are appropriate. It is important to realize that particle tracking includes only the effects of advective flow and neglects dispersion, sorption, and degradation. These factors must be kept in mind when comparing the particle tracking results to the observed contaminant distribution.

### 3.2.2 Finite Difference Grid

The solute transport model uses the same three-dimensional finite difference grid developed and described previously for the groundwater flow model (see Figure 2-1). Consequently, development of the numerical solute transport model required the specification of appropriate solute transport specific properties for this three-dimensional model grid.

### 3.2.3 Solute Transport Specific Properties

**3.2.3.1 Initial Conditions** - The initial conditions consist of the initial dissolved-phase concentrations of PCE, TCE, and 1,1-DCE. For future predictive simulations (i.e., simulations starting at the present time), the current PCE, TCE, and 1,1-DCE plumes as presented in Section 3-1 were used as the initial dissolved-phase concentrations in each of the Zone A, Zone B, and Zone C-upper (see Figure 3-1 through Figure 3-3). Again, the PCE, TCE, and 1,1-DCE concentration used for each well was the maximum value determined for that well based on analysis of groundwater samples collected in 2006, or if no 2006 data existed, then the value used was the maximum detected values from samples collected in earlier years.

**3.2.3.2 Specified Concentration Boundary Conditions** - Specified concentration cells were used to represent the assumed presence of a residual dense non-aqueous phase liquid (DNAPL) PCE source in the area of monitoring well BP-14B as shown in Figure 3-1. Also, a continuous TCE source was assumed in the area of monitoring wells EW-7C and EW-10D as shown in Figure 3-2. TCE concentrations in this area are not sufficiently elevated to indicate the presence there of DNAPL TCE, but concentrations are relatively constant over time. Therefore, an upgradient source is likely, but the location and magnitude are not known. Consequently, a constant concentration source area was assigned in the model at EW-7C/EW-10D to best represent the observed conditions (given the unknowns). The concentration assigned was based on TCE analytical data for these wells. Similarly, a continuous 1,1-DCE source was assumed in the area of monitoring wells MW-10C, EW-10D, and BP-14B as shown in Figure 3-3.

**3.2.3.3 Dispersivity** - The dispersivities were specified as 30 feet, 3 feet, and 1 foot in the longitudinal, transverse horizontal, and transverse vertical directions, respectively, throughout the model domain. These are reasonable values for the size of the plumes observed, but these are not calibrated values.

**3.2.3.4 Porosity** - An effective transport porosity value of 0.30 was specified. This is a reasonable value for the type of materials observed in the model domain but is not a calibrated or measured value.

**3.2.3.5 Bulk Density** - Bulk density ( $\rho_b$ ) values of 1.8 grams per cubic meter ( $\text{g}/\text{cm}^3$ ) were used for the aquifers (Zone A, Zone B, and Zone C). This is a reasonable value for the type of materials observed in the model domain but is not a calibrated or measured value.

**3.2.3.6 Sorption** - Sorption of the chlorinated solvents to the aquifer material was specified using a linear sorption isotherm. In this case, the sorbed- and dissolved-phased concentrations are assumed to be in equilibrium, and the sorbed-phase concentration divided by the dissolved-phase concentration is the equilibrium distribution coefficient ( $K_d$ ). For organics, sorption occurs predominantly onto organic carbon in the matrix (unless organic carbon content is very low). Consequently,  $K_d$  is generally taken as the product of the organic carbon fraction in the matrix ( $f_{oc}$ ) and the organic carbon partition coefficient ( $K_{oc}$ ). A  $f_{oc}$  value of 0.001 (0.1%) was assumed. This is a reasonable value for the type of materials observed in the model domain but is not a calibrated or measured value. The organic carbon partition coefficient  $K_{oc}$  is a chemical-specific property available from the literature. The  $K_{oc}$  values for PCE, TCE, and 1,1-

DCE are presented in Table 3-4. Also included in Table 3-4 are the  $K_d$  values computed based upon a  $f_{oc}$  of 0.001; these values were used throughout the model domain. The low end of the  $K_{oc}$  range for TCE (87 milliliters per gram [ml/g]) and PCE (209 ml/g) were used to calculate the  $K_d$ . This results in a lower  $K_d$  value, which conservatively underestimates sorption of TCE and PCE onto the aquifer matrix. Finally, retardation factors ( $R_f = 1 + K_d \cdot \rho_b / \eta$ , where  $\rho_b$  is bulk density and  $\eta$  is porosity) are shown in Table 3-4. The retardation factor is the factor (multiple) by which contaminant movement is retarded (slowed) relative to groundwater flow due to sorption onto the matrix. A retardation factor of 1 indicates the chemical advectively moves at the same rate as the bulk groundwater. For example, a retardation factor of 2.25 means the PCE moves 2.25 times slower than a conservative tracer would migrate in the groundwater.

**3.2.3.7 Degradation** - PCE, TCE, and 1,1-DCE were simulated assuming no decay. Site-specific redox potentials are greater than 50 millivolts, and dissolved oxygen concentrations are generally greater than 0.5 milligrams per liter (mg/L) (see Table A-1, Appendix A), indicating that the detected PCE, TCE, and 1,1-DCE plumes are generally in an aerobic state. According to Surez and Rafia, 1999; PCE, TCE, and 1,1-DCE could have a degradation rate as low as zero in the aerobic state. Review of the chemical data over time also indicates that the chemicals are not significantly degrading over time. At well EW-7C, the TCE concentration has increased from 900 micrograms per liter ( $\mu\text{g/L}$ ) in February 2005 to 1,400  $\mu\text{g/L}$  in February/July 2006 (for detail, please see Appendix A). Therefore, for this analysis, it was assumed that there was no decay of the chemicals. There may be some bio-decay occurring in the source zone area(s), resulting in the formation of DCE, but the rate and sustainability of this bio-decay process are not known, either within the source zone or within the plume (ITRC, 2007). The PCE, TCE, and DCE plumes are modeled as individual, non-decaying plumes.

### 3.2.4 Particle Tracking Analysis

Particle tracking analysis was conducted for wells EW-7, EW-9, and MW-10 (see Figure 3-5). The particle tracking analysis was done for both forward and backward tracking for wells EW-7, EW-9, and MW-10. As mentioned earlier, it is important to realize that particle tracking includes only the effects of advective flow and neglects dispersion, sorption, and degradation. These factors must be kept in mind when comparing the particle-tracking results to the observed contaminant distribution. Particle tracks are shown in red (forward track) and green (backward track), with travel times indicated in years (each arrow indicates one year). The result of this particle tracking shows the possible source of contamination and the future flow path of the contamination.

EW-7 and EW-9 are located upgradient of suspected source areas at Claremont and exhibit solvent contamination. Backward particle tracking from these two wells helps to identify possible upgradient source areas. Although dissolved solvent concentrations at EW-9 are relatively low, this well was included in the particle tracking analysis because it is located at the west side of the Claremont site and roughly defines the western extent of the plume coming onto the site. Areas to the northeast of the EW-9 reverse particle track may contribute to the plume moving onto the Claremont site, while areas to the southwest may not. The results of this particle tracking analysis indicate that contamination in monitoring wells EW-7 and EW-9 is apparently originating in an area north and northwest of the Claremont site. These results also

show that any contamination originating upgradient of these wells or from the Claremont site downgradient of these wells is captured by the Claremont extraction well field.

The particle tracking for monitoring well MW-10 indicates that contaminants in this well are likely originating from a source east of the Claremont site, and contaminants passing through this well area migrate downgradient, passing to the northeast of municipal well N-07852 and southwest of the two Suffolk County municipal water supply wells shown on Figure 3-5. These results are different than the results from the previous model which indicated this particle track to be captured by the TOB groundwater extraction well field.

Particle tracking analysis was also done for several municipal supply wells (Suffolk County S-20042 and S-39709; Village of Farmingdale N-7852), Claremont recovery wells (EXT-1, EXT-2, and EXT-3) TOB recovery wells (RW-1 through RW-5), and for the NCDPW groundwater extraction wells (RW-1 and ORW-4 through ORW-7). Reverse particle tracking was conducted for each of these wells, and the particle tracking results were used to map starting locations for particles discharging to these wells. The result of this capture zone analysis is shown in Figure 3-6. The Claremont recovery wells capture water originating on and upgradient of the Claremont site. The Nassau County wells capture water originating in the western portion of the FTC. The TOB wells capture water originating in the area of the FTC and the Old Bethpage Landfill (OBL), as well as water originating immediately east of the Claremont site. The Village of Farmingdale well N-7852 captures water originating at the TOB OBL western infiltration basin, and upgradient. The Suffolk County wells S-20042 and S-39709 capture water east of the currently projected eastern edge of any of the contaminant plumes. As shown in Figure 3-6, water captured by these wells originates at the northern model boundary. These Suffolk County wells are in Zone “C-Lower” in the model and, given the current model configuration, are predicted not to capture any shallow contamination that may be present directly upgradient within the model area. Flow model verification (Section 2.2.11) will increase the confidence in this (and other) model predictions. Final definition of the eastern plume boundary will be required to make a final determination of the degree of risk to these wells (or other wells further downgradient outside of the model area) from the contaminant plumes addressed in this study.

A comparison of the capture analysis on Figure 3-6 to the TCE, PCE, and 1,1-DCE plumes as illustrated on Figures 3-1, 3-2, and 3-3 indicates that contaminants in the easternmost edge of the groundwater plumes are likely not being captured by any of the currently operating groundwater extraction well fields. This conclusion is tentative, however, since the eastern edge of the plumes in this area can only be estimated (indicated by dashed lines on Figures 3-1, 3-2, and 3-3) due to a lack of groundwater TCE, PCE, and 1,1-DCE data from this area of the plume.

Backward particle tracking was also conducted from public supply wells N-7515, N-7516, and N-7852 (see Figure 3-7) to show the possible migration pathway and times to these public supply wells. These results indicate that water moving toward municipal water supply wells N-7515 and N-7516 originates in areas of no known groundwater contamination. Water moving toward well N-7852, however, originates in the areas of the FTC and OBL, both of which are known sources of groundwater contamination. This information is to be interpreted within the uncertainty of the modeled versus observed flow field, as discussed above.



The backward particle tracks and travel times for the two Suffolk County municipal water supply wells (S-39709 and S-20042) are also presented on Figure 3-7. These results further illustrate that water moving to these wells originates east of the Claremont facility, beyond the currently defined eastern edge of the contaminant plumes. Again, final plume definition will be required to conclude that these wells are at no risk of impact by downgradient migration of the contaminant plumes.

### **3.2.5 Predictive PCE, TCE, and 1,1-DCE Simulations**

Solute transport was conducted with advection, sorption, dispersion, and no degradation. The future simulation time frame was taken as 5 years and 10 years. The 5- and 10-year future PCE, TCE, and 1,1-DCE simulation results are presented in Figures 3-8 through 3-17.

The results of the solute transport modeling of the PCE plumes are presented in Figures 3-8, 3-9, 3-10, and 3-11. These results indicate a general downgradient migration, along with decreasing PCE concentrations in each of the four zones modeled. Of particular importance is that the modeling indicates that the migrating PCE plume will impact the Village of Farmingdale municipal water supply well N-7852 in 10 years. The modeling indicates that this well is at risk of contamination. This interpretation needs to be tempered by the fact that the southern extent of the plume used in this modeling effort is not completely defined due to a lack of data in this area. This indicates that additional plume delineation in this area is critical to the further evaluation of this situation.

The results of the solute transport modeling of the TCE plumes are presented in Figures 3-12, 3-13, 3-14, and 3-15. These results, similar to the results of the PCE modeling, indicate a general downgradient migration, along with decreasing TCE concentrations, in each of the four zones modeled. Of particular importance again is that the modeling indicates that the migrating TCE plume will impact the Village of Farmingdale municipal water supply well N-7852 in possibly as few as five years. The modeling again indicates that this well is at risk of contamination, but this interpretation needs to be tempered by the lack of firm plume definition in this southern area of the plume.

The results of the solute transport modeling of the 1,1-DCE plumes are presented in Figures 3-16 and 3-17. These results indicate a general downgradient migration along with decreasing 1,1-DCE concentrations in each of the four zones modeled. Unlike the results of the PCE and TCE modeling, however, there are no projected impacts by the 1,1-DCE plumes on any municipal groundwater supply wells.

### 3.3 Transport Model Summary

The PCE, TCE, and 1,1-DCE initial plume map was estimated based on the most recent sampled data and applied to the model as the initial plume. The transport simulation predicted the possible potential paths of the contaminants and the extent of the plumes in next 5 and 10 years. Transport validation is possible through chemical data collected at future times and is recommended. Additional monitoring points will be required to define the plume boundaries to allow a final assessment of the risk of plume migration to downgradient municipal water supplies.

## 4.0 SUMMARY AND CONCLUSIONS

An extensive data analysis was conducted, and a regional numerical flow and transport model was developed. The calibrated groundwater model accurately reproduces observed March 2006 heads within the model domain, under steady-state conditions including multiple extraction/injection points. Additionally, model-simulated heads closely match the blind July 2006 water level dataset (although the value of this comparison is limited, as discussed in Section 2.2.10). The current model can be applied for screening level design and analysis of hypothetical scenarios. As recommended in Section 2.2.11, model verification should be conducted prior to using the model to support any significant treatment system redesign, or reconfiguration/construction recommendations.

Optimal remedial well field design can be accomplished by using this model in tandem with MODOFC, the optimal flow control algorithm developed by David Ahlfeld. This tool automates the pumping rate and location of injection and remediation wells, given user-specified controls on desired groundwater flow directions at key locations.

While the model is an excellent decision tool as it currently stands, the following limitations and recommendations must be borne in mind:

1. The current model can be applied for screening level design and analysis of hypothetical scenarios. As recommended in Section 2.2.11, model verification should be conducted prior to using the model to support final treatment system configuration/construction recommendations. Model verification involves reproducing observed heads under a different set of conditions than were used for the model calibration, and increases the likelihood that the model accurately represents the physical system.
2. Additional monitoring wells are required to define (1) the eastern plume boundary to establish whether it is being captured by the existing extraction systems and (2) the relationship between the northern and southern portions of the PCE and TCE plumes.
3. Refinement of the model grid may be necessary to perform flow or transport calculations in specific regions of the model for specific purposes. Both horizontal (row, column) and vertical (layer) grid refinement may be required.

4. The groundwater flow field has some uncertainty depending on the method used to interpret the information. Three analysis techniques are presented: Kriging and triangulation (Figure 2-3) and the modeled results (Figures 2-7 through 2-11, inclusive). Particle tracking and transport interpretation is to be assessed within this level of uncertainty.
5. The local area around the site is not modeled as a DNAPL source area and is modeled in a regional scale. This averages the effect of DNAPL flow paths in heterogeneous materials such as sand/clay lenses. This effect can be modeled, and remedial designs can be optimized. This would require a numerical model capable of handling DNAPL flow and transport, such as the UTCHEM simulator.
6. The regional model has five model layers for the transport simulations. This approach also averages out the effect of local sand/clay lenses and does not account for matrix diffusion and rebound of these systems. This can have the effect of prolonging the time for a plume to reach maximum contaminant level (MCL).
7. The initial plumes were developed using plume maps constructed from recent field data. The plumes were not recreated from initial spill conditions as sufficient information does not exist from which to perform that analysis. The transport solution was not validated. It can be validated over time as additional chemical data are collected in the future. Deviation in transport prediction, if any, for future conditions may require model refinement.
8. The pumping rates for the public supply wells from best available data from 2004-2005 were used and the flow field modeled as steady-state. The pumping and injection rates for the wells are shown on Figure 2-4. Data from actual well withdrawal and injection should be collected over time. If rates change, the flow model should be validated to be certain these data did not introduce an inadvertent bias into the model calibration.



## 5.0 REFERENCES

- ASTM, 2004. ASTM D5447-04 Standard Guide for Application of a Ground-Water Flow Model to a Site-Specific Problem.
- Camp, Dresser and McKee, 2008. Nassau County Department of Public Works Fireman's Training Center Groundwater Model, Final Report, April 2008.
- Department of Army, August 1994. 100% Final Remedial Design Phase Submittal, Operable Unit 1, Phase I Design, Claremont Polychemical Corporation, Superfund Site, Old Bethpage, New York, Volume 3.
- Ebasco, 1990. Remedial Investigation Report, Draft Final, Claremont Polychemical site, Old Bethpage, NY. Ebasco Services Inc. July 1990
- Environmental Simulations, Inc., 2004. *Guide to Using Groundwater Vistas Version 4: Environmental Simulations, Inc.*, 358 p.
- Firemen's Training Center, 2004. Hard Copy data received from Nassau County for the Fire training area on-site/off-site well construction details, geological logs for recovery and injection wells, boring logs and well construction diagrams for available monitoring wells. Data transmittal date: June 2004.
- G&M, 1987. OBSWDC Aquifer Test for Evaluating Hydraulic Control of Leach Impacted Groundwater, Old Bethpage, Long Island, New York. Geraghty & Miller, Inc., September 1987.
- Geraghty & Miller, Inc., Undated. Summary of Construction Details for Phase 3 off-site wells, Old Bethpage, New York.
- Harbaugh, A. W., and M. G. McDonald, 1996. User's documentation for MODFLOW-96, an update to the U.S. Geological Survey modular finite-difference ground-water flow model: U.S. Geological Survey Open-File Report 96-485, 56 p.
- Isbister, 1966. Remedial Investigation Report (Appendix H, 4<sup>th</sup> page), Draft Final, Claremont Polychemical site, Old Bethpage, NY. Ebasco Services Inc., July 1990.
- ITRC, 2007. Deschaine, L. M., Simulation and Optimization of Subsurface Environmental Impacts; Investigations, Remedial Design and Long Term Monitoring of BioNAPL Remediation Systems, Chapter 9, in In-Situ Bioremediation of Chlorinated Ethene DNAPL Source Zones: Case Studies, Prepared by The Interstate Technology and Regulatory Council, Bioremediation of Dense Non-Aqueous Phase Liquids (Bio DNAPL) Team, 2007. [www.itrcweb.org/Documents/bioDNPL\\_Docs/BioDNAPL-2.pdf](http://www.itrcweb.org/Documents/bioDNPL_Docs/BioDNAPL-2.pdf)

- Nassau County Department of Public Works, 2004. Review of off-site Volatile Organic Plume Characteristics, Department of Public Works, Nassau County, Database Development Meeting at EPA Region II Headquarters, New York, NY, March 2004.
- NYSDEC, 2004. Public water supply well data for year 2004, New York State Department of Environmental Conservation, NY.
- Pollock, D. W., 1994. *User's Guide for MODPATH/MODPATH-PLOT, Version 3: A particle tracking post-processing package for MODFLOW, the U.S. Geological Survey finite-difference ground-water flow model*. U.S. Geological Survey Open-File Report 94-464, 234 p.
- SAIC, 2003. Report on Aquifer Recovery Monitoring Results. Letter report to Mr. Brad Vann, USACE, dated November 20, 2003.
- SAIC, 2007. Groundwater Data Base and Plume Modeling Report for the Claremont Polychemical Superfund Site. September 2007.
- Surez and Rafia, 1999. Biodegradation Rates for Fuel Hydrocarbons and Chlorinated Solvents in Groundwater, Civil and Environmental Engineering, University of Houston, CRC Press, 1999.
- Zheng, C., and P. P Wang, 1999. *MT3DMS®: A Modular Three-Dimensional Multispecies Transport Model for Simulation of Advection, Dispersion, and Chemical Reactions of Contaminants in Groundwater Systems; Documentation and User's Guide*, U.S. Army Engineer Research and Development Center Contract Report SERDP-99-1, Vicksburg, Mississippi.

## TABLES

# TABLES

**Table 2-1. Borehole Data Used to Interpret the Conceptual Model**

Well	Zone	Screen Elevation Top (FT amsl)	Screen Elevation Bottom (FT amsl)	Ground Elevation (FT amsl)
BP-11	A	4	-16	81.76
BP-12A	A	9	-11	78.33
BP-3A	A	70.54	50.54	124.54
BP-4A	A	74	54	92.69
BP-5A	A	67	47	96.34
BP-6A	A	79	59	102.55
BP-7A	A	73	53	148.35
BP-8A	A	72	52	92.29
DW-1	A	37.69	32.69	131.19
DW-2	A	42.61	37.61	137.61
EW-1A	A	64.85	55.02	130.02
EW-1B	A	40.39	30.56	130.56
EW-2A	A	64.97	55.14	157.14
EW-3A	A	63.75	53.92	158.92
EW-6A	A	67.31	57.48	130.48
OSEB-1 (5A)	A	52	47	137
OSEB-2 (6A)	A	60	55	160
OSEB-3 (7A)	A	73	58	148
OSEB-4 (8A)	A	50	45	125
OSEB-5 (9A)	A	75	60	153
OSEB-6 (10A)	A	61	56	165
SW-1	A	66.31	61.31	131.5
SW-2	A	73.93	63.93	131.19
TU-3	A	35	30	92.9
W-20A	A	57	37	113.17
W-21A	A	55	35	100.95
WT-1	A	66.98	56.98	162.38
RW-2	A	70	-6	104
RB-1	A	58	38	136
MW-5A	A	50.9	45.9	135.9
MW-6A	A	58.8	53.8	158.8
MW-7A	A	71.9	56.9	146.9
MW-9A	A	74	59	152
MW-10A	A	59.8	54.8	159.8
MW-11A	B	-55	-60	85
BP-10B	B	-129	-149	81.21
BP-12B	B	-103	-123	78.24
BP-13B	B	-147	-311	133.37
BP-14B	B	-119	-159	81.5
BP-4B	B	-78	-98	91.72
BP-5B	B	-84	-104	96.58
BP-6B	B	-77	-97	102.58

Well	Zone	Screen Elevation Top (FT amsl)	Screen Elevation Bottom (FT amsl)	Ground Elevation (FT amsl)
BP-7B	B	-80	-100	147.9
BP-8B	B	-39	-59	91.43
BP-9B	B	-99	-119	85.09
EW-1C	B	15.3	5.47	130.47
EW-2B	B	37.44	27.61	157.61
EW-2C	B	17.37	7.54	157.54
EW-3B	B	33.89	24.06	159.06
EW-3C	B	4.75	-5.08	158.92
EW-4A	B	61.72	46.89	161.89
EW-4B	B	41.5	31.67	161.67
EW-4C	B	16.24	6.41	161.41
EW-5	B	-29.62	-39.45	135.55
EW-6B	B	20.44	10.61	130.61
EW-6C	B	-29.77	-39.6	130.9
LF-2	B	8.7	3.7	161.12
MW-10B	B	-11.88	-16.88	134.24
MW-6D	B	-24.61	-29.61	130.9
MW-8B	B	-20.76	-25.76	160.39
OBS-2	B	-64	-84	105
OSEB-2 (6B)	B	30	25	160
OSEB-2 (6C)	B	5	0	160
OSEB-2 (6D)	B	-27	-32	160
OSEB-2 (6E)	B	-85	-90	160
OSEB-3 (7B)	B	-82	-87	150
OSEB-4 (8C)	B	-110	-115	135
OSEB-5 (9C)	B	-67	-72	153
OSEB-6 (10C)	B	-113	-118	165
UM-1	B	-35	-4	115.64
W-20B	B	20	0	113.5
W-20C	B	-42	-62	112.91
W-21B	B	9	-11	100.1
W-21C	B	-38	-58	100.73
W-7B	B	25	5	104.52
ORW-1	B	-39	-119	146
ORW-2	B	-44.06	-144.86	96.94
ORW-3	B	-64.1	-132.1	90.9
ORW-4	B	-88	-148	84
ORW-5	B	-65	-140	100
ORW-6	B	-92.7	-152.7	82.3
ORW-7	B	-131.2	-181.2	74.8
IW-1	B	56	6	156
IW-2	B	54	4	154
IW-3	B	55	5	155
OBS-1	B	-65	-85	110

Well	Zone	Screen Elevation Top (FT amsl)	Screen Elevation Bottom (FT amsl)	Ground Elevation (FT amsl)
MW-5B	B	24.9	19.9	136.9
MW-6B	B	23.7	18.7	158.7
MW-6C	B	3.5	-1.5	158.5
MW-8A	B	48.5	-53.5	133.5
MW-9B	B	-10.9	-15.9	152.1
MW-11B	C	-150	-155	90
BP-10C	C	-276	-296	80.94
BP-12C	C	-291	-311	78.56
BP-13C	C	-321	-341	133.67
BP-14C	C	-229	-269	81.48
BP-3B	C	-91.43	-111.43	123.57
BP-3C	C	-156.32	-176.32	123.68
BP-4C	C	-188	-208	91.57
BP-5C	C	-154	-174	96.28
BP-6C	C	-154	-174	102.35
BP-7C	C	-162	-182	148.4
BP-8C	C	-169	-189	91.48
BP-9C	C	-239	-259	84.88
MW-10C	C	-112.73	-117.73	135.72
MW-10D	C	-147.83	-152.83	160.27
MW-8C	C	-109.28	-114.28	104.58
OSEB-2 (6F)	C	-185	-190	160
OSEB-5 (9D)	C	-158	-163	153
OSEB-6 (10D)	C	-148	-153	165
W-20D	C	-119	-139	113.15
W-21D	C	-116	-136	100.44
W-7D	C	-106	-126	104.68
MW-6E	C	-85.7	-90.7	159.3
MW-6F	C	-186.5	-191.5	158.5
MW-7B	C	-83.3	-88.3	146.7
MW-9C	C	-67.9	-72.9	152.1
MW-9D	C	-159.5	-164.5	151.5

*FT amsl: Feet above mean sea level*

**Table 2-2. Hydraulic Conductivities of the Aquifer (ft/day)**

	Source			
	(SAIC, 2003) <sup>1</sup>	Public wells <sup>1</sup> (Appendix B)	(Nassau County Department of Public works, 2004)	1987 Geraghty and Miller pump test
<b>Zone A</b>	<b>31.5</b>	<b>--</b>	<b>150</b>	<b>--</b>
<b>Zone B</b>	<b>52.3</b>	<b>--</b>	<b>150</b>	<b>251</b>
<b>Zone C</b>	<b>36.9</b>	<b>2.76-29.83</b>	<b>150</b>	<b>253</b>

<sup>1</sup>: assuming saturated thickness of the aquifer is 690 ft.

**Table 2-3. Modeled Aquifer Parameters**

Hydraulic Conductivity						
Zone	Kx (ft/d)		Ky (ft/day)		Kz (ft/day)	
	Initial value	Value after calibration	Initial value	Value after calibration	Initial value	Value after calibration
A	31.5	282	31.5	282	3.15	28.2
B	52.3	125	52.3	125	5.23	12.5
C-upper	36.9	135	36.9	135	3.69	13.5
C-middle	36.9	690	36.9	690	3.69	69
C-lower	36.9	98	36.9	98	3.69	9.8
Recharge						
Zone	ft/day		in/yr		cm/yr	
A	0.0047		20.58		52.28	
Effective Porosity						
Zone	-		—		—	
A	0.30		—		—	
B	0.30		—		—	
C	0.30		—		—	



**Table 2-4. Model Calibration Result**

<b>Well</b>	<b>X</b>	<b>Y</b>	<b>Observed Head</b>	<b>Computed Head</b>	<b>Residual</b>
BP-11	1138404	210663	59.77	59.10	0.67
BP-12A	1137808	209996.5	58.73	58.67	0.06
BP-4A	1137813	211407.6	61.27	61.00	0.27
BP-5A	1136488	211132.6	61.59	61.99	-0.40
BP-6A	1135510	212074.4	64.21	64.48	-0.27
BP-7A	1135260	213639.5	66.50	67.48	-0.98
BP-8A	1136542	212426.9	63.60	64.24	-0.64
DW-1	1138500	215549.6	67.34	67.29	0.05
DW-2	1138799	215542.4	65.99	66.89	-0.90
EW-1A	1138388	215352.9	67.06	67.07	-0.01
EW-1B	1138392	215362.2	67.10	67.08	0.02
EW-2A	1138990	215434.3	65.61	66.34	-0.73
EW-3A	1140105	214282.4	64.59	63.70	0.89
EW-6A	1138479	216174.6	68.92	68.62	0.30
MW-05A	1137775	213289.1	66.03	64.58	1.45
MW-06A	1138695	214331.8	65.69	65.17	0.52
MW-07A	1139663	212801.7	62.76	61.31	1.45
RB-1	1137946	217261.2	70.90	70.98	-0.08
SW-1	1138491	215550.4	67.36	67.31	0.05
WT-1	1139327	215791.6	68.07	67.83	0.24
MW-08A	1138580	215212	65.89	66.49	-0.60
MW-10A	1139726	214857.4	65.94	64.99	0.95
N-9880	1139695	209098.3	57.00	55.96	1.04
TW-1	1135750	214858.4	70.43	69.29	1.14
TW-2	1135951	214318	67.80	68.07	-0.27
BP-10B	1138982	209498.6	57.58	57.06	0.52
BP-12B	1137808	209996.5	58.37	58.64	-0.27
BP-14B	1138073	210590.6	59.27	59.32	-0.05
BP-3B	1139436	211723.4	59.76	60.09	-0.33
BP-4B	1137813	211407.6	60.97	61.04	-0.07
BP-5B	1136488	211132.6	61.37	62.00	-0.63
BP-6B	1135510	212074.4	63.57	64.48	-0.91
BP-8B	1136542	212426.9	63.76	64.18	-0.42
EW-1C	1138381	215355.8	66.91	66.98	-0.07
EW-2B	1138995	215447.2	66.12	66.27	-0.15
EW-2C	1138988	215444.8	65.82	66.24	-0.42
EW-3B	1140104	214302.4	64.49	63.74	0.75
EW-3C	1140110	214301.4	64.45	63.73	0.72
EW-4A	1138937	215734.7	67.32	67.31	0.01
EW-4B	1138937	215728.4	67.22	67.29	-0.07
EW-4C	1138937	215722	67.21	67.27	-0.06
EW-5	1138811	215530.1	67.23	66.52	0.71

**Table 2-4. Model Calibration Result (Continued)**

Well	X	Y	Observed Head	Computed Head	Residual
EW-6C	1138487	216170.7	68.91	68.57	0.34
LF-2	1137938	215192.2	67.26	67.41	-0.15
MW-05B	1137775	213289.1	66.05	64.36	1.69
MW-06B	1138695	214331.8	65.61	65.14	0.47
MW-06C	1138695	214331.8	65.70	65.14	0.56
MW-06D	1138496	214310.4	65.76	65.35	0.41
MW-08B	1138634	215202.5	66.21	65.61	0.60
MW-09B	1138788	212993.9	62.59	62.35	0.24
MW-10B	1139743	214813.2	64.58	64.99	-0.41
OBS-1	1137924	212227.3	62.49	62.21	0.28
OBS-2	1138767	211943.8	60.03	60.95	-0.92
MW-11A	1139540	209612.2	57.86	56.82	1.04
EW-7C	1138857	216155.1	68.39	68.30	0.09
EW-10C	1139102	216072.1	68.34	68.11	0.23
BP-10C	1138982	209498.6	56.02	57.10	-1.08
BP-12C	1137808	209996.5	57.91	58.82	-0.91
BP-13B	1136607	209238.6	57.55	58.80	-1.25
BP-13C	1136614	209242.5	56.79	58.80	-2.01
BP-14C	1138073	210590.6	58.74	59.50	-0.76
BP-3C	1139446	211755.4	59.66	60.21	-0.55
BP-4C	1137813	211407.6	60.59	61.12	-0.53
BP-5C	1136488	211132.6	61.20	62.01	-0.81
BP-6C	1135510	212074.4	63.73	64.50	-0.77
BP-7B	1135260	213639.5	66.36	67.37	-1.01
BP-7C	1135260	213639.5	66.26	67.37	-1.11
BP-8C	1136542	212426.9	62.91	64.13	-1.22
BP-9C	1138518	210207.8	58.07	58.47	-0.40
EW-2D	1139005	215488.1	66.80	66.81	-0.01
MW-06E	1138695	214331.8	65.53	65.16	0.37
MW-06F	1138695	214331.8	65.37	65.16	0.21
MW-07B	1139663	212801.7	61.41	61.58	-0.17
MW-09C	1138788	212993.9	61.73	62.66	-0.93
MW-09D	1138788	212993.9	62.27	62.66	-0.39
MW-10C	1139676	214834.3	65.46	65.13	0.33
MW-10D	1139678	214820.6	65.37	65.10	0.27
MW-11B	1139540	209612.2	57.63	56.83	0.80
MW-08C	1138634	215202.5	66.76	66.58	0.18
EW-7D	1138847	216156.7	68.31	68.19	0.12
EW-8D	1138323	215998.8	68.24	68.36	-0.12
EW-9D	1138632	216075.7	68.28	68.21	0.07
PPW-1	1138492	215820.2	67.68	67.88	-0.20

**Table 2-5. Steady State Calibration Statistics**

Statistic	
Number of wells	83
Residual Mean	-0.05
Residual Standard Deviation	0.68
Sum of Squares of residuals	38.66
Absolute Residual Mean	0.53
Minimum Residual	-2.01
Maximum. Residual	1.69
Residual Standard Deviation / Range in Observed Heads	4.58%

**Table 2-6. Mass Balance**

Parameter	Fluxes (ft <sup>3</sup> /day)		
	Inflow	Outflow	Net
Storage	NA	NA	NA
Wells	319,761.40	-1,381,424.24	-1,061,662.84
Constant Head Boundaries (Model North and South boundary)	4,269,852.32	-4,485,687.59	-215,835.27
Recharge	1,277,498.19	0.00	1,277,498.19
Total	5,867,111.91	-5,867,111.83	0.08
% Error	1.4E-06%		

**Table 2-7. Blind Test Result  
(July 2006 Water Level Data)**

Well	X	Y	Observed	Computed	Residual
BP-10B	1138982.40	209498.56	58.04	57.03	1.01
BP-10C	1138982.40	209498.56	55.40	57.07	-1.67
BP-11	1138404.28	210662.98	60.04	59.07	0.97
BP-12A	1137808.08	209996.53	58.84	58.64	0.20
BP-12B	1137808.08	209996.53	58.36	58.61	-0.25
BP-12C	1137808.08	209996.53	57.34	58.79	-1.45
BP-13B	1136613.78	209242.51	56.42	58.78	-2.36
BP-13C	1136613.78	209242.51	55.47	58.78	-3.31
BP-14B	1138073.14	210590.58	59.29	59.29	0.00
BP-14C	1138073.14	210590.58	58.30	59.47	-1.17
BP-3B	1139436.28	211723.43	59.98	60.05	-0.07
BP-3C	1139446.28	211755.43	59.83	60.17	-0.34
BP-4A	1137813.39	211407.64	61.12	60.97	0.15
BP-4B	1137813.39	211407.64	60.96	61.00	-0.04
BP-4C	1137813.39	211407.64	60.10	61.09	-0.99
BP-5A	1136488.28	211132.63	61.47	61.96	-0.49
BP-5B	1136488.28	211132.63	61.06	61.97	-0.91
BP-5C	1136488.28	211132.63	60.71	61.98	-1.27
BP-6A	1135510.39	212074.43	63.63	64.44	-0.81
BP-6B	1135510.39	212074.43	62.85	64.44	-1.59
BP-6C	1135510.39	212074.43	62.70	64.46	-1.76
BP-7A	1135259.81	213639.49	66.50	67.43	-0.93
BP-8A	1136542.44	212426.94	63.26	64.20	-0.94
BP-8B	1136542.44	212426.94	63.40	64.14	-0.74
BP-8C	1136542.44	212426.94	62.37	64.09	-1.72
BP-9B	1138518.41	210207.84	58.14	57.67	0.47
BP-9C	1138518.41	210207.84	57.60	58.44	-0.84
DW-1	1138499.95	215549.63	67.28	67.22	0.06
DW-2	1138798.68	215542.45	65.87	66.82	-0.95
EW-1A	1138387.75	215352.87	67.02	67.00	0.02
EW-1B	1138392.25	215362.20	67.99	67.01	0.98
EW-1C	1138381.05	215355.83	67.18	66.91	0.27
EW-2A	1138989.80	215434.34	65.26	66.27	-1.01
EW-2B	1138995.00	215447.23	65.99	66.20	-0.21
EW-2C	1138987.52	215444.75	65.89	66.17	-0.28
EW-2D	1139004.81	215488.09	65.87	66.73	-0.86
EW-3A	1140105.28	214282.44	64.50	63.64	0.86
EW-3B	1140104.27	214302.44	64.45	63.67	0.78
EW-3C	1140110.28	214301.44	64.37	63.67	0.70
EW-4A	1138937.09	215734.67	67.28	67.24	0.04
EW-4B	1138936.94	215728.38	67.26	67.22	0.04

**Table 2-7. Blind Test Result (Continued)**  
**(July 2006 Water Level Data)**

Well	X	Y	Observed	Computed	Residual
EW-4C	1138936.91	215722.04	67.21	67.20	0.01
EW-5	1138811.04	215530.12	67.23	66.45	0.78
EW-6A	1138478.86	216174.62	68.92	68.54	0.38
EW-6C	1138486.72	216170.72	68.60	68.49	0.11
LF-2	1137937.86	215192.20	67.09	67.34	-0.25
MW-05A	1137775.16	213289.10	66.03	64.53	1.50
MW-05B	1137775.16	213289.10	64.64	64.31	0.33
MW-06B	1138694.66	214331.77	65.22	65.08	0.14
MW-06C	1138694.66	214331.77	65.44	65.08	0.36
MW-06D	1138496.28	214310.44	65.51	65.29	0.22
MW-06E	1138694.66	214331.77	65.24	65.10	0.14
MW-06F	1138694.66	214331.77	65.02	65.10	-0.08
MW-07A	1139663.00	212801.75	62.76	61.27	1.49
MW-07B	1139663.00	212801.75	61.52	61.53	-0.01
MW-08A	1138579.99	215211.98	65.84	66.42	-0.58
MW-08B	1138634.22	215202.46	66.47	65.54	0.93
MW-08C	1138634.23	215202.46	66.61	65.54	1.07
MW-09B	1138788.10	212993.93	62.59	62.30	0.29
MW-09C	1138788.10	212993.93	61.59	62.61	-1.02
MW-09D	1138788.10	212993.93	62.05	62.61	-0.56
MW-10B	1139742.59	214813.17	65.36	64.92	0.44
MW-10C	1139676.14	214834.27	64.15	65.06	-0.91
MW-10D	1139677.93	214820.62	65.19	65.04	0.15
OBS-1	1137923.81	212227.33	62.36	62.16	0.20
OBS-2	1138766.85	211943.83	61.28	60.91	0.37
SW-1	1138491.46	215550.40	67.29	67.23	0.06
WT-1	1139326.83	215791.58	67.37	67.75	-0.38

**Table 3-1. PCE Data Used to Develop Current PCE plume**

WELL	X	Y	PCE (ug/L)
BP-12B	1137808	209997	21.800
BP-14B	1138073	210591	631.000
BP-14C	1138073	210591	5.900
BP-3B	1139436	211723	13.000
BP-3C	1139446	211755	3.400
BP-4B	1137813	211408	28.600
BP-4C	1137813	211408	76.800
BP-9B	1138518	210208	8.500
BP-9C	1138518	210208	3.100
DW-1	1138500	215550	0.450
DW-2	1138799	215542	0.330
EW-10C	1139102	216072	15.000
EW-11D	1139684	215472	0.720
EW-13D	1139347	216036	1.200
EW-14D	1140845	213111	5.900
EW-1A	1138388	215353	80.700
EW-1B	1138392	215362	3.000
EW-1C	1138381	215356	0.300
EW-2A	1138990	215434	0.300
EW-2B	1138995	215447	1.600
EW-2C	1138988	215445	2.600
EW-2D	1139005	215488	0.300
EW-3B	1140104	214302	0.200
EW-3C	1140110	214301	0.800
EW-4A	1138937	215735	31.000
EW-4B	1138937	215728	18.000
EW-4C	1138937	215722	34.000
EW-4D	1138953	215747	0.650
EW-5	1138811	215530	3.300
EW-6A	1138479	216175	0.180
EW-7C	1138857	216155	46.000
EW-7D	1138847	216157	3.600
EW-9D	1138632	216076	0.130
EXT-1	1138684	215226	75.000
EXT-2	1138776	215333	76.000
EXT-3	1138899	215476	34.000
MW-10B	1139743	214813	1.200
MW-10C	1139676	214834	43.000
MW-10D	1139678	214821	2.700
OBS-1	1137924	212227	3.500
SW-1	1138491	215550	100.000

**Table 3-1. PCE Data Used to Develop Current PCE plume (Continued)**

WELL_ID	X	Y	PCE (ug/L)
BP-10B	1138982	209499	-
BP-10C	1138982	209499	-
BP-12A	1137808	209997	-
BP-12C	1137808	209997	-
BP-13B	1136614	209243	-
BP-13C	1136614	209243	-
BP-2A	1137607	213043	-
BP-2B	1137607	213043	-
BP-3A	1139432	211706	-
EW-12D	1139217	215589	-
EW-3A	1140105	214282	-
EW-6C	1138487	216171	-
EW-8D	1138323	215999	-
EXT-3	1138899	215476	-
FTC-W-14A	1137092	213482	-
FTC-W-14B	1137082	213486	-
FTC-W-23	1137128	214004	-
FTC-W-31	1137117	213737	-
FTC-W-32	1137020	213810	-
FTC-W-35	1137165	213639	-
FTC-W-4A	1137207	214252	-
FTC-W-4B	1137199	214256	-
FTC-W-7A	1137225	213382	-
FTC-W-7B	1137210	213382	-
FTC-W-7C	1137202	213390	-
FTC-W-7D	1137242	213387	-
FTC-W-9A	1137484	213567	-
FTC-W-9B	1137488	213573	-
LF-1	1137113	214355	-
LF-2	1137938	215192	-
MW-06D	1138496	214310	-
MW-08C	1138634	215202	-
MW-09D	1138788	212994	-
OBS-2	1138767	211944	-
PPW-1	1138492	215820	-
RB-1	1137946	217261	-
RW-1	1138101	212732	-
RW-2	1138712	212758	-
RW-3	1139286	212942	-
RW-4	1139748	213178	-
RW-5	1139522	213974	-
WT-1	1139327	215792	-

-: Non detect or the value is below reported limit

**Table 3-2. TCE Data Used to Develop Current TCE plume**

WELL_ID	X	Y	TCE (ug/L)
BP-12B	1137808.00	209997.00	8.000
BP-14B	1138073.00	210591.00	50.100
BP-3B	1139436.00	211723.00	0.640
BP-3C	1139446.00	211755.00	13.000
BP-4B	1137813.00	211408.00	5.700
BP-4C	1137813.00	211408.00	8.300
BP-9B	1138518.00	210208.00	3.800
DW-1	1138500.00	215550.00	0.120
EW-10C	1139102.00	216072.00	22.000
EW-11D	1139684.00	215472.00	0.900
EW-12D	1139217.00	215589.00	0.350
EW-13D	1139347.00	216036.00	5.500
EW-14D	1140845.00	213111.00	400.000
EW-1A	1138388.00	215353.00	8.800
EW-1B	1138392.00	215362.00	0.300
EW-1C	1138381.00	215356.00	0.100
EW-2A	1138990.00	215434.00	0.400
EW-2B	1138995.00	215447.00	0.700
EW-2C	1138988.00	215445.00	27.400
EW-2D	1139005.00	215488.00	1.800
EW-3B	1140104.00	214302.00	0.300
EW-3C	1140110.00	214301.00	4.800
EW-4A	1138937.00	215735.00	0.530
EW-4B	1138937.00	215728.00	150.000
EW-4C	1138937.00	215722.00	640.000
EW-4D	1138953.00	215747.00	1.900
EW-5	1138811.00	215530.00	41.000
EW-6C	1138487.00	216171.00	0.540
EW-7C	1138857.00	216155.00	1400.000
EW-7D	1138847.00	216157.00	38.000
EW-9D	1138632.00	216076.00	0.500
EXT-1	1138684.00	215226.00	210.000
EXT-2	1138776.00	215333.00	24.000
EXT-3	1138899.00	215476.00	640.000
MW-06D	1138496.00	214310.00	0.200
MW-10B	1139743.00	214813.00	1.200
MW-10C	1139676.00	214834.00	273.000
MW-10D	1139678.00	214821.00	60.000
OBS-1	1137924.00	212227.00	0.600
SW-1	1138491.00	215550.00	3.200
WT-1	1139327.00	215792.00	0.190



**Table 3-2. TCE Data Used to Develop Current TCE plume (Continued)**

WELL_ID	X_COORDINA	Y_COORDINA	TCE (ug/L)
BP-10B	1138982	209499	-
BP-10C	1138982	209499	-
BP-12A	1137808	209997	-
BP-12C	1137808	209997	-
BP-13B	1136614	209243	-
BP-13C	1136614	209243	-
BP-14C	1138073	210591	-
BP-2A	1137607	213043	-
BP-2B	1137607	213043	-
BP-3A	1139432	211706	-
BP-9C	1138518	210208	-
DW-2	1138799	215542	-
EW-3A	1140105	214282	-
EW-6A	1138479	216175	-
EW-8D	1138323	215999	-
FTC-W-14A	1137092	213482	-
FTC-W-14B	1137082	213486	-
FTC-W-23	1137128	214004	-
FTC-W-31	1137117	213737	-
FTC-W-32	1137020	213810	-
FTC-W-35	1137165	213639	-
FTC-W-4A	1137207	214252	-
FTC-W-4B	1137199	214256	-
FTC-W-7A	1137225	213382	-
FTC-W-7B	1137210	213382	-
FTC-W-7C	1137202	213390	-
FTC-W-7D	1137242	213387	-
FTC-W-9A	1137484	213567	-
FTC-W-9B	1137488	213573	-
LF-1	1137113	214355	-
LF-2	1137938	215192	-
MW-08C	1138634	215202	-
MW-09D	1138788	212994	-
OBS-2	1138767	211944	-
PPW-1	1138492	215820	-
RB-1	1137946	217261	-
RB-1	1137946	217261	-
RW-1	1138101	212732	-
RW-2	1138712	212758	-
RW-3	1139286	212942	-
RW-4	1139748	213178	-
RW-5	1139522	213974	-

--: Non detect or the value is below reported limit

**Table 3-3. 1,1-DCE Data Used to Develop Current 1,1-DCE Plume**

WELL	X	Y	1,1-DCE
BP-14B	1138073	210591	31.70
BP-3C	1139446	211755	1.40
EW-10C	1139102	216072	6.60
EW-13D	1139347	216036	0.33
EW-14D	1140845	213111	42.00
EW-2C	1138988	215445	0.30
EW-4D	1138953	215747	0.35
EW-5	1138811	215530	0.88
EXT-1A	1138684	215226	4.00
EXT-2	1138776	215333	2.80
EXT-3	1138899	215476	12.00
MW-10C	1139676	214834	29.10
MW-10D	1139678	214821	0.34
EW-9D	1138632	216076	0.11
BP-10BC	1138982	209499	-
BP-12ABC	1137808	209997	-
BP-13B	1136614	209243	-
BP-13C	1136614	209243	-
BP-2AB	1137607	213043	-
BP-4BC	1137813	211408	-
BP-9BC	1138518	210208	-
DW-1	1138500	215550	-
DW-2	1138799	215542	-
EW-11D	1139684	215472	-
EW-12D	1139217	215589	-
EW-1A	1138388	215353	-
EW-1B	1138392	215362	-
EW-1C	1138381	215356	-
EW-2A	1138990	215434	-
EW-2B	1138995	215447	-
EW-2D	1139005	215488	-
EW-3A	1140105	214282	-
EW-3B	1140104	214302	-
EW-3C	1140110	214301	-
EW-4A	1138937	215735	-
EW-4B	1138937	215728	-
EW-4C	1138937	215722	-
EW-6A	1138479	216175	-
EW-6C	1138487	216171	-

**Table 3-3. 1,1-DCE Data Used to Develop Current 1,1-DCE Plume  
(Continued)**

WELL	X	Y	1,1-DCE
EW-7C	1138857	216155	-
EW-7D	1138847	216157	-
EW-8D	1138323	215999	-
FTC-W-14A	1137092	213482	-
FTC-W-14B	1137082	213486	-
FTC-W-23	1137128	214004	-
FTC-W-31	1137117	213737	-
FTC-W-32	1137020	213810	-
FTC-W-35	1137165	213639	-
FTC-W-4A	1137207	214252	-
FTC-W-4B	1137199	214256	-
FTC-W-7A	1137225	213382	-
FTC-W-7B	1137210	213382	-
FTC-W-7C	1137202	213390	-
FTC-W-7D	1137242	213387	-
FTC-W-9A	1137484	213567	-
FTC-W-9B	1137488	213573	-
LF-1	1137113	214355	-
LF-2	1137938	215192	-
MW-06D	1138496	214310	-
MW-08C	1138634	215202	-
MW-09D	1138788	212994	-
MW-10B	1139743	214813	-
OBS-1	1137924	212227	-
OBS-2	1138767	211944	-
PPW-1	1138492	215820	-
RB-1	1137946	217261	-
RW-1	1138101	212732	-
RW-2	1138712	212758	-
RW-3	1139286	212942	-
RW-4	1139748	213178	-
RW-5	1139522	213974	-
SW-1	1138491	215550	-
WT-1	1139327	215792	-

--: Non detect or the value is below reported limit

**Table 3-4. Sorption Parameters**

<b>Contaminant</b>	<b>Koc (ml/g)</b>	<b>Kd (ml/g)<sup>2</sup></b>	<b>Retardation Factor (Rf) in Aquifer Material<sup>3</sup></b>
PCE	209 -238 <sup>1</sup>	0.209	2.25
TCE	87 - 150 <sup>1</sup>	0.087	1.52
1,1-DCE	64.6 <sup>1</sup>	0.064	1.38

<sup>1</sup>USEPA 1998

<sup>2</sup> Kd values computed from  $foc \cdot K_{oc}$ , using  $foc=0.001$ .

<sup>3</sup> Rf values for aquifer material computed from  $Rf = 1 + Kd \cdot \rho_b / \rho_e$ , where  $\rho_b=1.8g/cm^3$  (Section 2) and  $\rho_e=0.3$  (Section 1).

## FIGURES

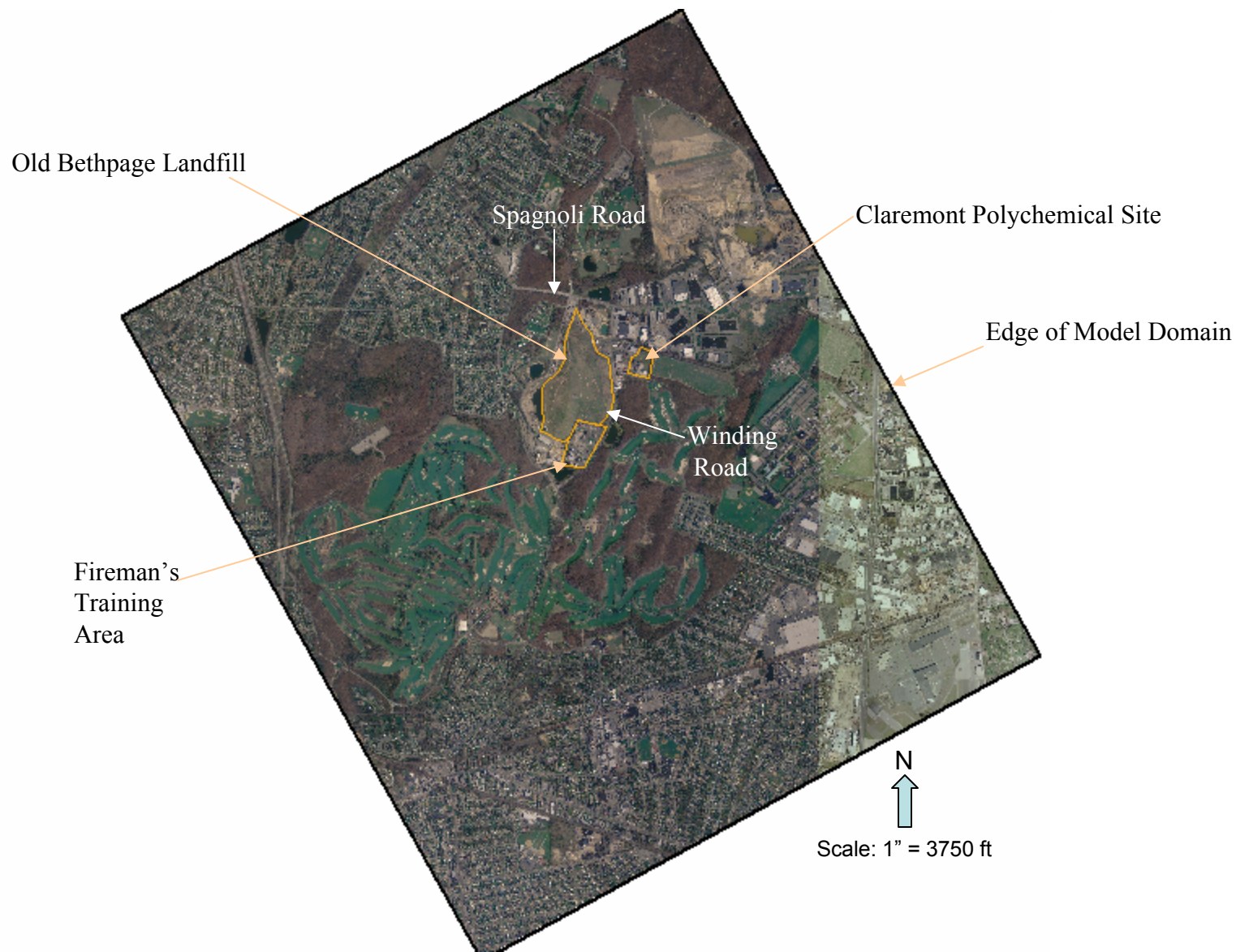


**Figure 2-1. Groundwater Model Domain**  
(model grid is 25 ft by 25 ft)

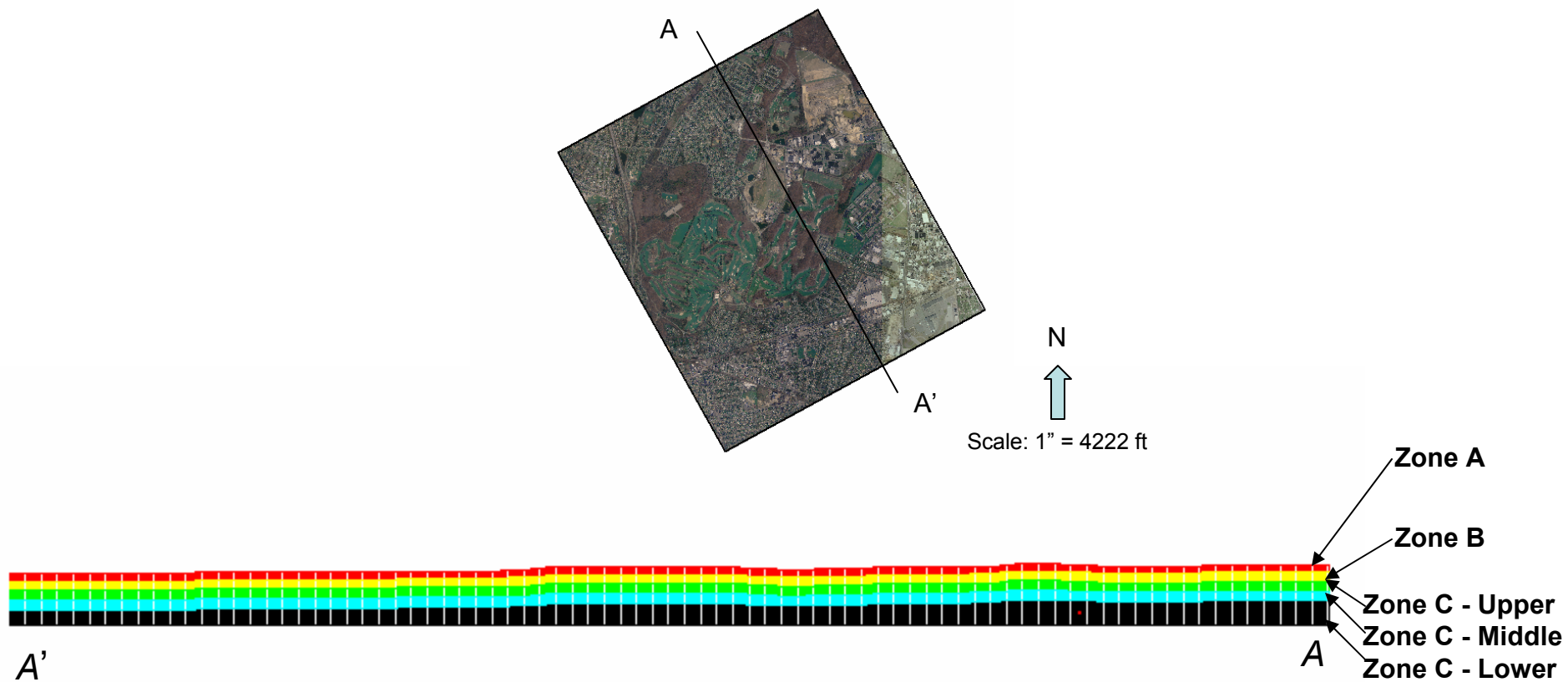
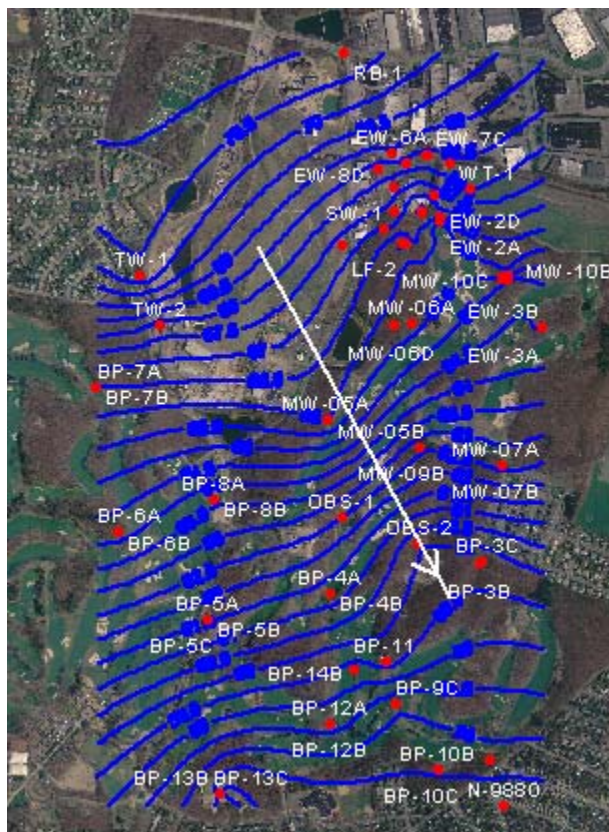
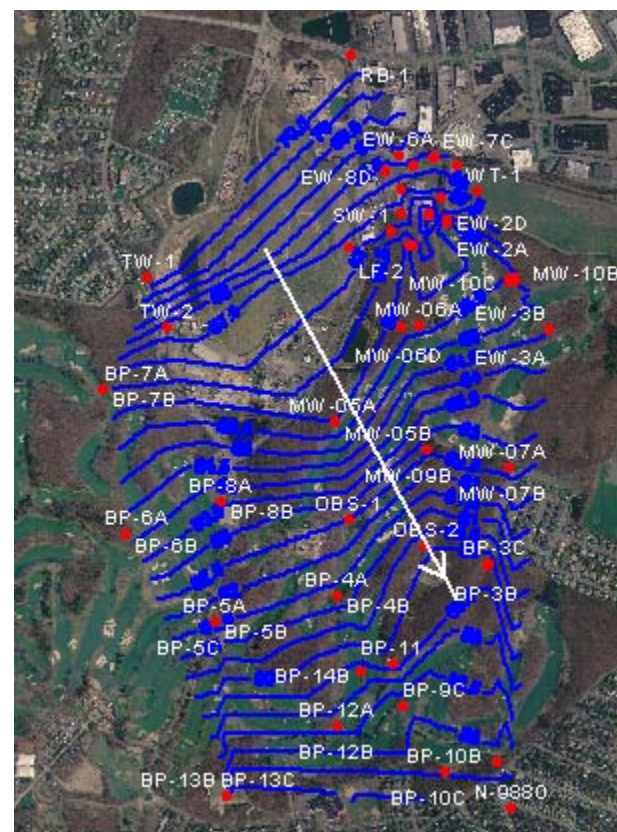


Figure 2-2. Vertical Discretization of the Model





Groundwater contour map plotted by kriging the March 2006 water level (contour interval =  $\frac{1}{2}$  ft)



Groundwater contour map plotted by trigulation with linear interpolation method for the March 2006 water level data (contour interval =  $\frac{1}{2}$  ft)



Scale: 1" = 2083 ft

Figure 2-3. Groundwater Counter Map and Principal Flow Direction Based on March 2006 Observed Water Level



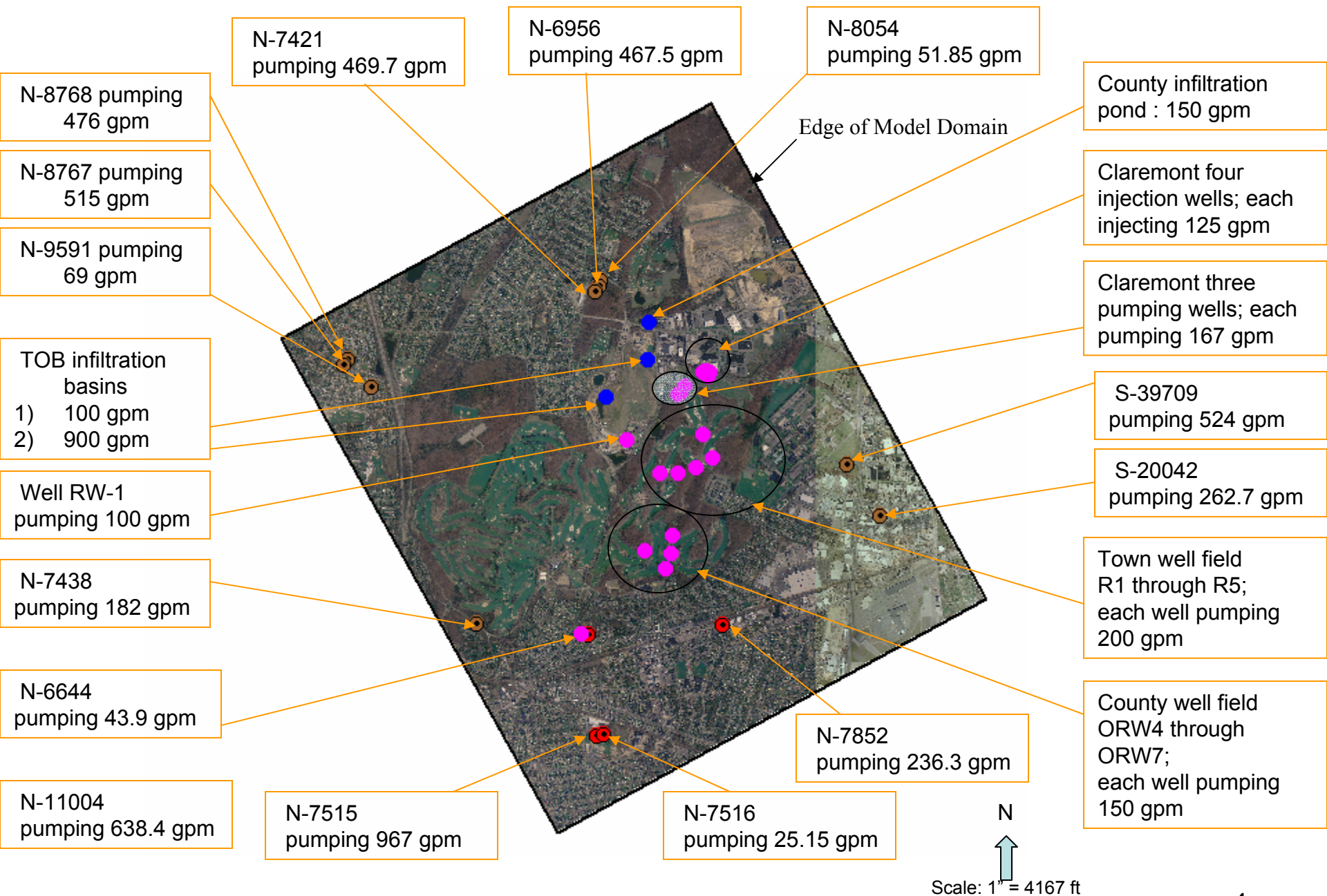


**Figure 2-4. Injection Wells, Pumping Wells, and Infiltration Basins Within the Model Domain**

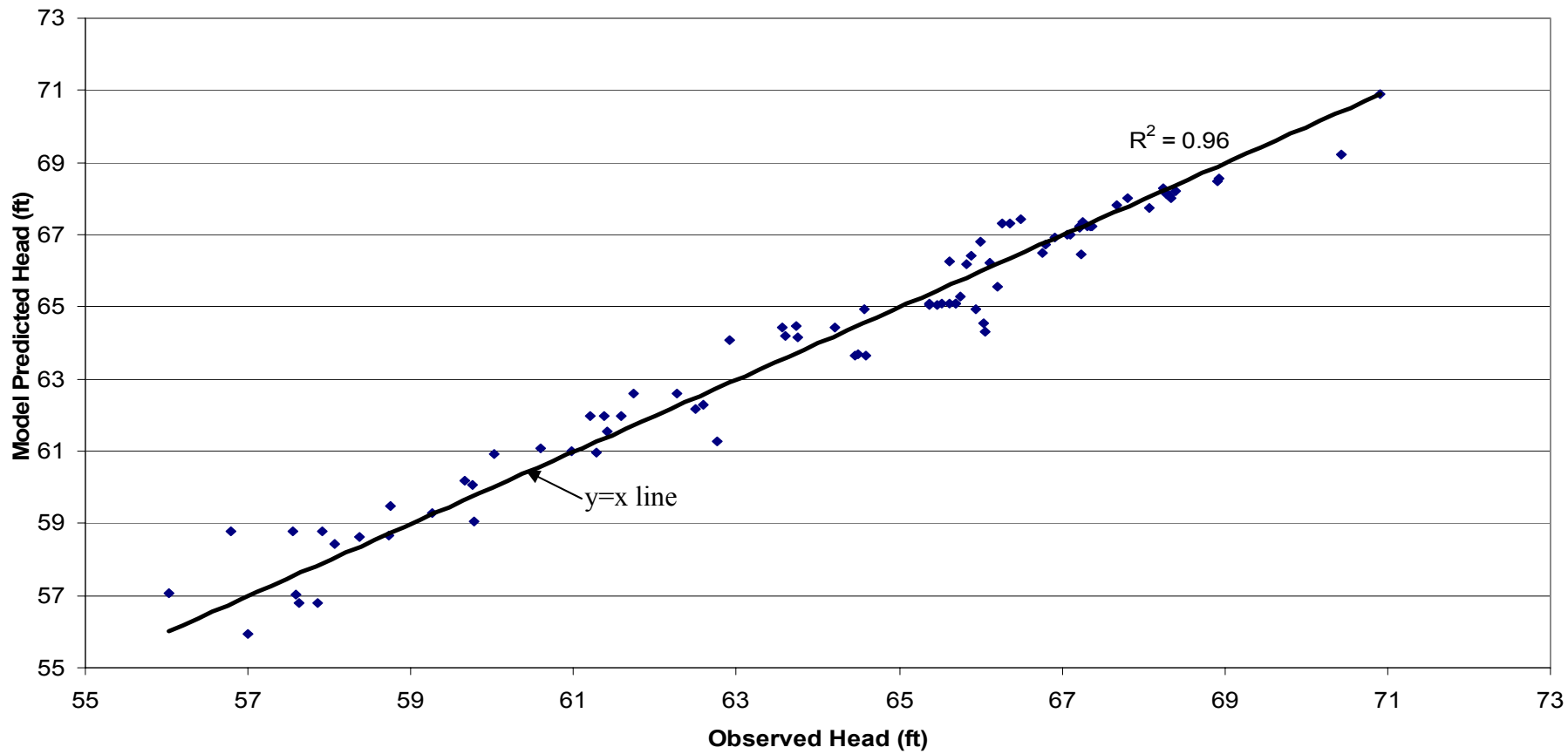


Figure 2-5. Observed Versus Model Predicted Head – March 2006







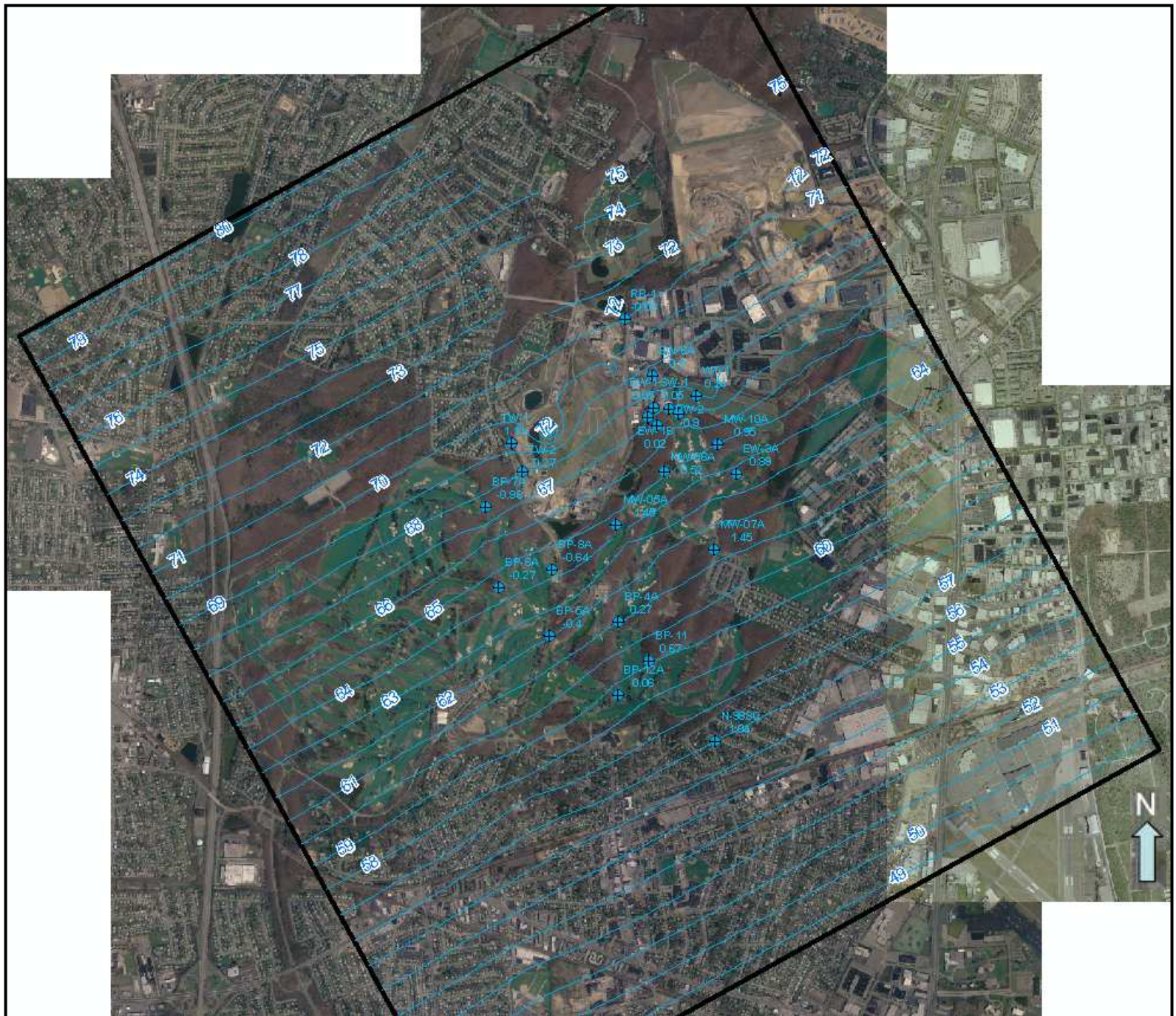


Figure 2-7. Model Predicted Groundwater Head at Zone A



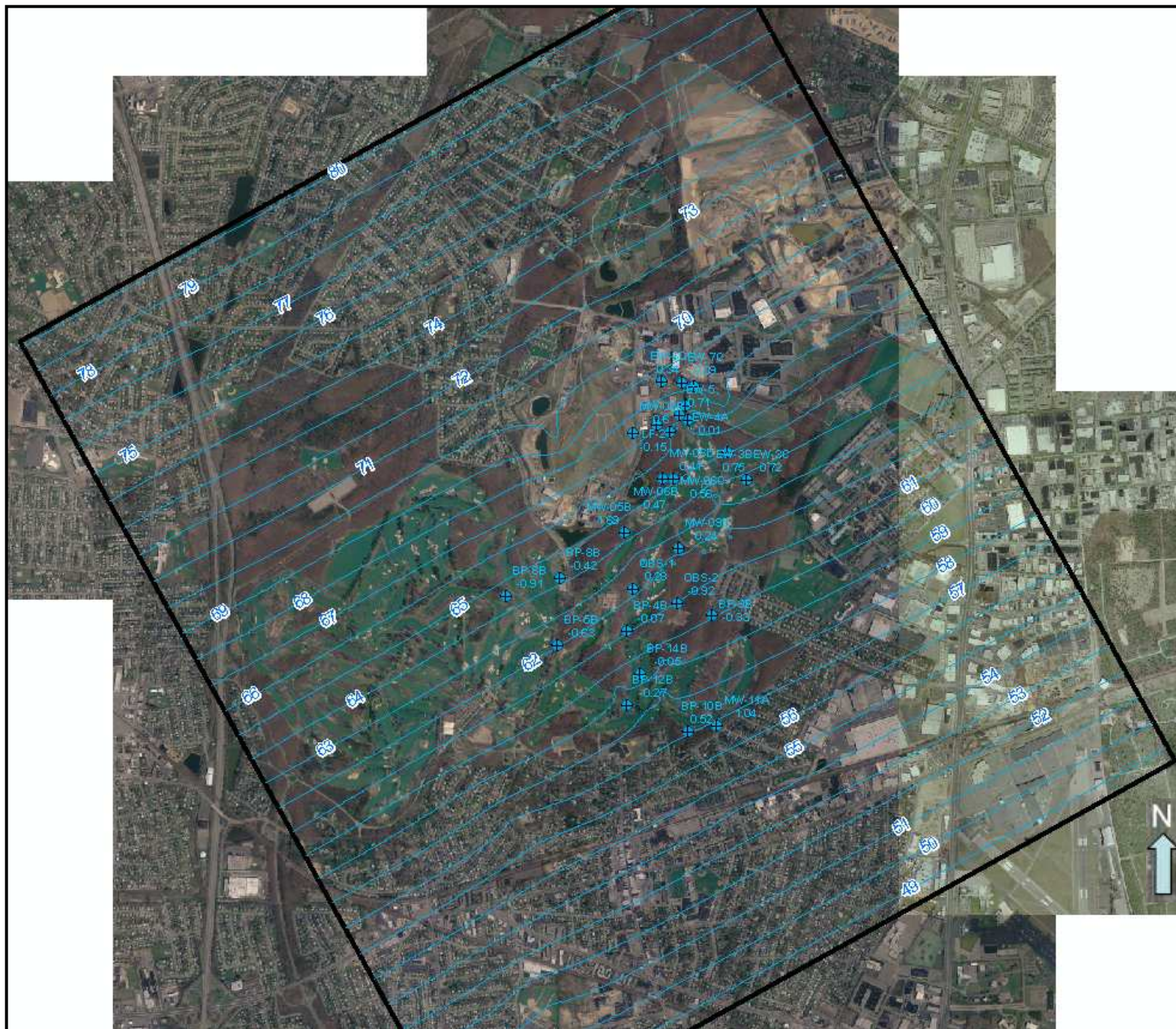
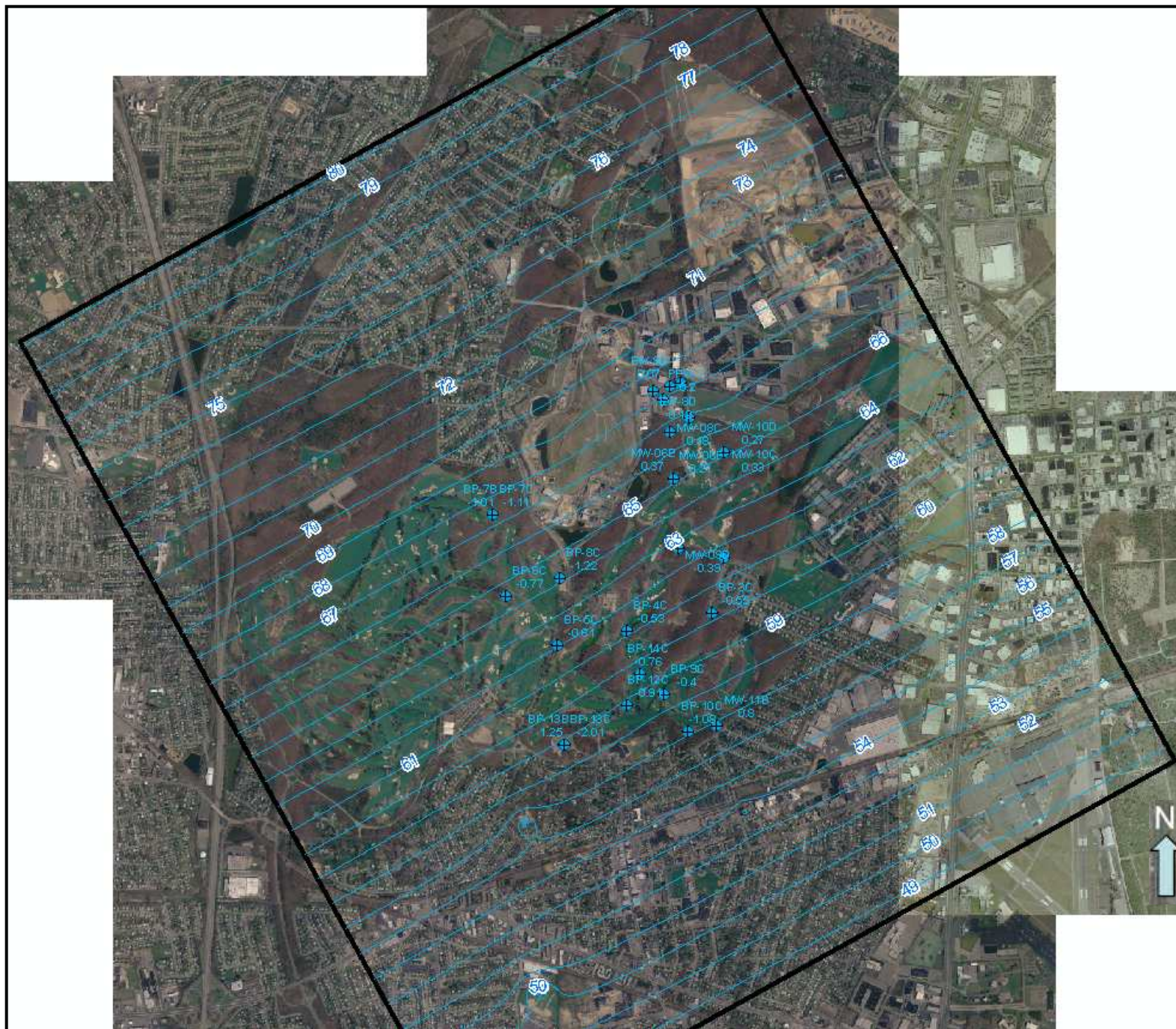


Figure 2-8. Model Predicted Groundwater Head at Zone B







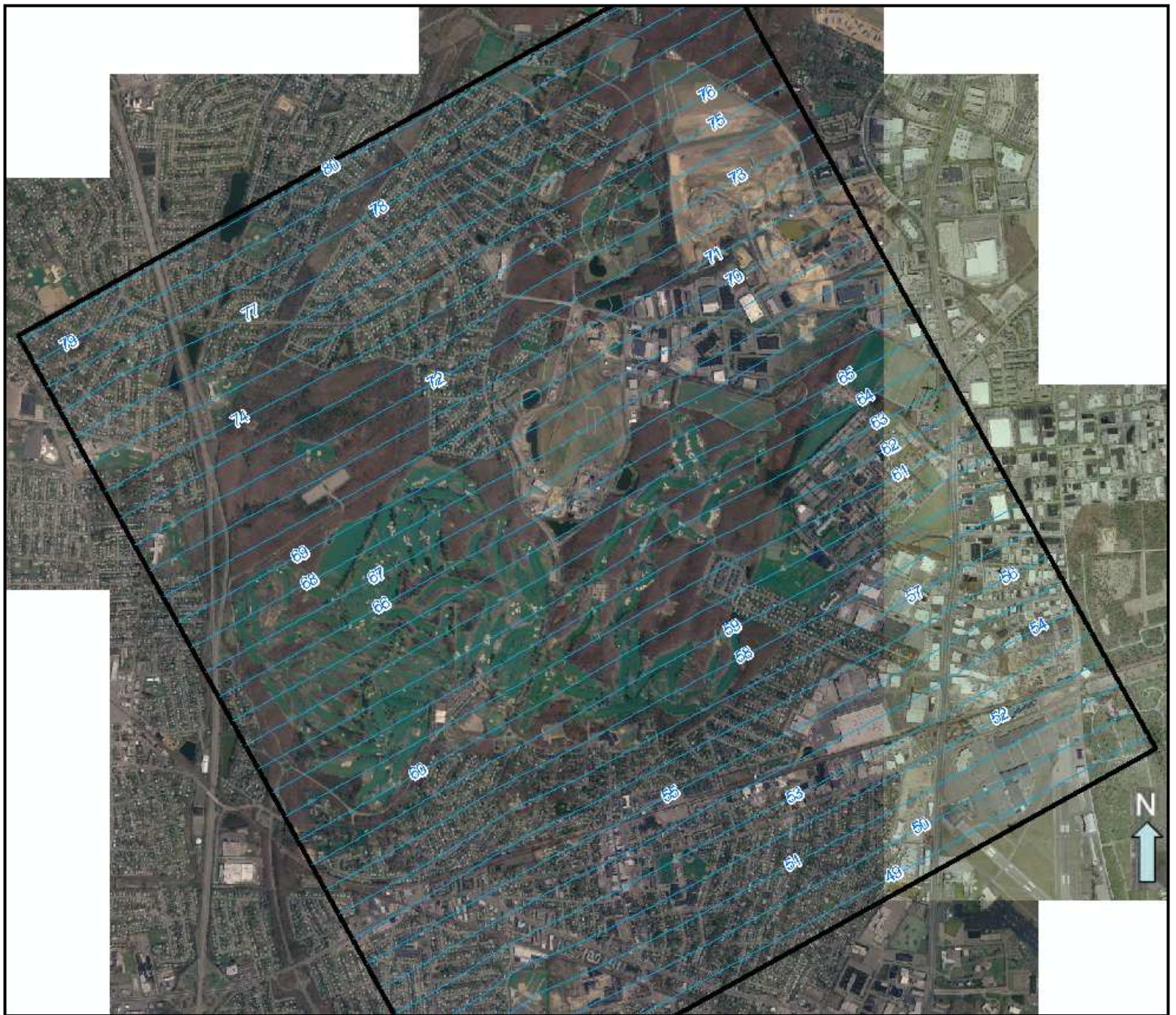


Figure 2-10. Model Predicted Groundwater Head at Zone C-Middle



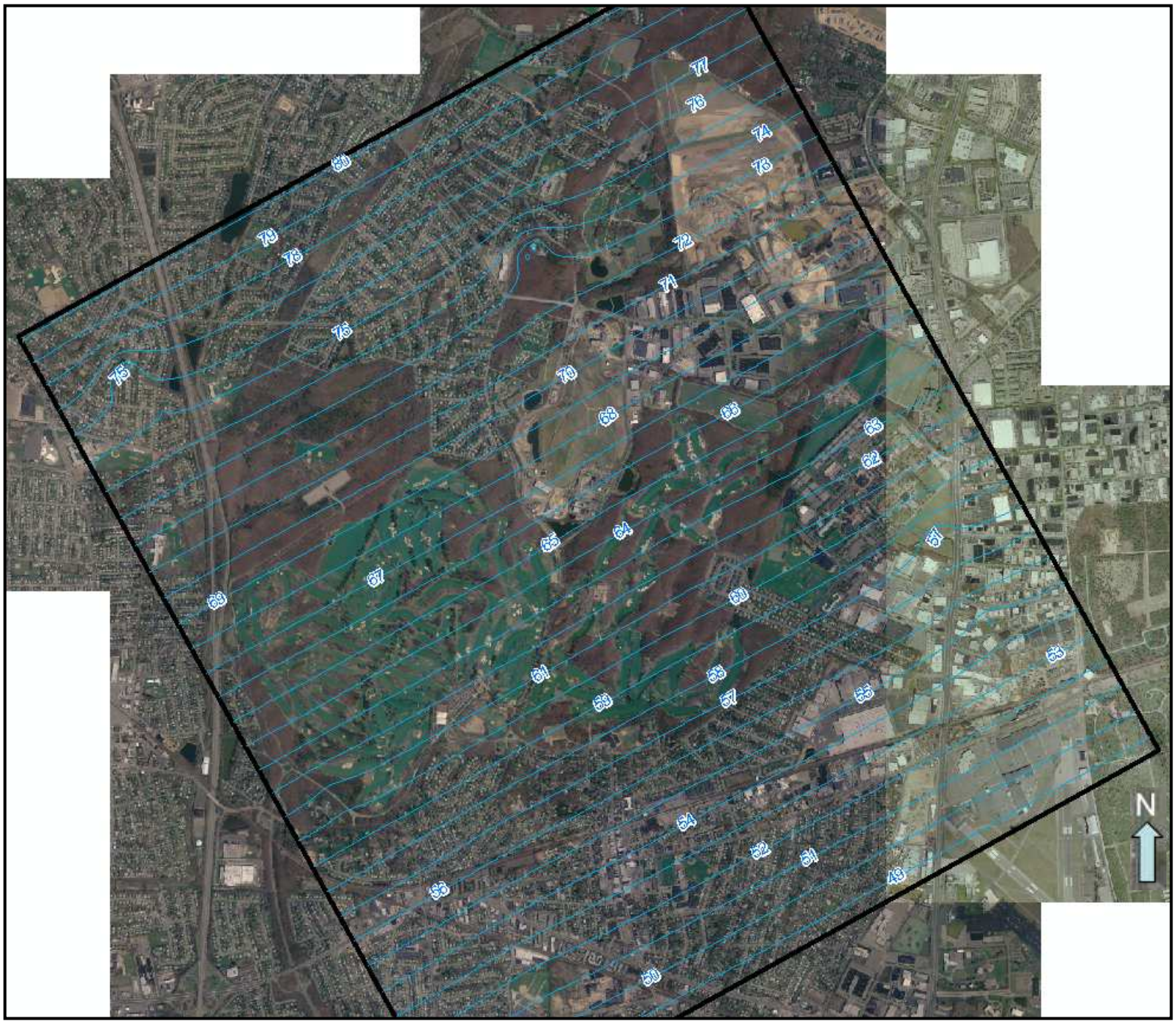
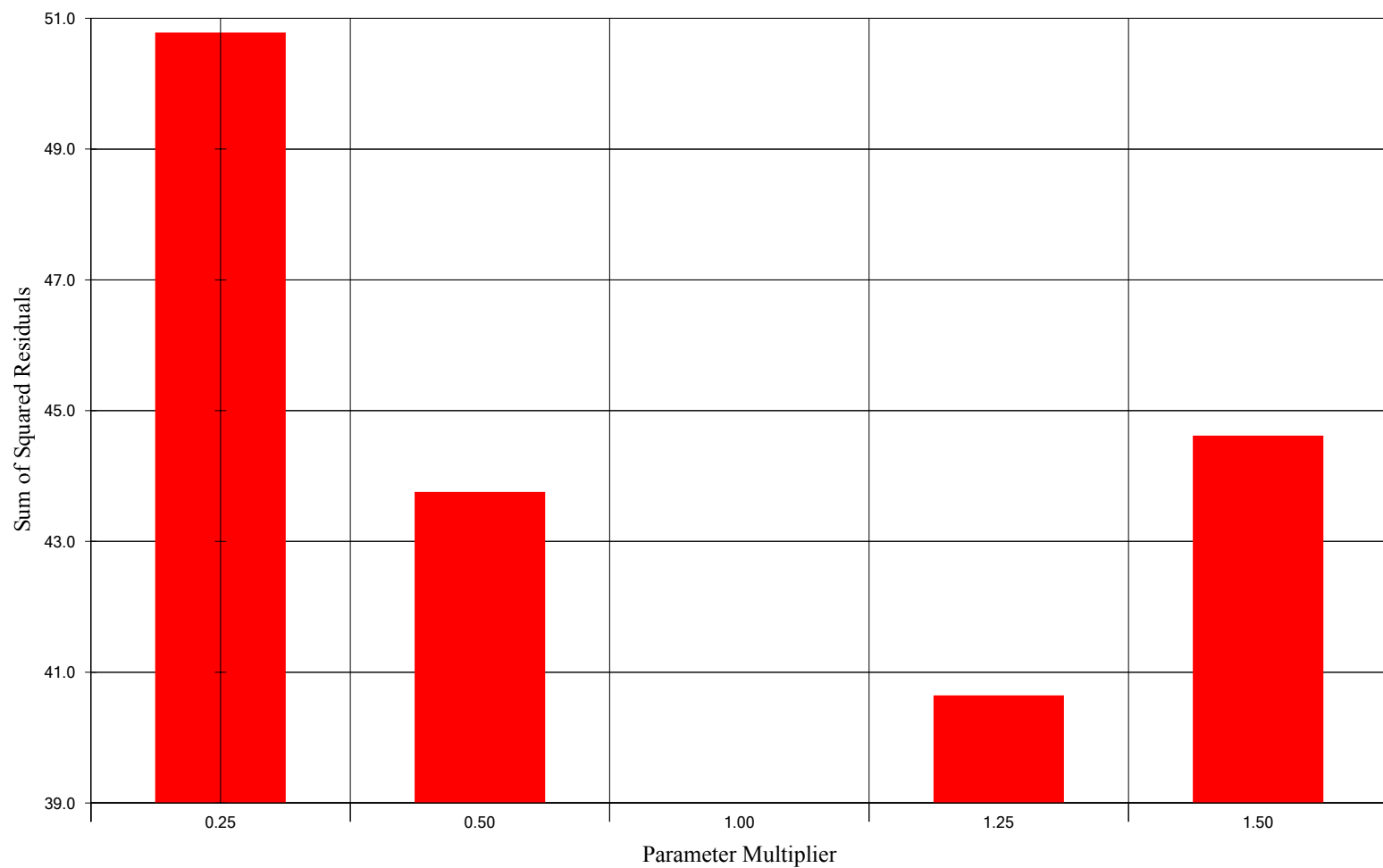
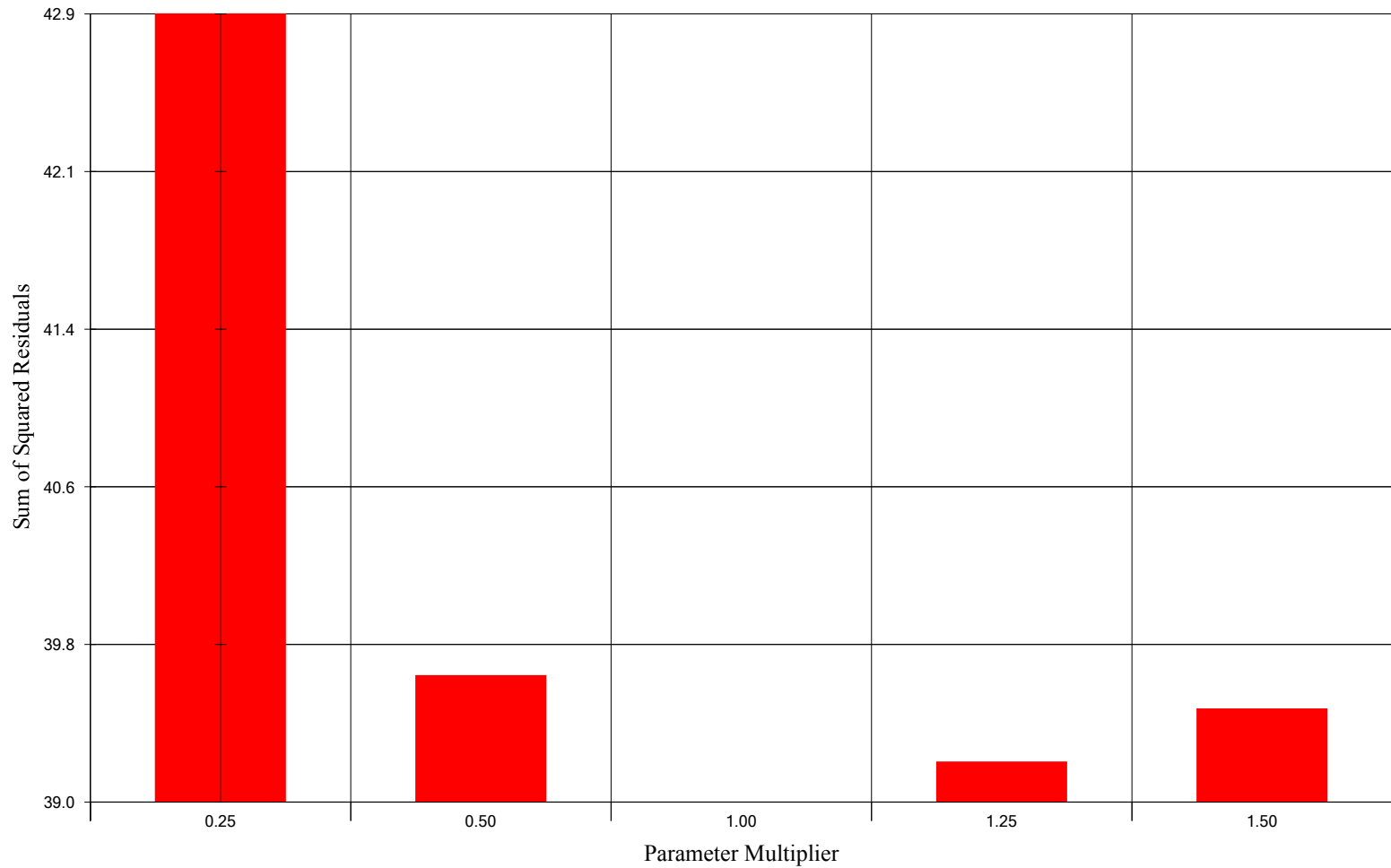


Figure 2-11. Model Predicted Groundwater Head at Zone C-Lower





**Figure 2-12. Sensitivity Analysis for Zone "A" Hydraulic Conductivity ( $K_x = K_y = 282$  ft/day)**



**Figure 2-13.Sensitivity Analysis for Zone "B" Hydraulic Conductivity ( $K_x = K_y = 125$  ft/day)**

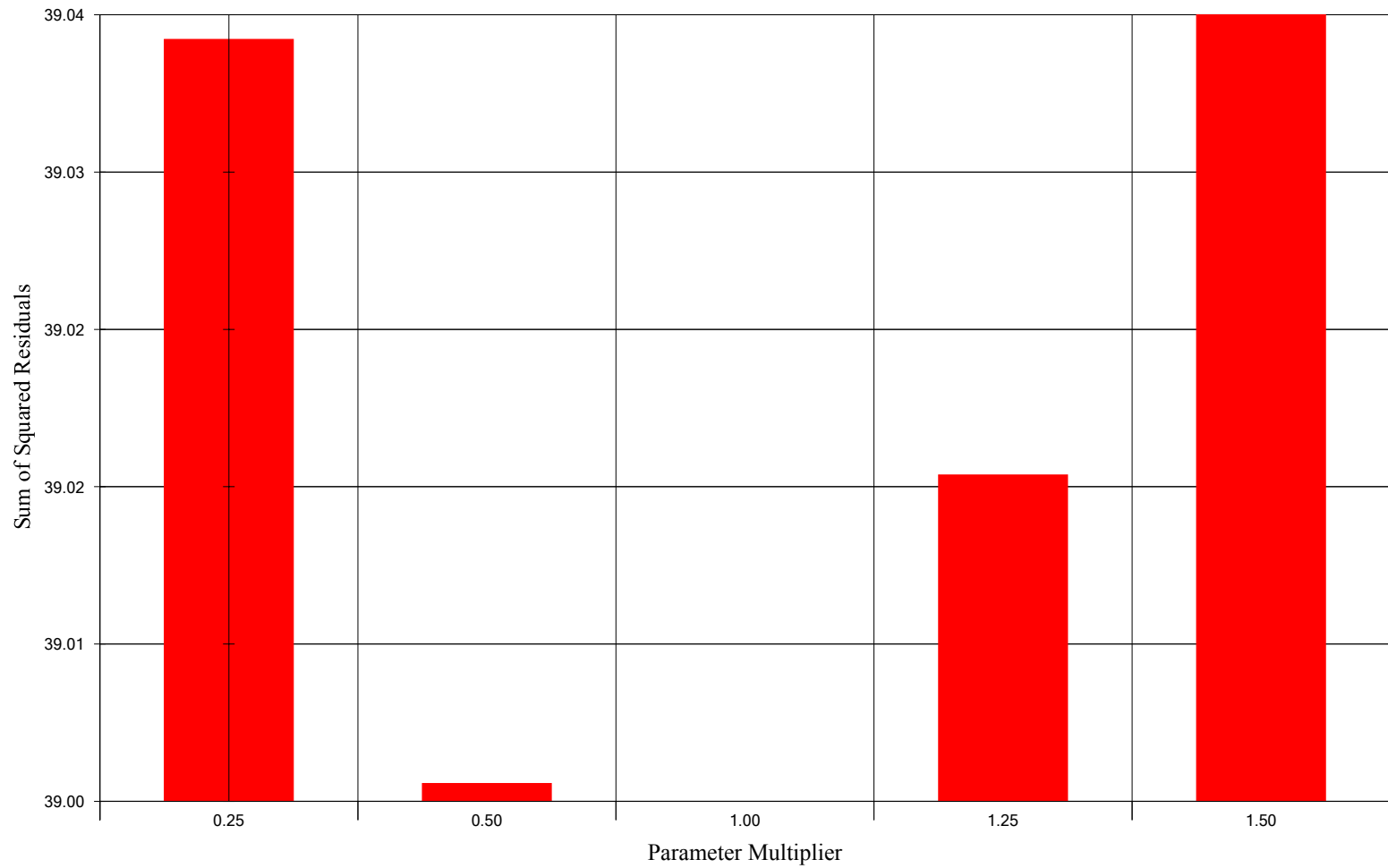


**Figure 2-14.Sensitivity Analysis for Zone "C -Upper" Hydraulic Conductivity ( $K_x = K_y = 135$  ft/day)**

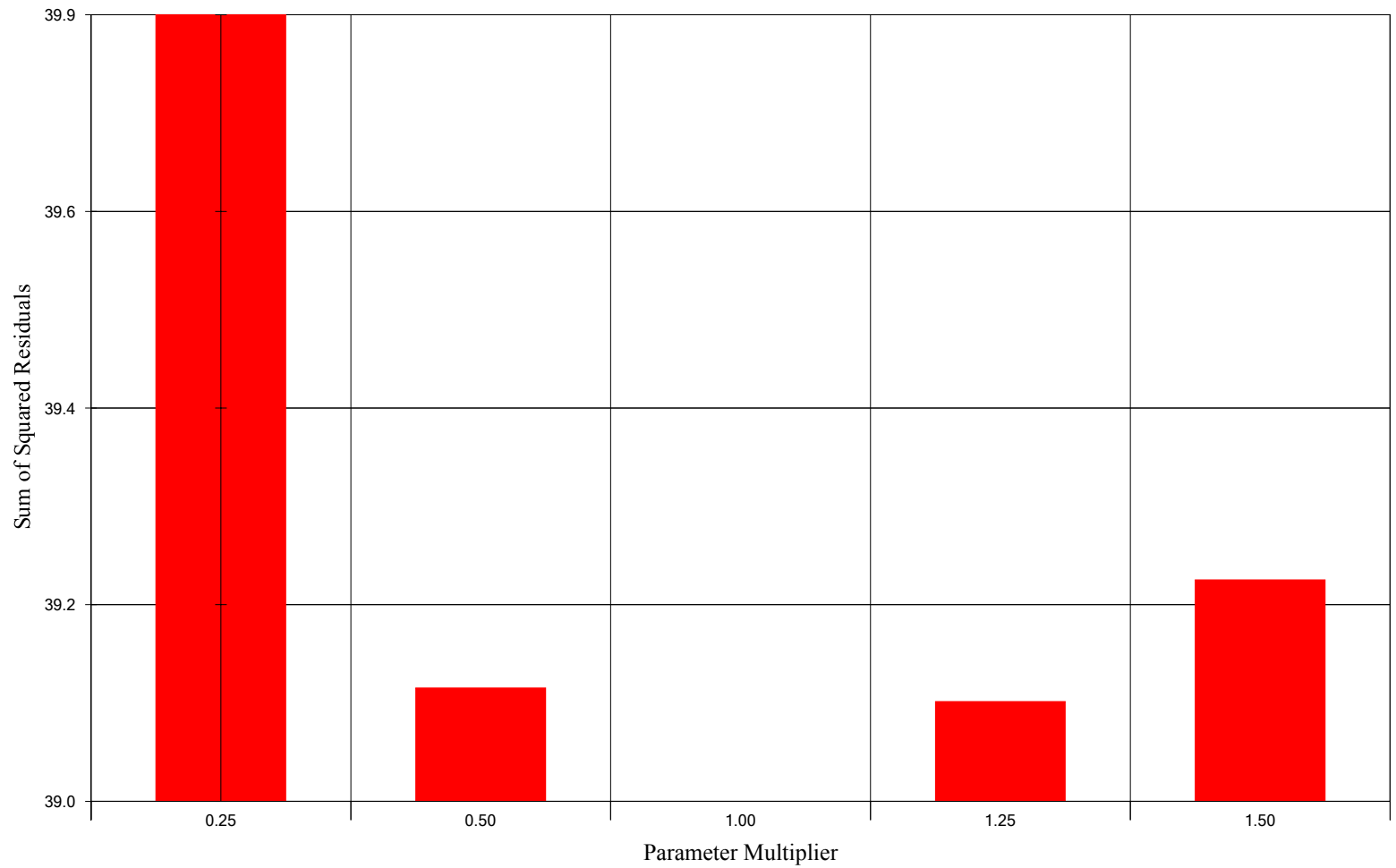


**Figure 2-15. Sensitivity Analysis for Zone "C - Middle" Hydraulic Conductivity ( $K_x = K_y = 690$  ft/day)**

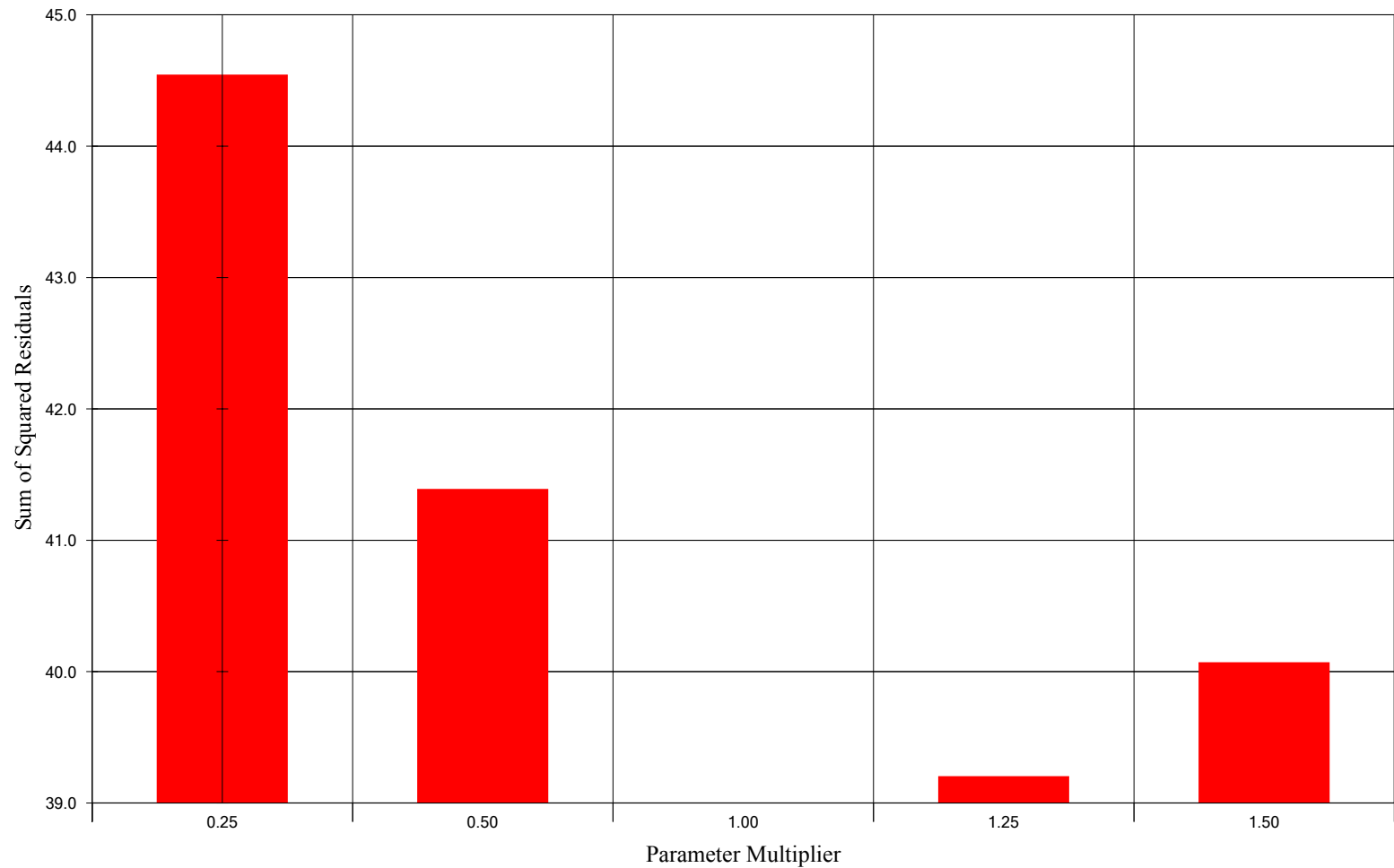


**Figure 2-16. Sensitivity Analysis for Zone "C -Lower" Hydraulic Conductivity ( $K_x = K_y = 98$  ft/day)**

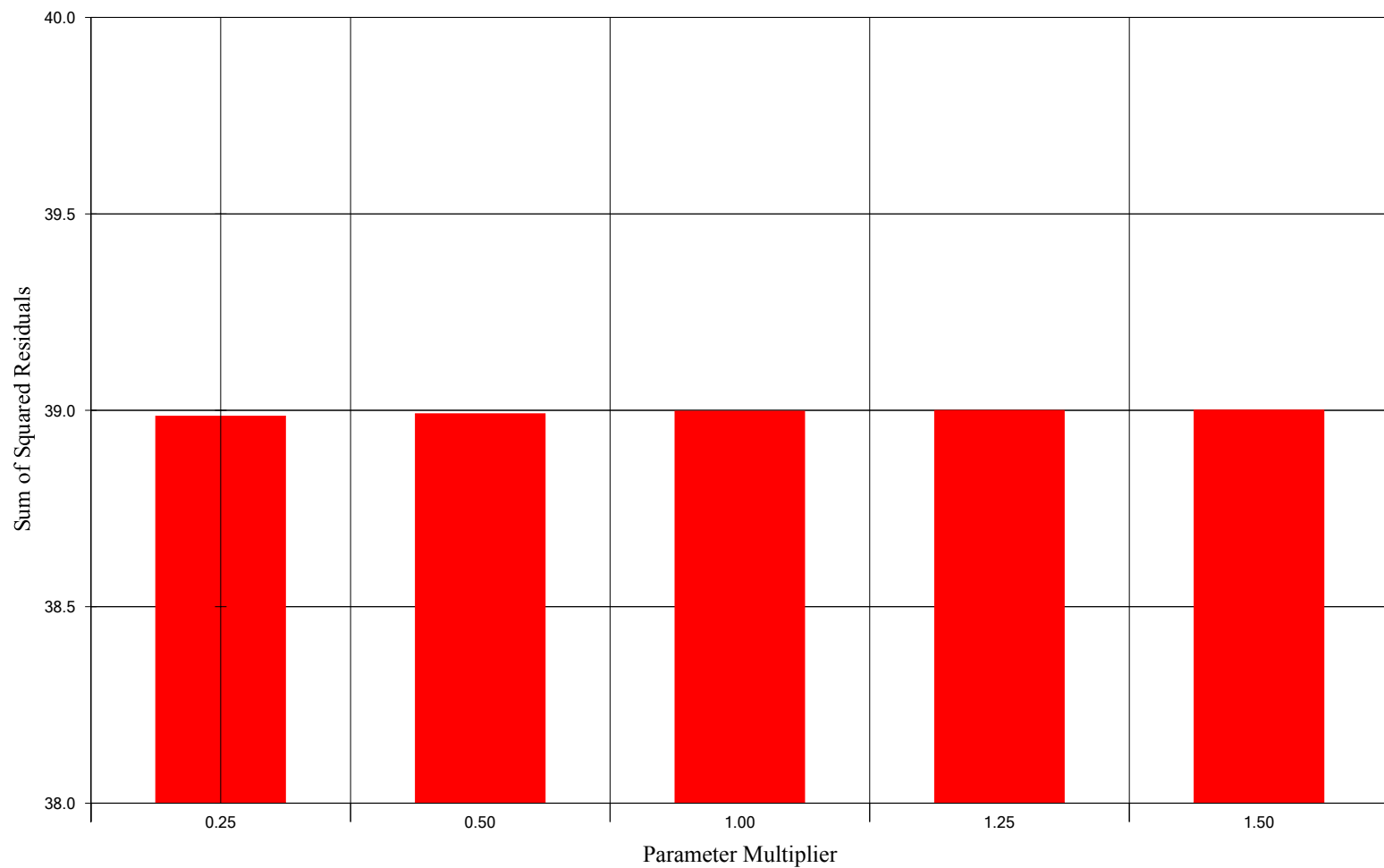


**Figure 2-17. Sensitivity Analysis for Zone "A" Hydraulic Conductivity ( $K_z = 28.2$  ft/day)**

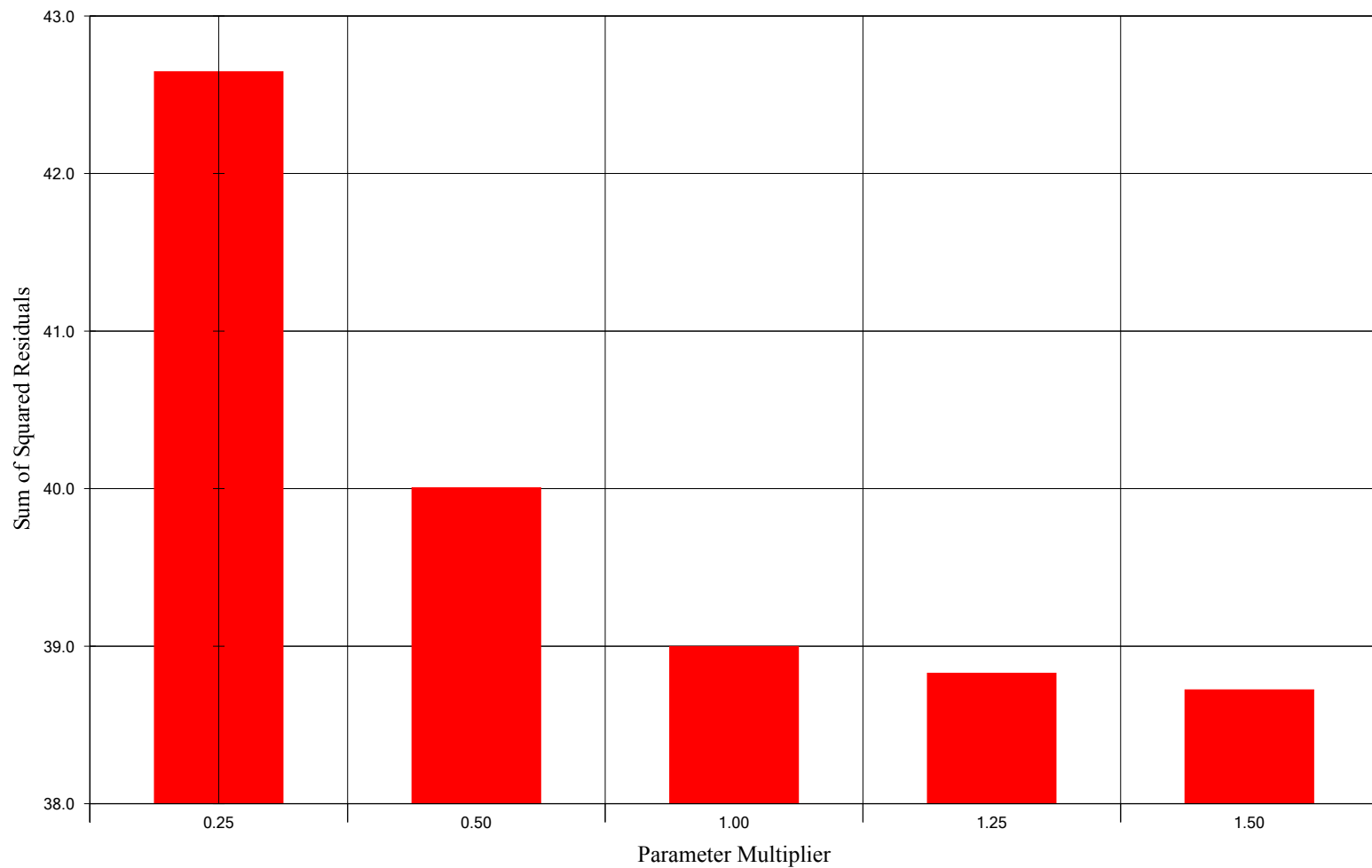


**Figure 2-18. Sensitivity Analysis for Zone "B" Hydraulic Conductivity ( $K_z = 12.5$  ft/day)**

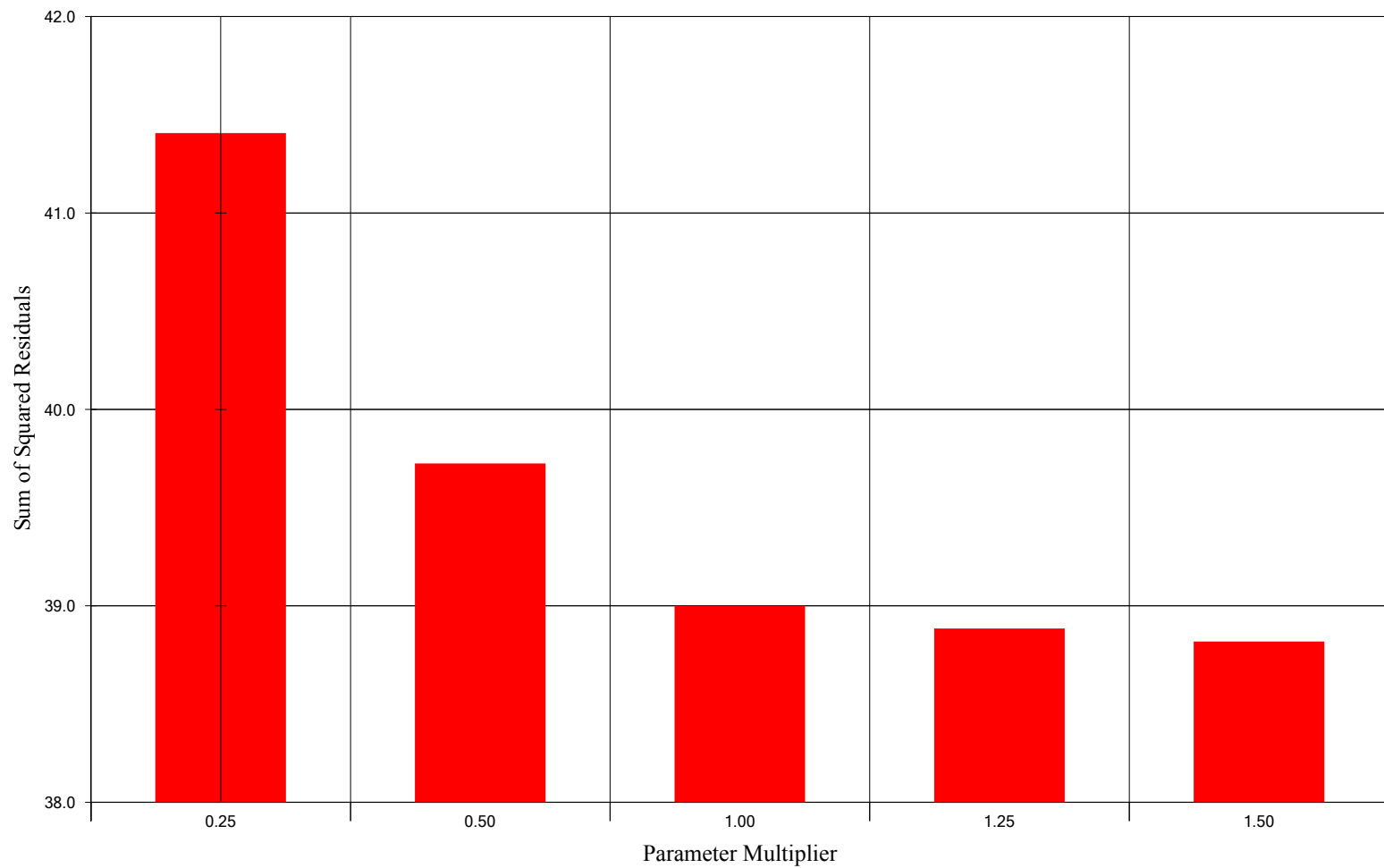


**Figure 2-19. Sensitivity Analysis for Zone "C-Upper" Hydraulic Conductivity ( $K_z = 13.5$  ft/day)**



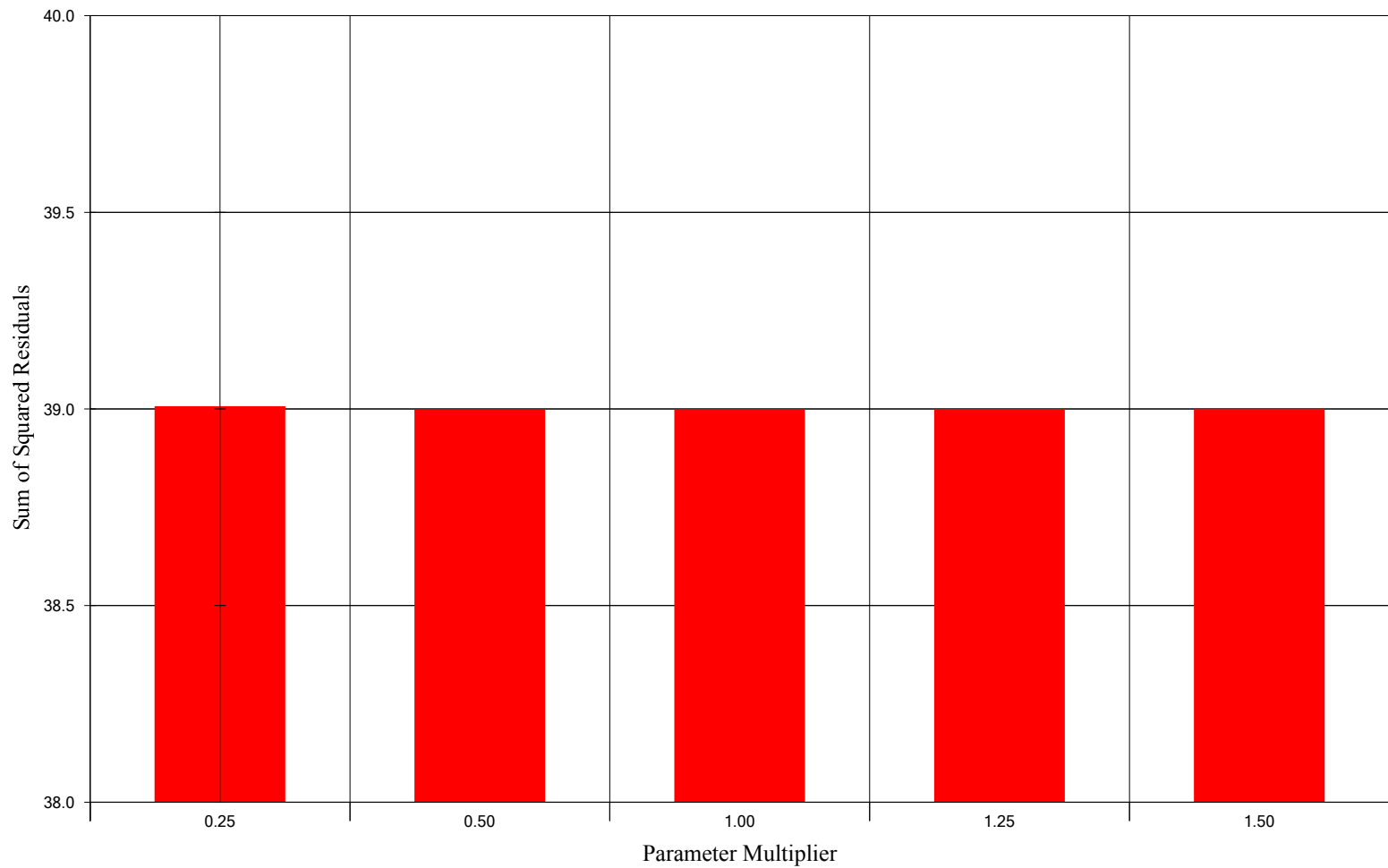


**Figure 2-20. Sensitivity Analysis for Zone "C-Middle" Hydraulic Conductivity ( $K_z = 69.0$  ft/day)**

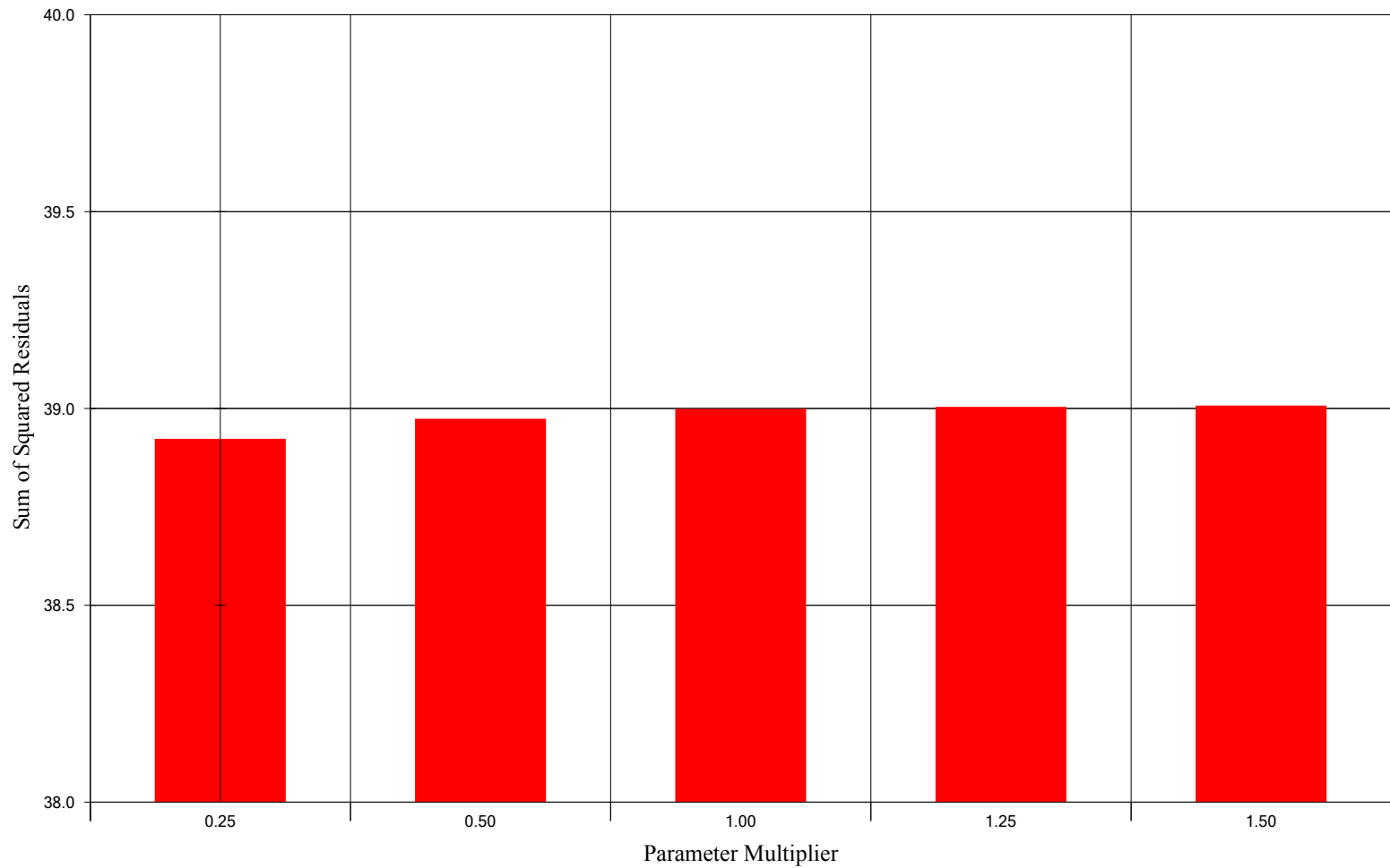


**Figure 2-21. Sensitivity Analysis for Zone "C-Lower" Hydraulic Conductivity ( $K_z = 9.8$  ft/day)**

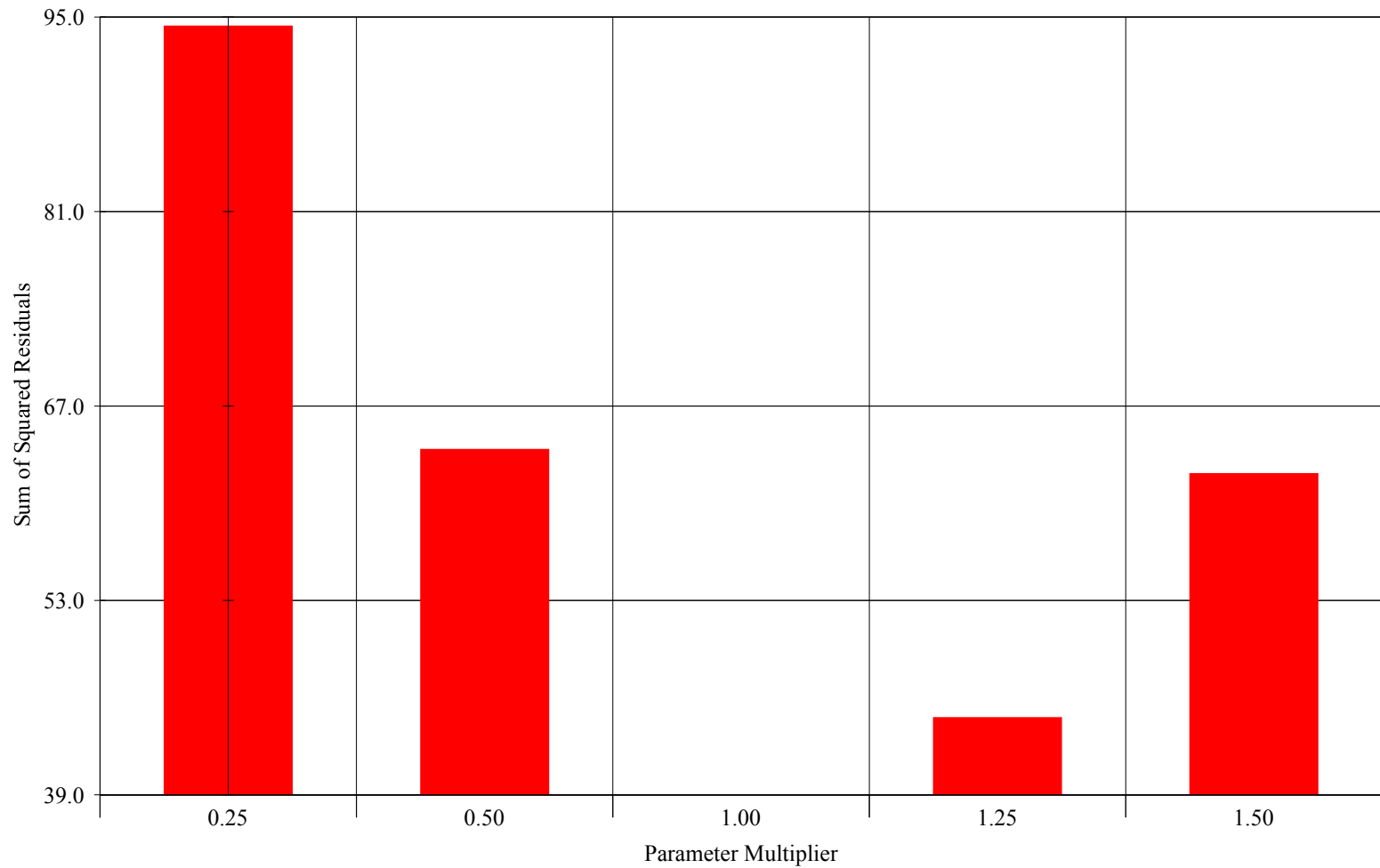


**Figure 2-22. Sensitivity Analysis for Groundwater Recharge (Recharge = 20.58 inch per year)**

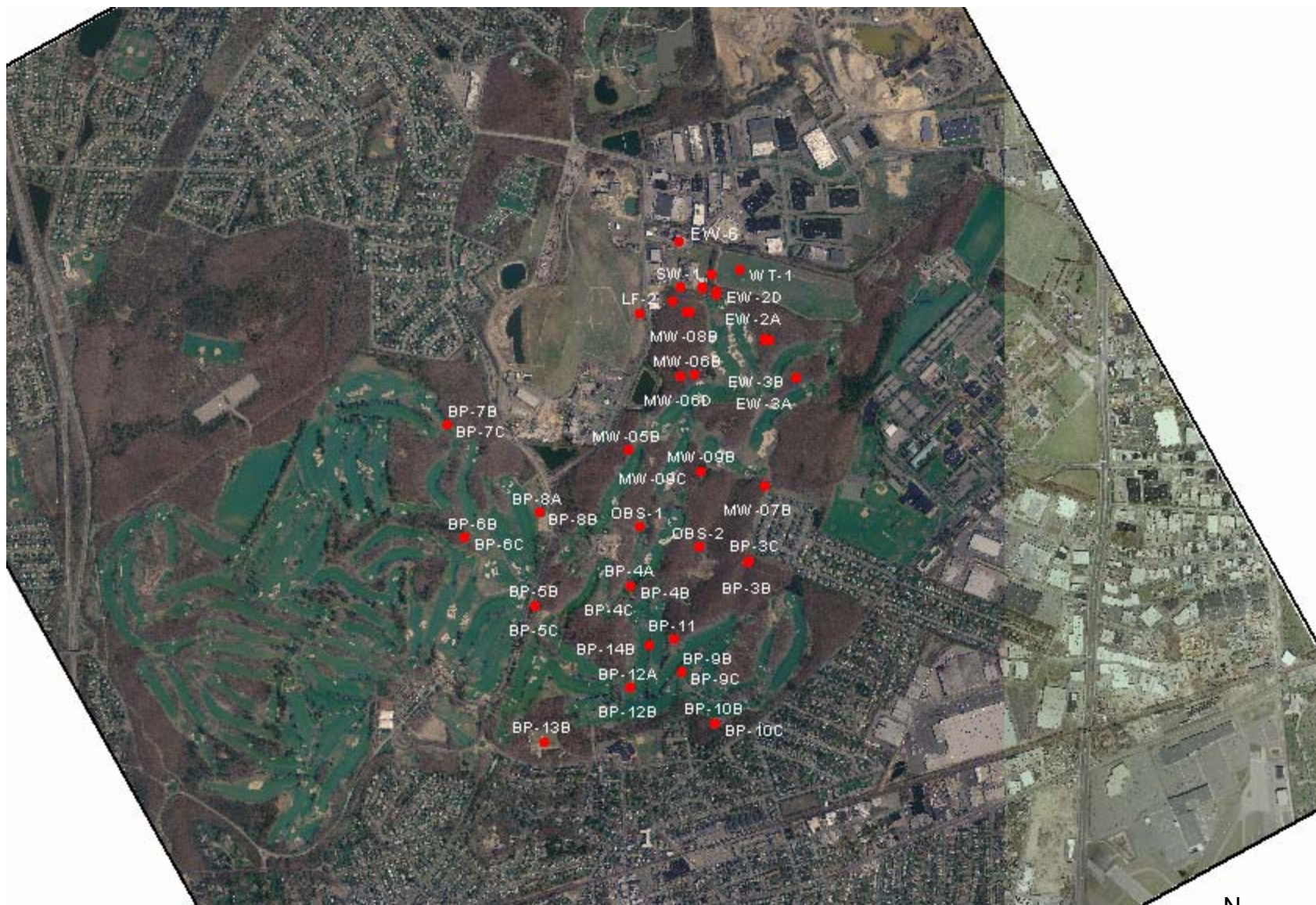


**Figure 2-23. Well Locations for Blind Test Data**



Scale: 1" = 2083 ft

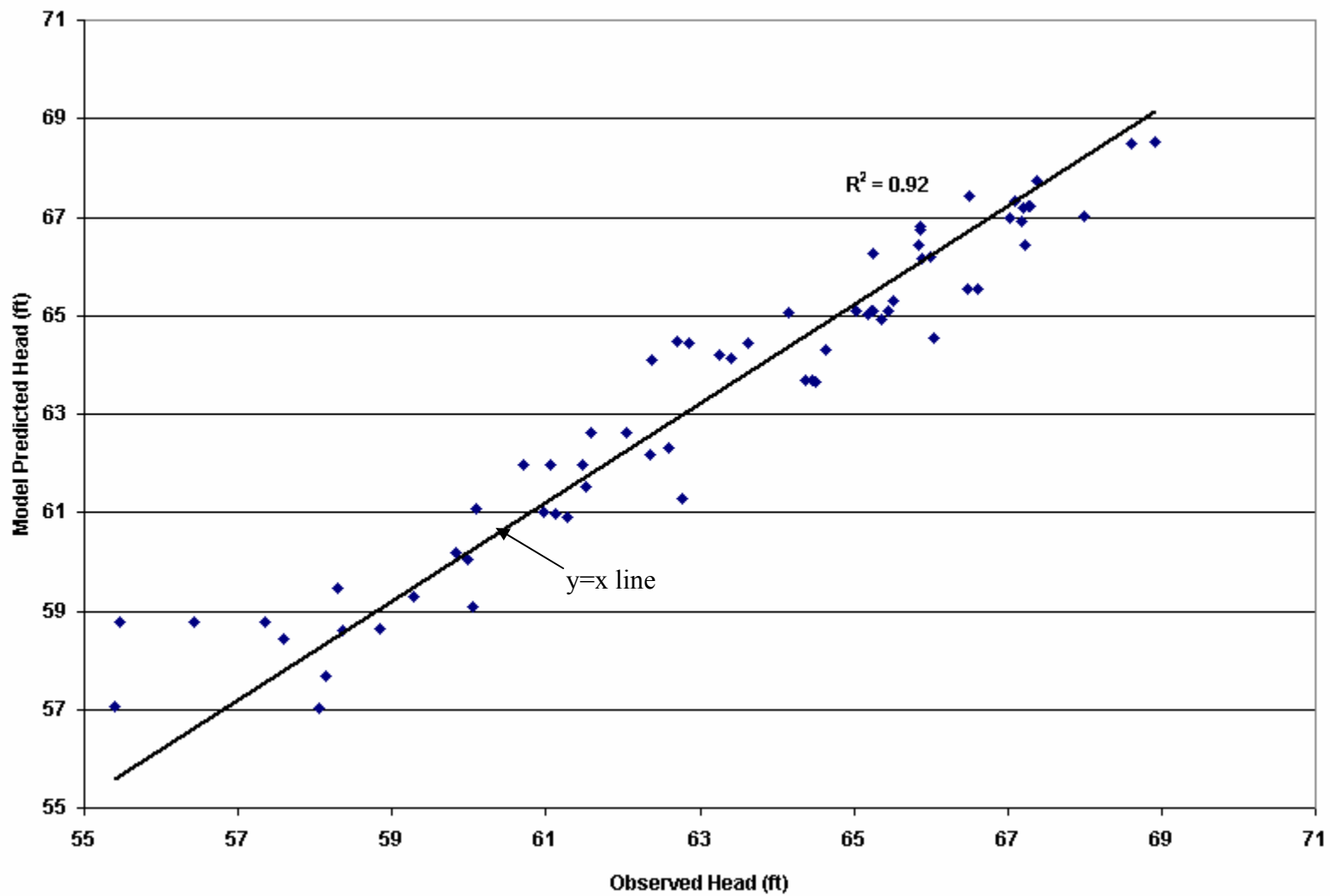
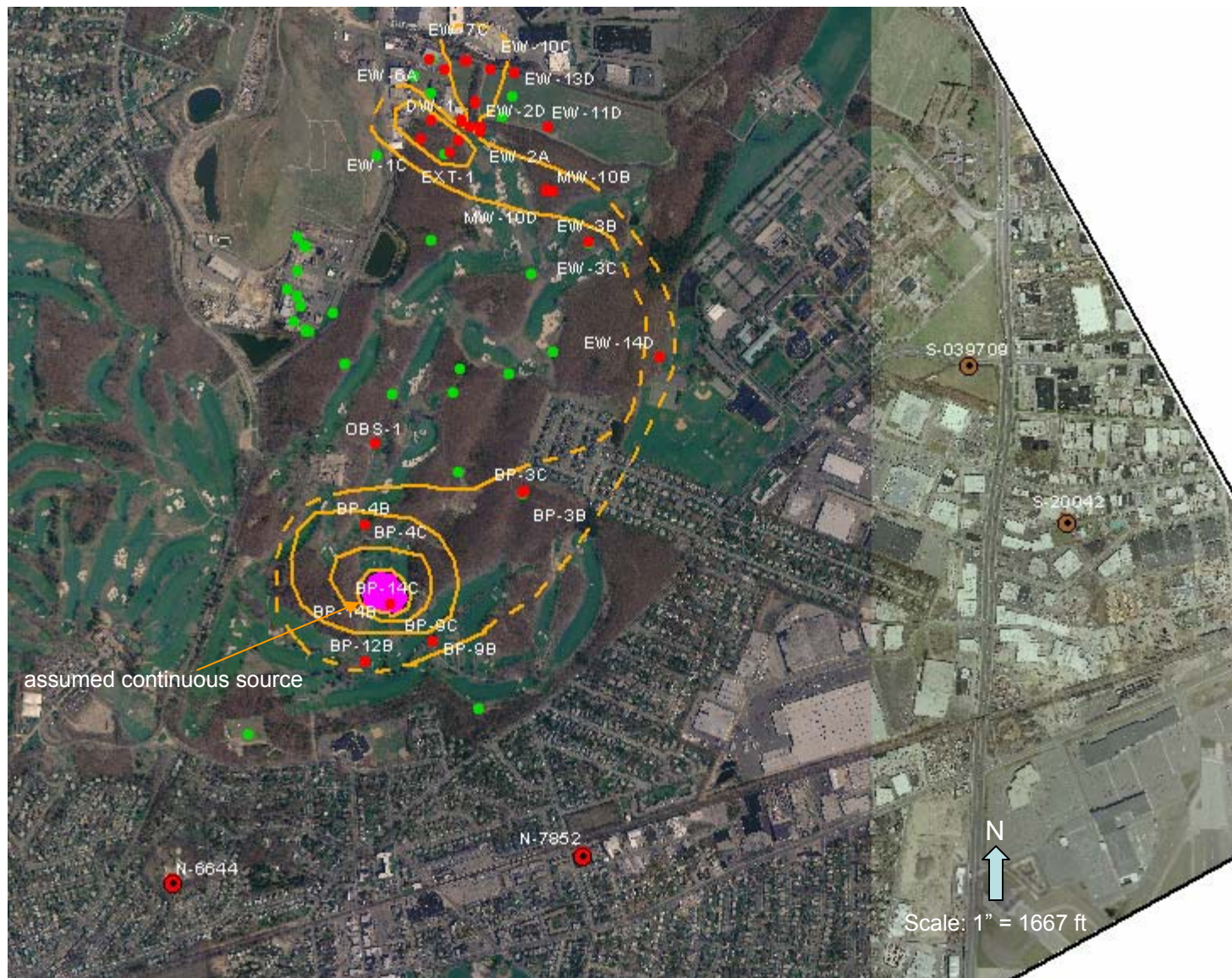


Figure 2-24. Simulated Head versus Observed Head for Blind Test Data





**Figure 3-1. PCE Plume Map**  
**Contour Interval = 5, 50, 100, and 500 ug/L**



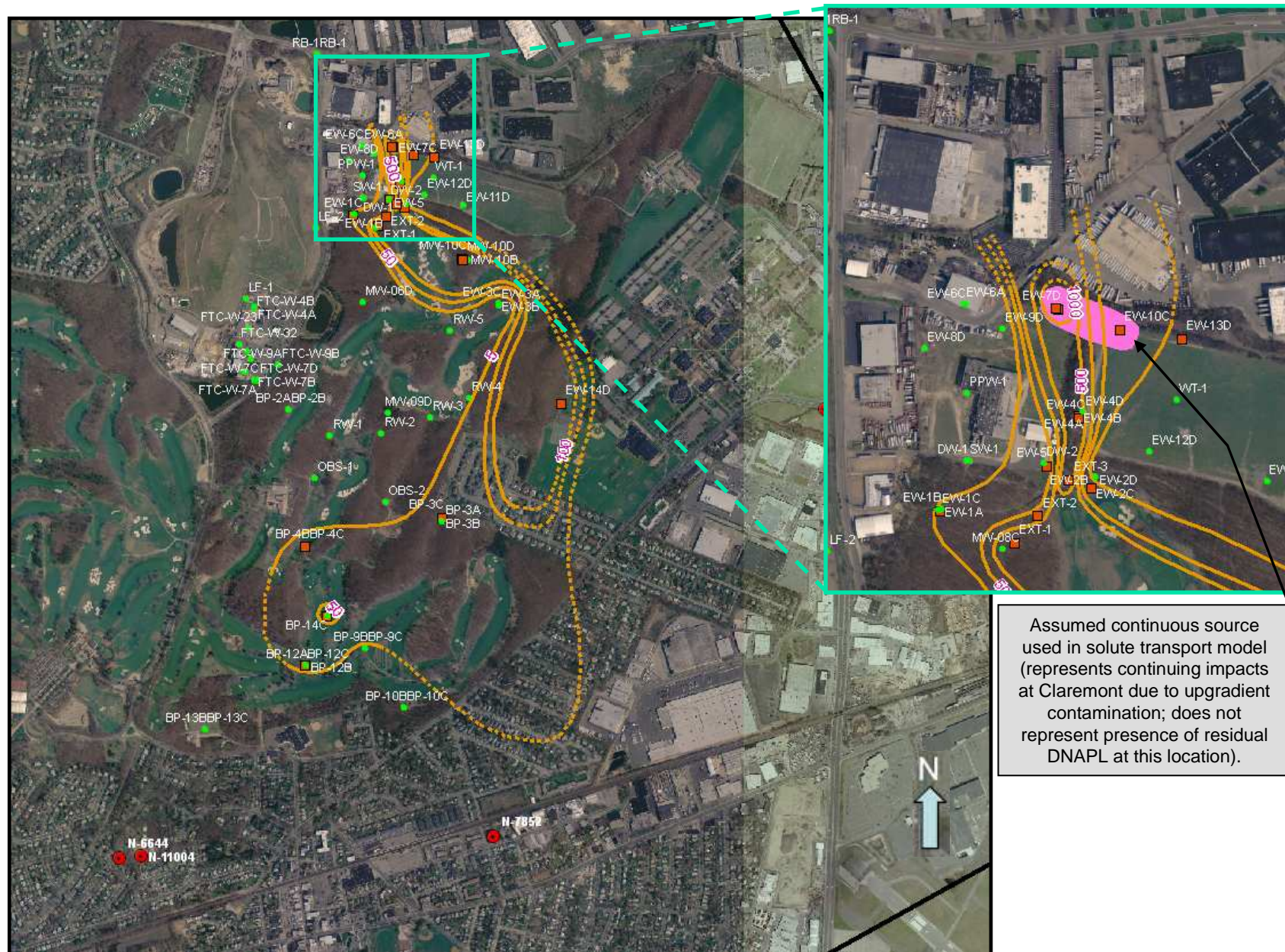
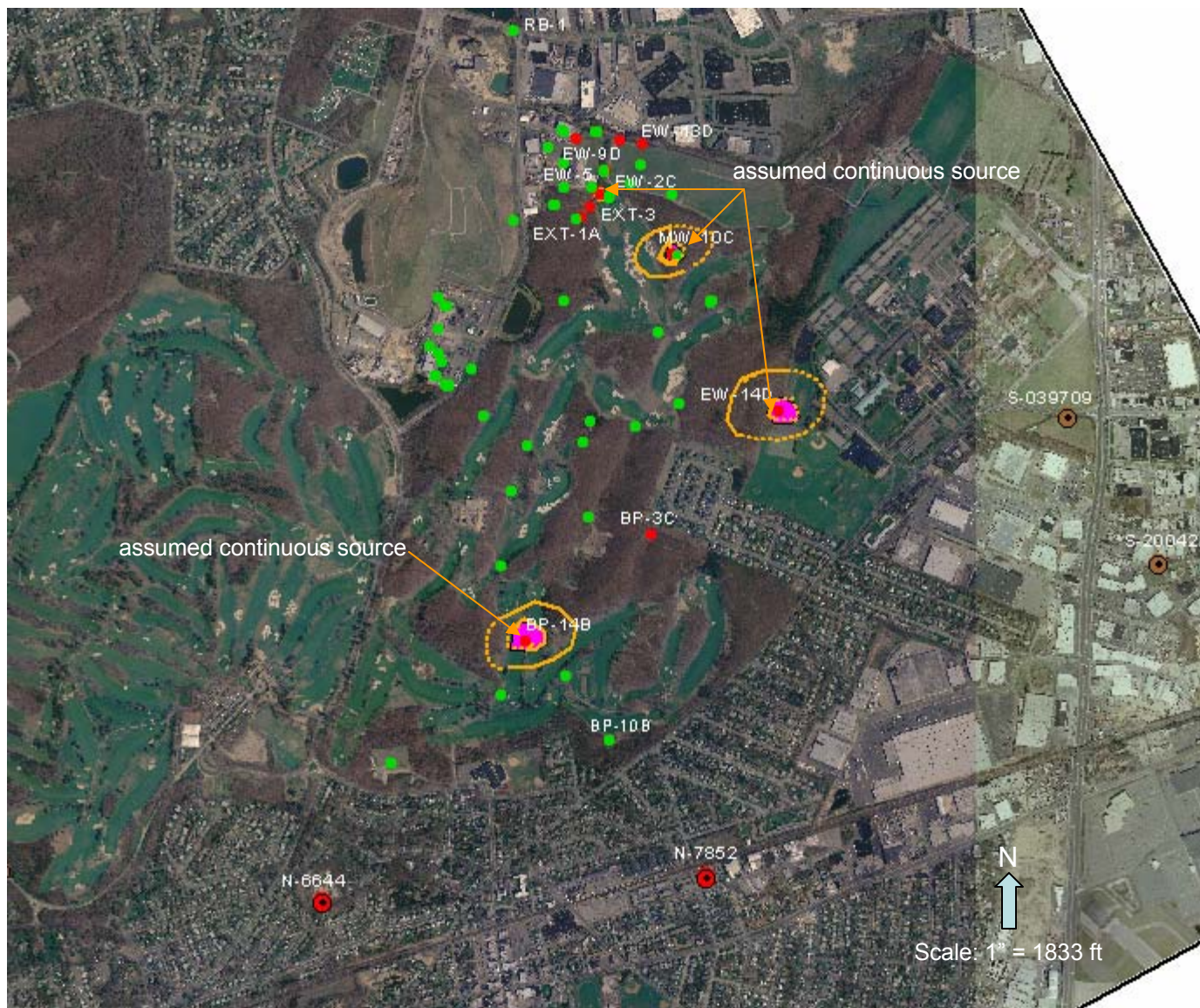


Figure 3-2. TCE Plume Map  
Contours 5, 50, 100, 500, and 1000 mg/L

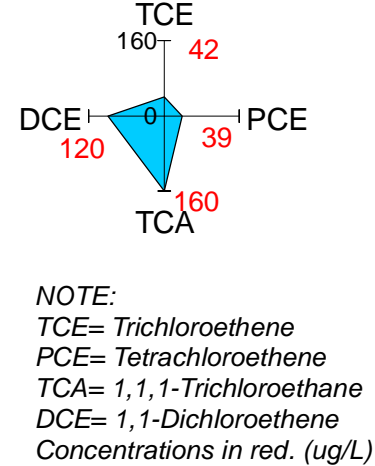
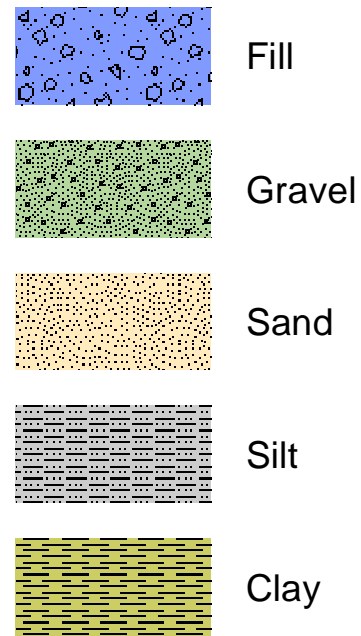




**Figure 3-3. 1,1- DCE Plume Map**  
**Contour Interval = 7, and 20 ug/L**



Legend



Monitoring Well Location/ Soil Boring Location

EW 13 D

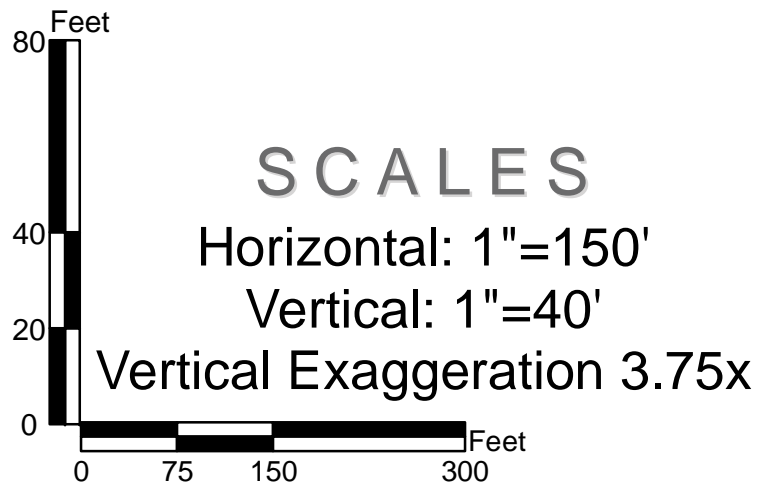
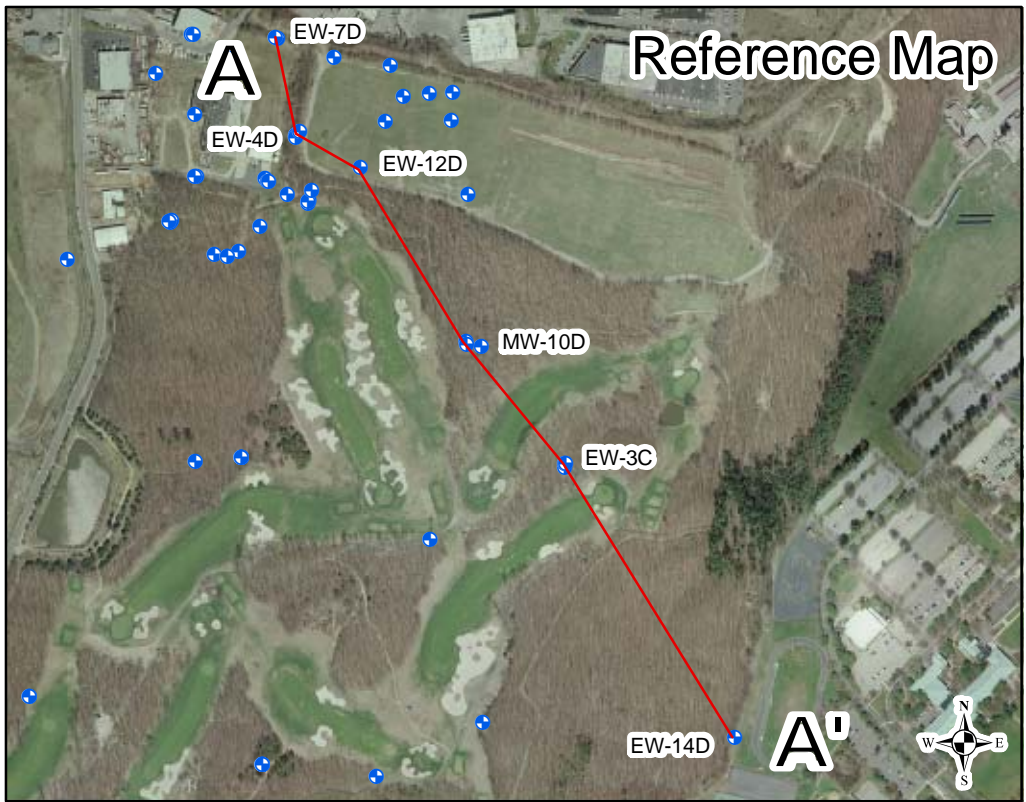
Land Surface

Casing

Screened Interval

Soil Boring (Abandoned)

- 1.) Lithologic interpretations are based on drilling logs from SAIC Ebasco Services, Inc. and Geraghty & Miller, Inc. (Logs from EW-7D, EW-4D, EW-12D, MW-10D, EW-3C, and EW-14D were used in the lithologic interpretation.)
- 2.) Colors are used for diagrammatic purposes only.
- 3.) Monitoring well widths are horizontally exaggerated for display purposes.
- 4.) Lithologic interpretation for MW-10D is missing bottom 27' due to missing data from job file.
- 5.) Data from graphing diagrams from 2007 Groundwater sampling events.




CLAREMONT POLYCHEMICAL

Old Bethpage, Nassau Co, New York

Stratigraphic Cross-Section A-A'

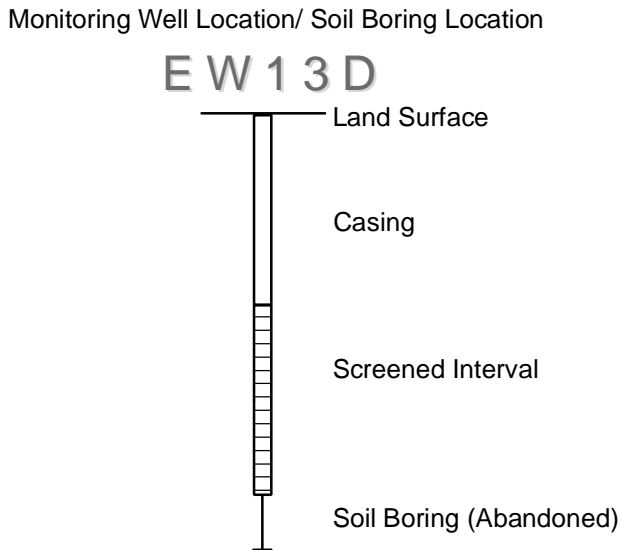
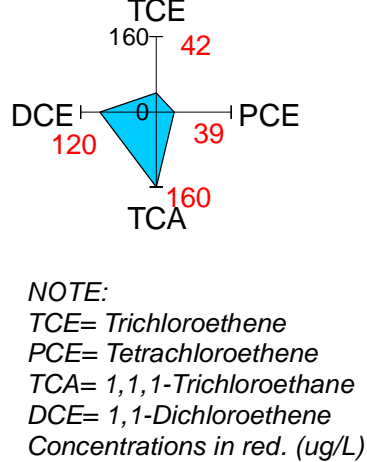
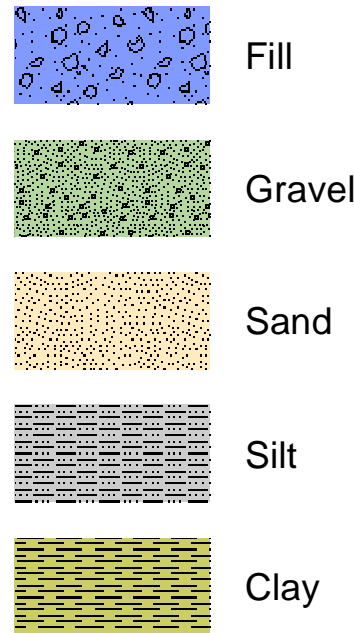
drawn	AGM	checked	approved	figure no.
date	7/14/06	date	date	3.4a
job no.	01-1633-08-5509-211		file no.	
initials	date	revision	A_A'.mxd	
AGM	8/11/08	Change X-section identifier to A-A'		



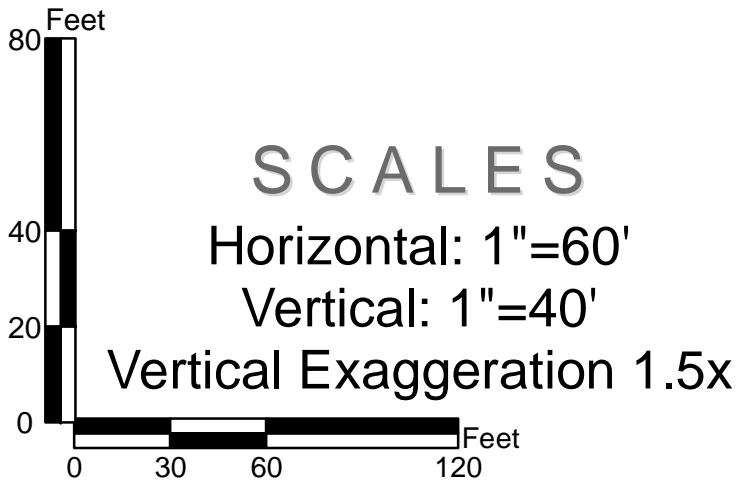
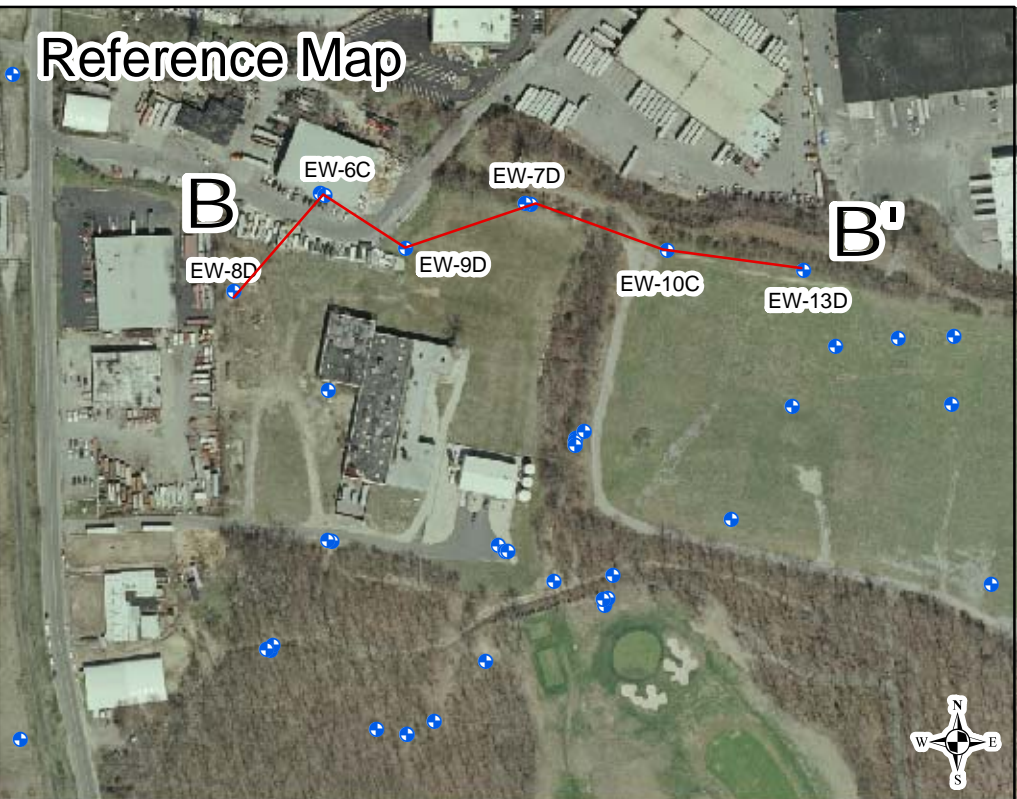
**SAIC**  
From Science to Solutions



Legend



- 1.) Chemistry for EW-6C,A from 10-5-05 sampling event.
- 2.) All other chemistry from discrete interval sampling during well drilling activities.
- 3.) Lithologic interpretations are based on drilling logs from SAIC and Ebasco Services, Inc. (Logs from EW-8D, EW-6C, EW-9D, EW-7D, EW-10C and EW-13D were used in the lithologic interpretation.)
- 4.) Colors are used for diagrammatic purposes only.
- 5.) Monitoring well widths are horizontally exaggerated for display purposes.
- 6.) Data from graphing diagrams from 2007 Groundwater sampling events.



CLAREMONT POLYCHEMICAL				
Old Bethpage, Nassau Co, New York				
Stratigraphic Cross-Section B-B'				
drawn AGM	checked	approved	figure no.	
date 1/23/06	date	date	3.4b	
job no. 01-1633-08-5509-211	file no. A_A.mxd			
initials AGM	date 8/11/08	revision Change X-section identifier to B-B'		













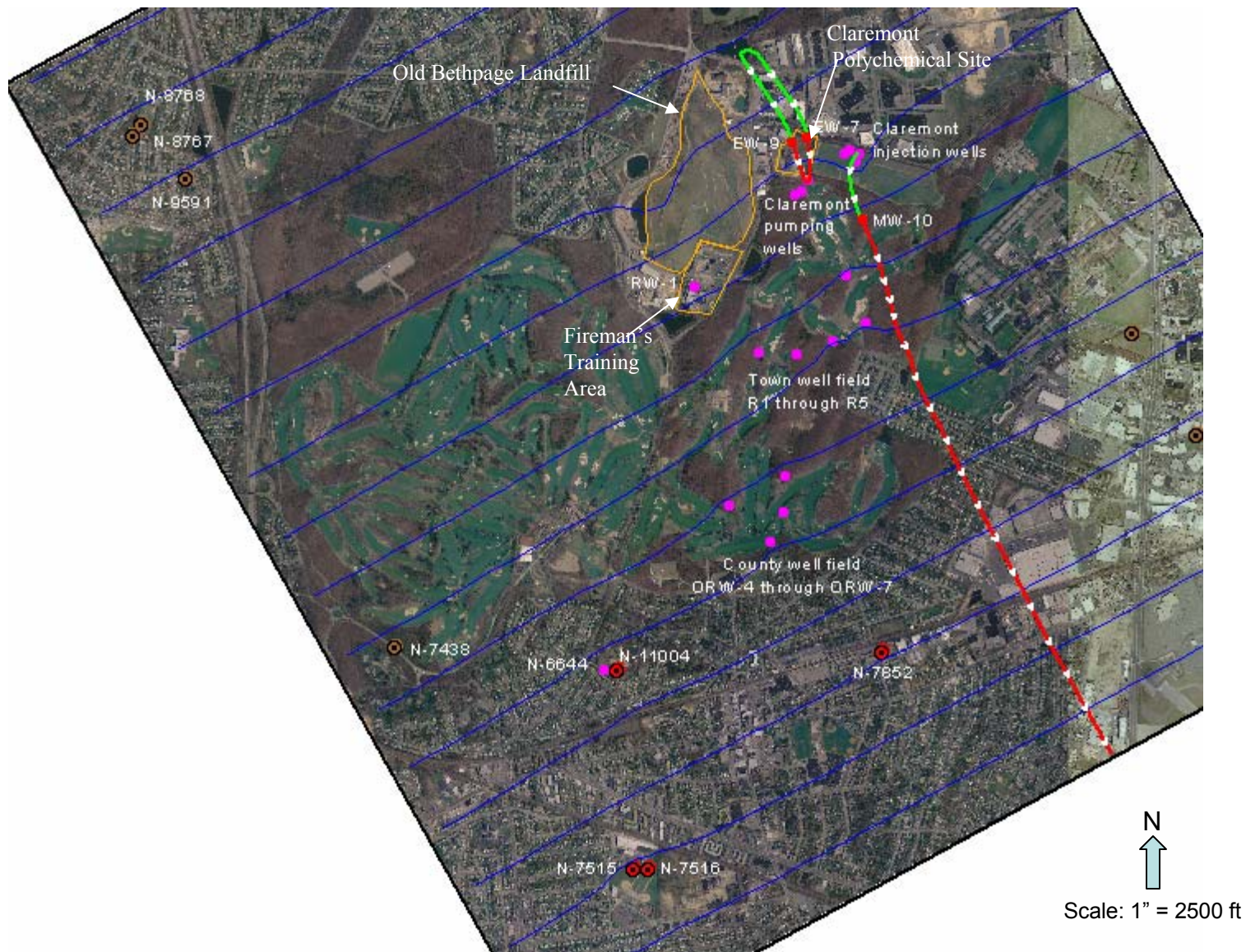


**Figure 3-5. Particle Tracking in Zone B from Wells EW-9, EW-7, and MW-10  
Backward Track in Green : Forward Track in Red, 1 Arrow = 1 yr**



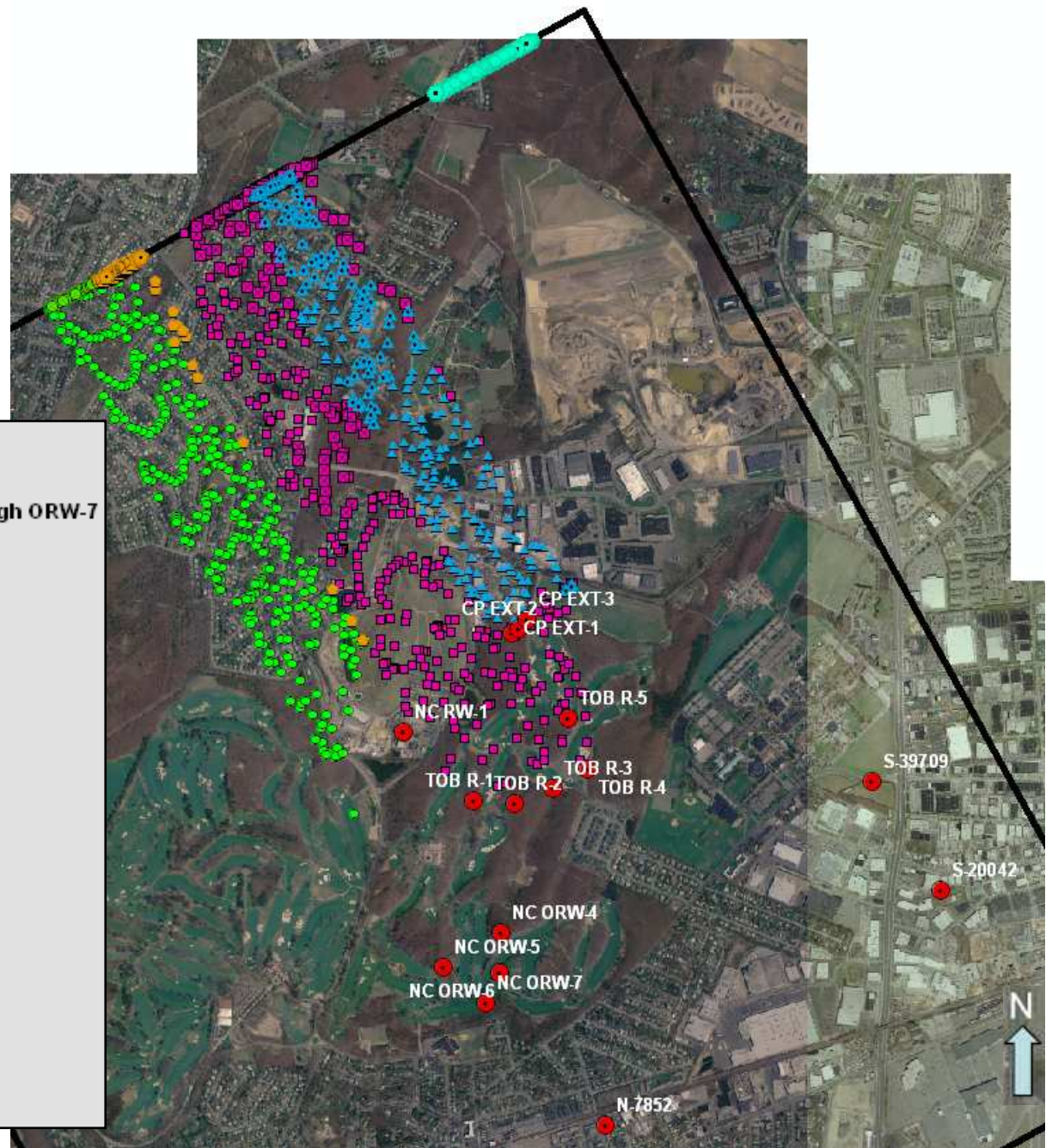
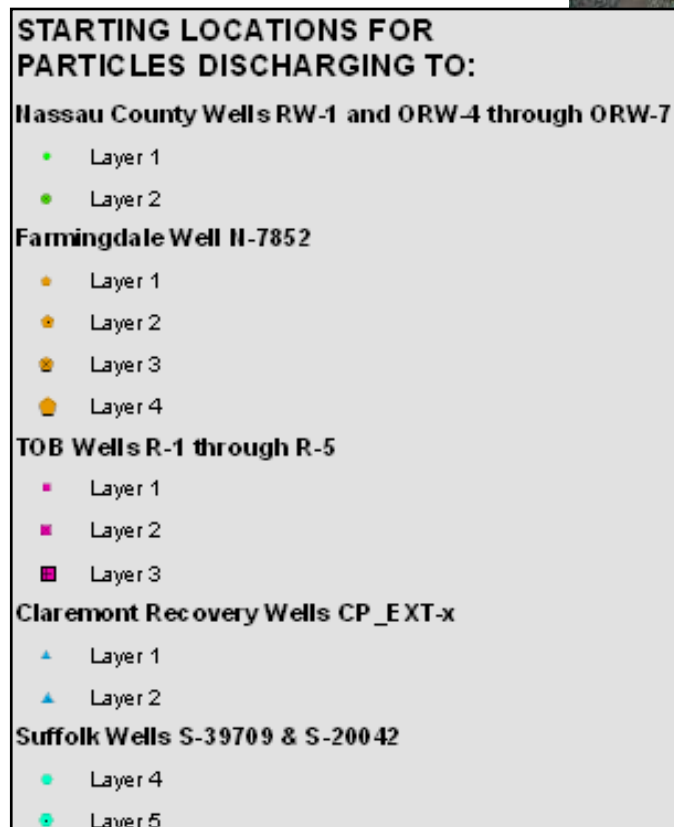


Figure 3-6. Starting Locations for Particles Discharging to Selected Wells  
Suffolk County S-20042 and S-39709; Village of Farmingdale N-7852; Claremont EXT-1, EXT-2, and EXT-3;  
TOB recovery wells RW-1 through RW-5; & NCDPW extraction wells RW-1 and ORW-4 through ORW-7



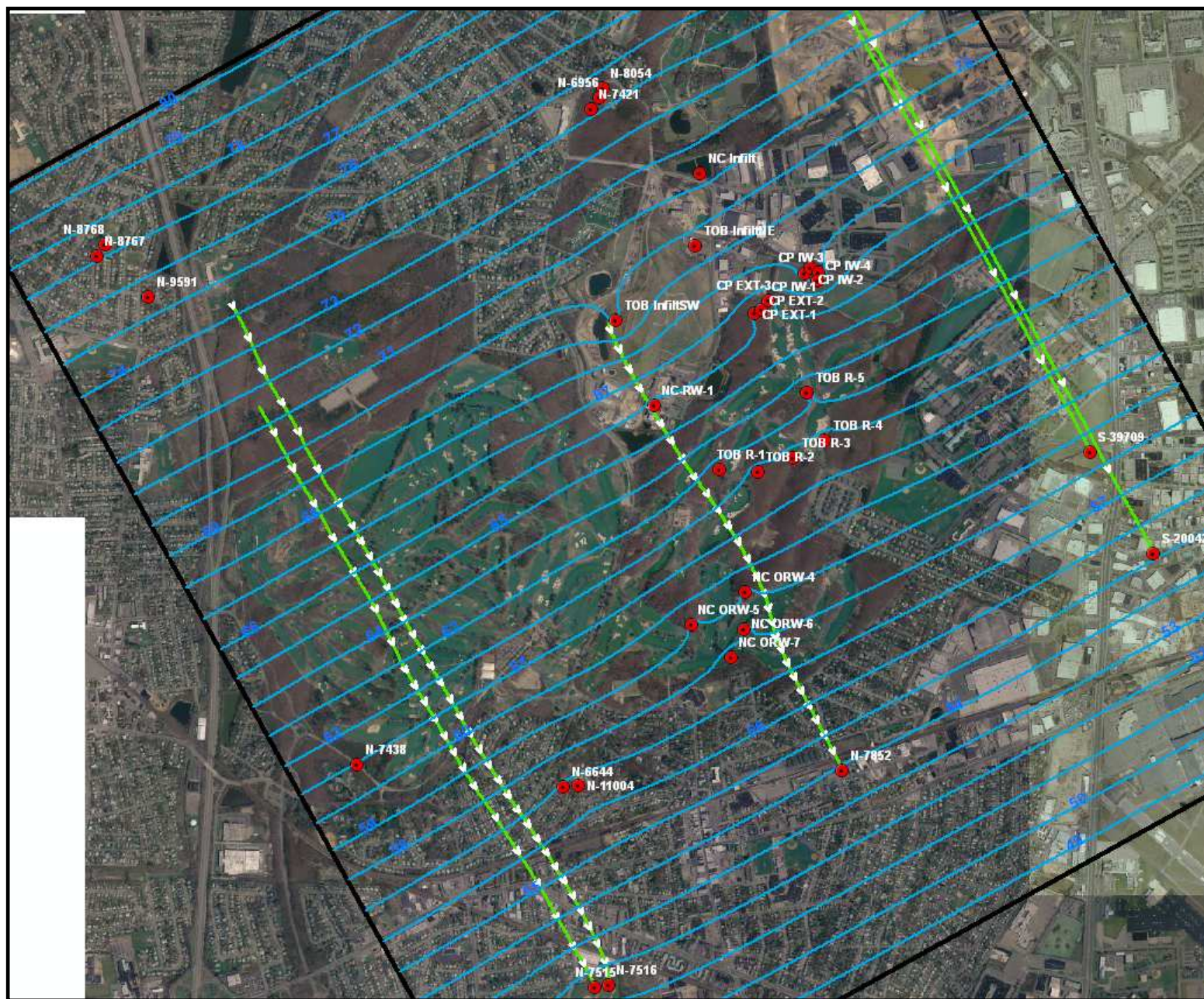


Figure 3-7. Backward Particle Tracking from Village of Farmingdale Municipal Supply Wells (N-7515, N-7516, N-7852) (wells in Zone C-Upper) and Suffolk County Water Supply Wells (S-39709 and S-20042) (wells in Zone C-Lower)





Zone A



Zone B



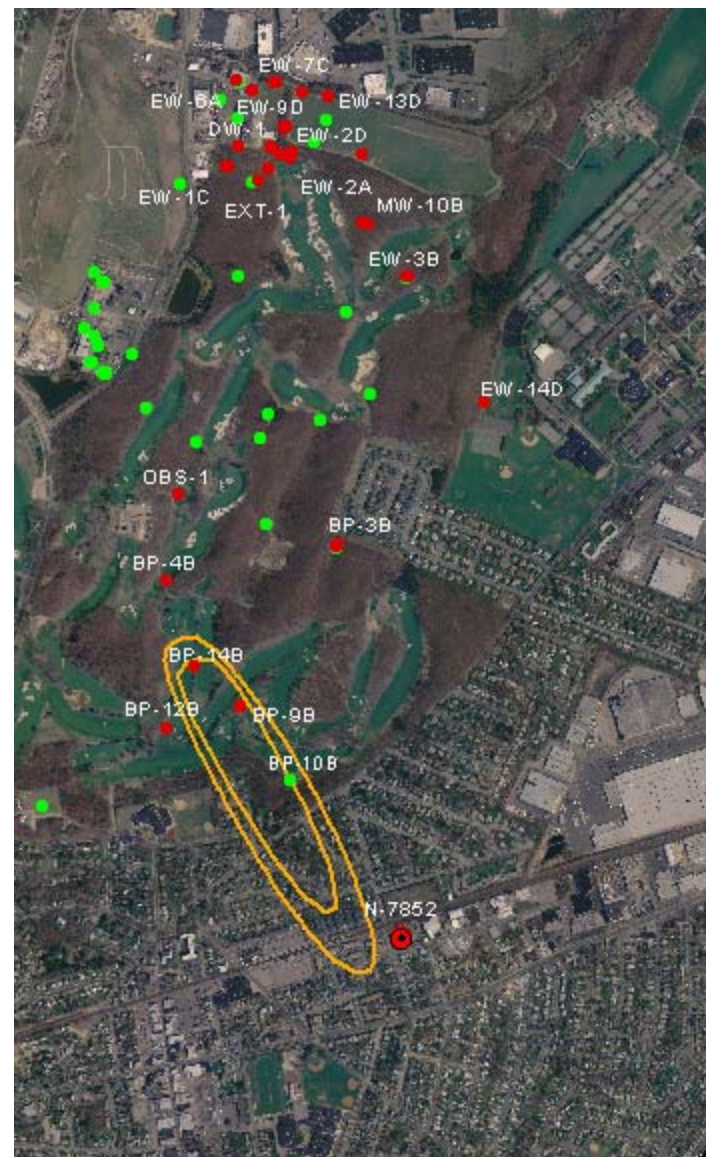
Scale: 1" = 1833 ft

**Figure 3-8. USGS/MODFLOW/MT3D Predicted PCE Plumes in 5 Years for Zone A and Zone B**  
**Plume Map Contour Interval = 5, 10, and 100 ug/L**





Zone C-Upper



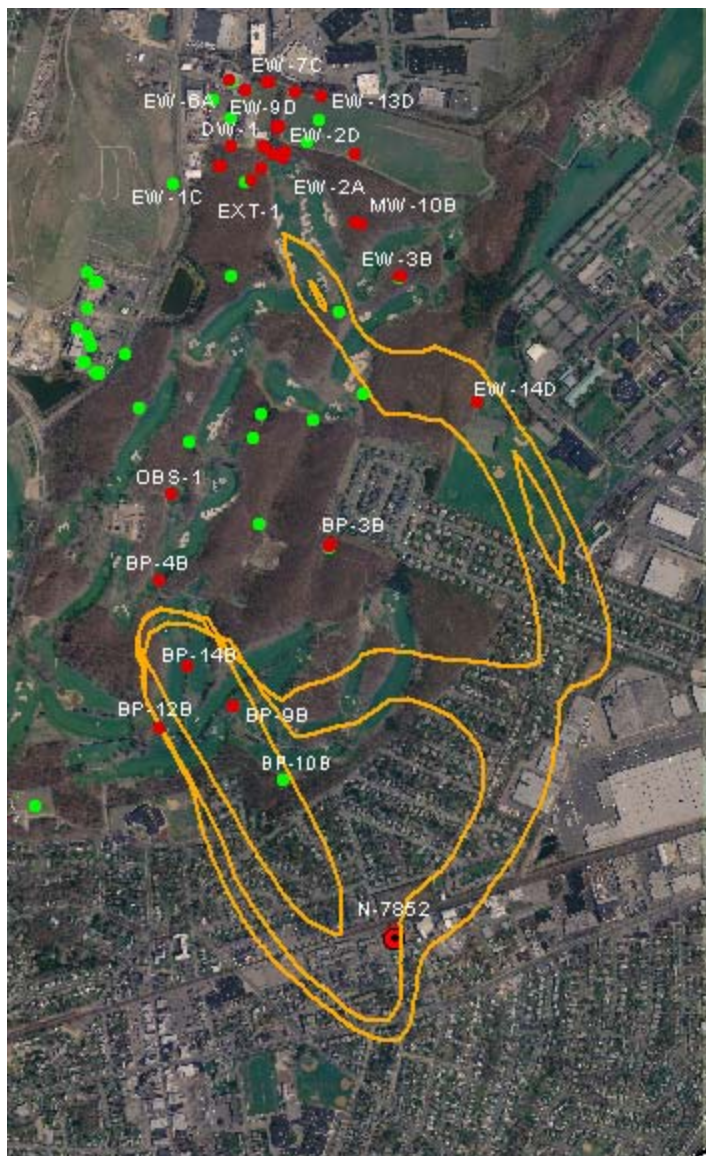
Zone C-Middle



Scale: 1" = 1833 ft

**Figure 3-9. USGS/MODFLOW/MT3D Predicted PCE Plumes in 5 Years for Zone C-Upper and Zone C-Middle**  
**Plume Map Contour Interval = 5, 10, and 100 ug/L**

*Predicted PCE concentration was below 5 ug/L in Zone C-Lower layer*



Zone A



Zone B



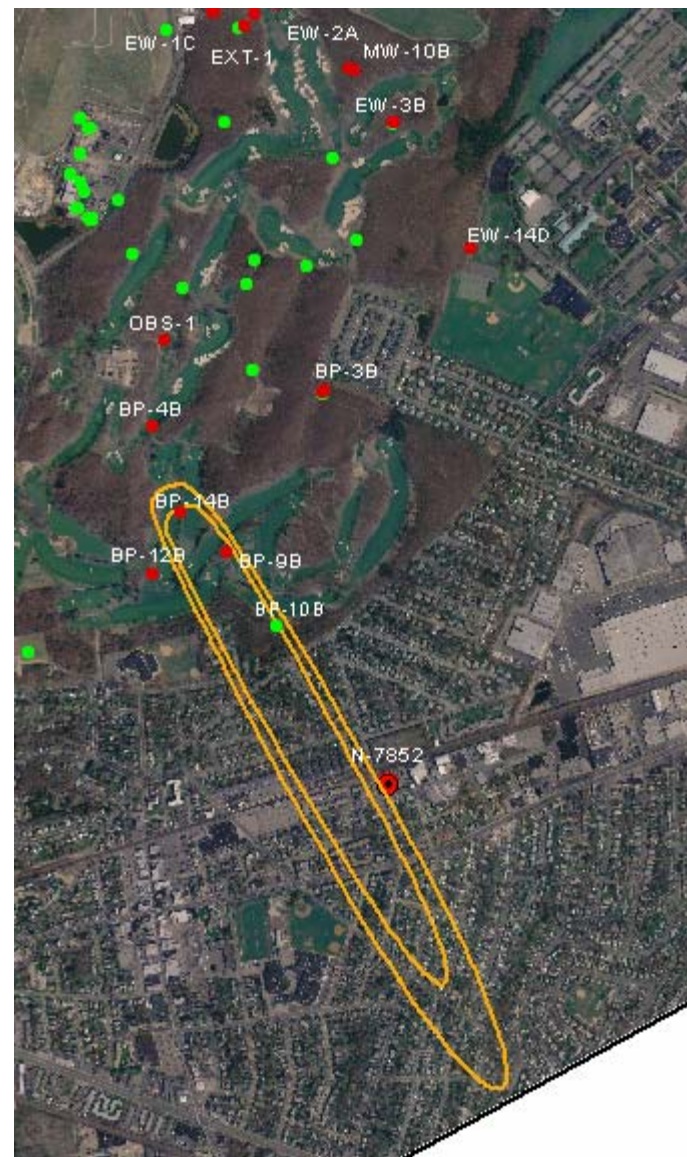
Scale: 1" = 1833 ft

**Figure 3-10. USGS/MODFLOW/MT3D Predicted PCE Plumes in 10 Years for Zone A and Zone B**  
**Plume Map Contour Interval = 5, 10, and 100 ug/L**





Zone C-Upper



Zone C-Middle



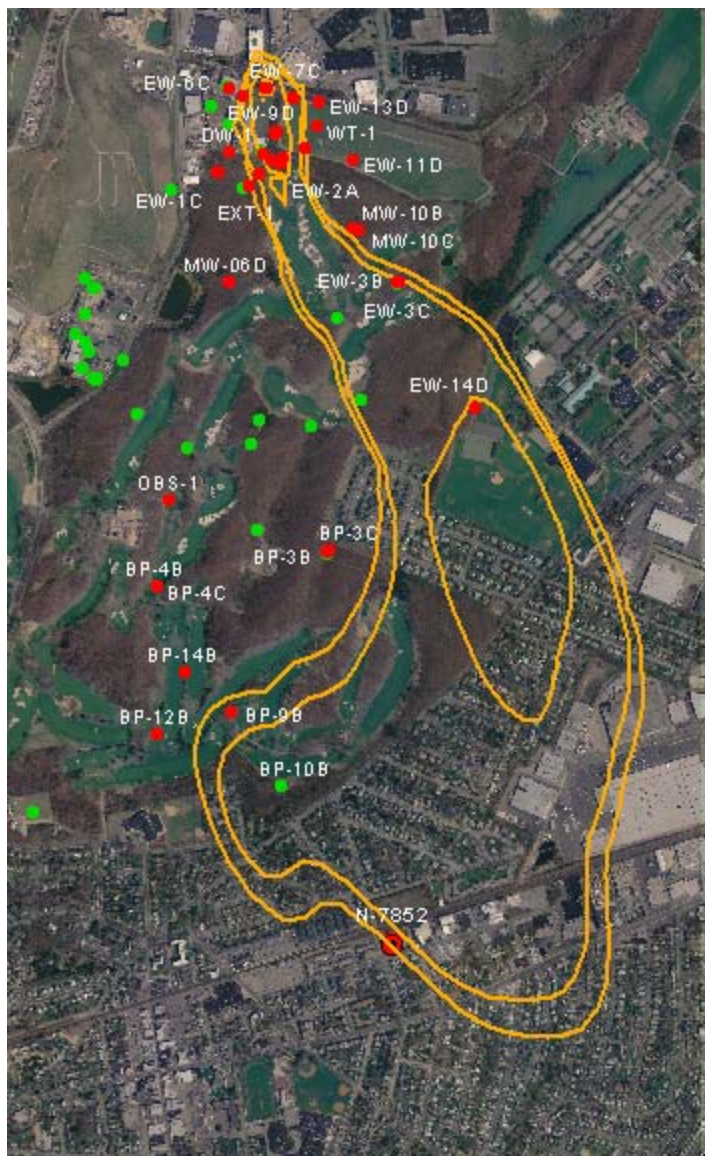
Scale: 1" = 1833 ft

**Figure 3-11. USGS/MODFLOW/MT3D Predicted PCE Plumes in 10 Years for Zone C-Upper and Zone C-Middle**  
**Plume Map Contour Interval = 5, 10, and 100 ug/L**

39

*Predicted PCE concentration was below 5 ug/L in Zone C-Lower layer*





Zone A



Zone B



Scale: 1" = 1833 ft

**Figure 3-12. USGS/MODFLOW/MT3D Predicted TCE Plumes in 5 Years for Zone A and Zone B**  
**Plume Map Contour Interval = 5, 10, 100, and 1000 ug/L**





Zone C-Upper

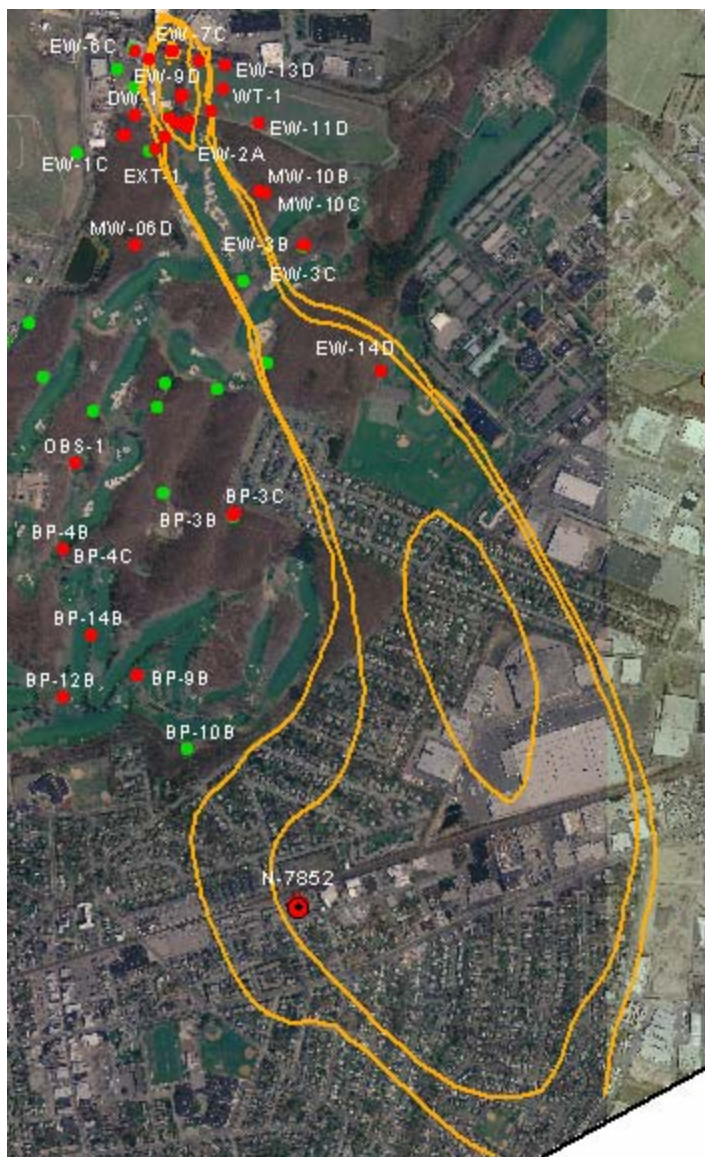


Zone C-Middle

N  
↑  
Scale: 1" = 1833 ft

**Figure 3-13. USGS/MODFLOW/MT3D Predicted TCE Plumes in 5 Years for Zone C-Upper and Zone C-Middle**  
Plume Map Contour Interval = 5, 10, 100, and 1000 ug/L





Zone A



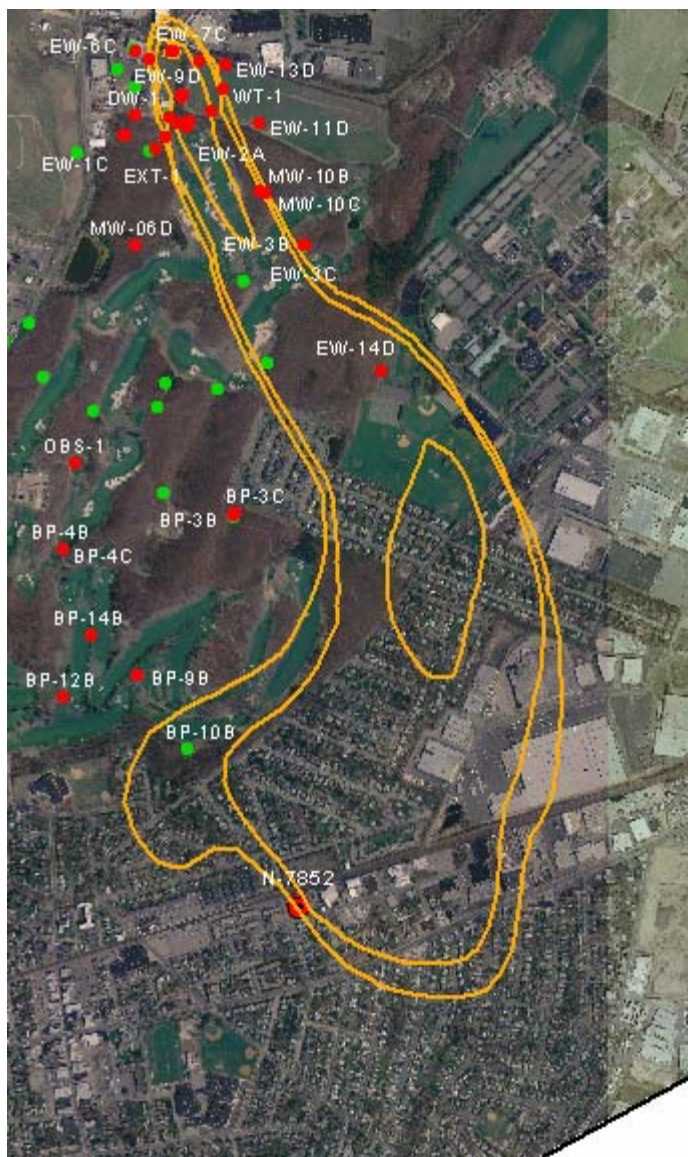
Zone B



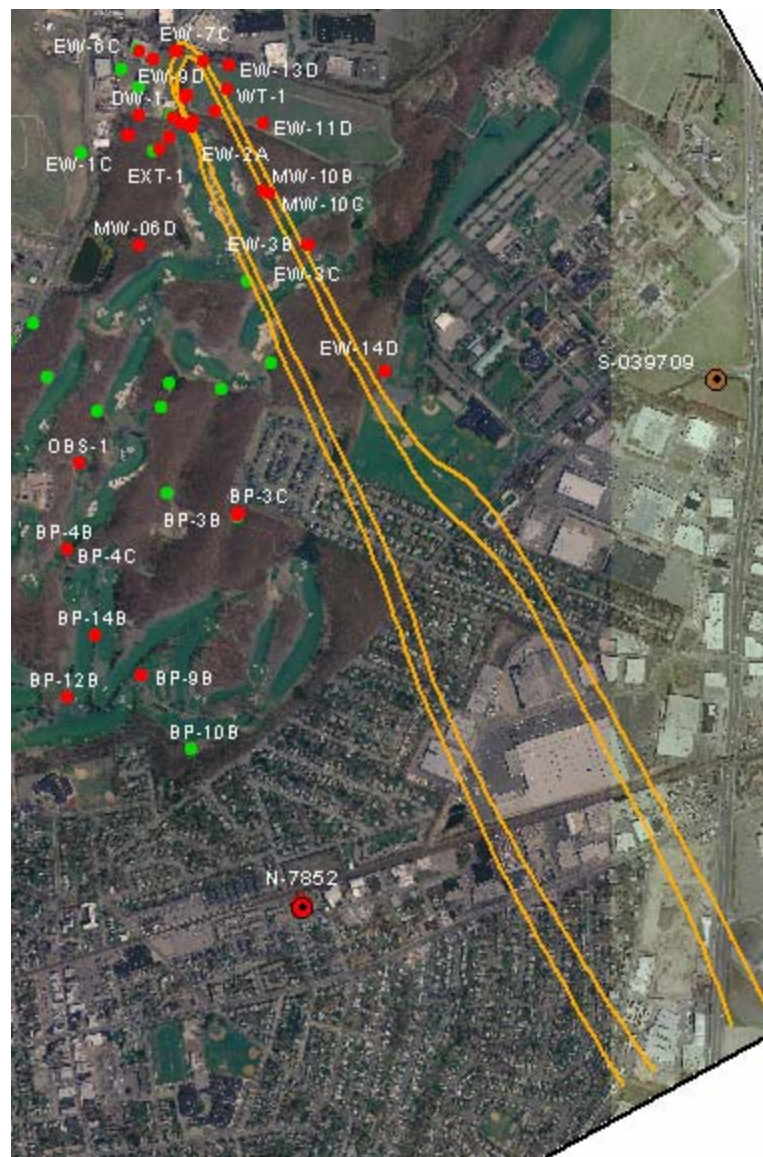
Scale: 1" = 1833 ft

**Figure 3-14. USGS/MODFLOW/MT3D Predicted TCE Plumes in 10 Years for Zone A and Zone B**  
**Plume Map Contour Interval = 5, 10, 100, and 1000 ug/L**





Zone C-Upper



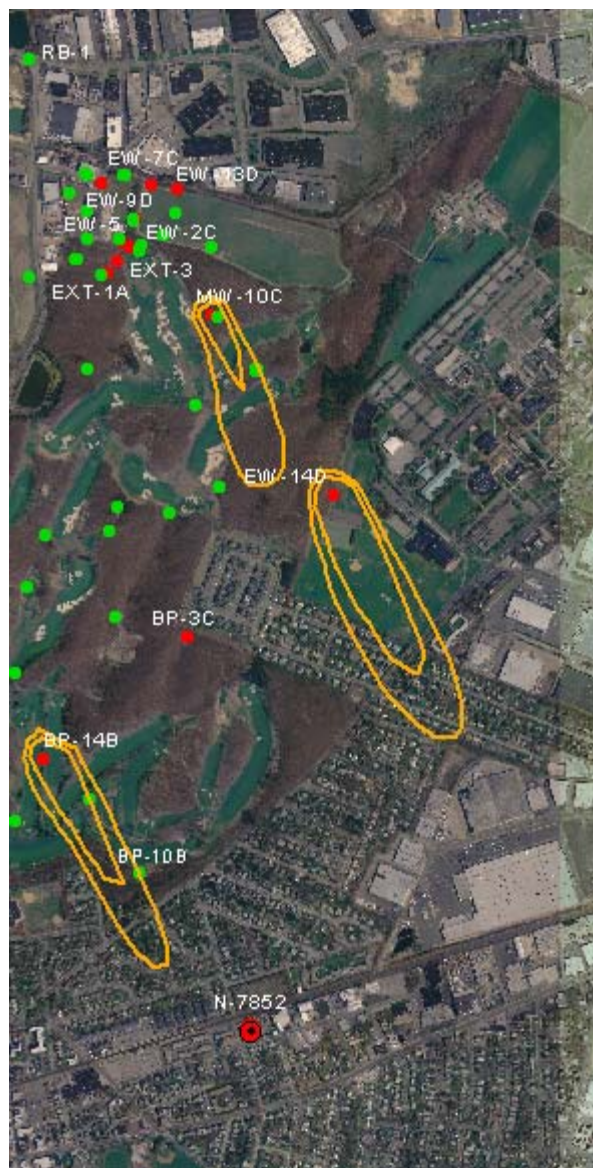
Zone C-Middle

N  
↑  
Scale: 1" = 1833 ft

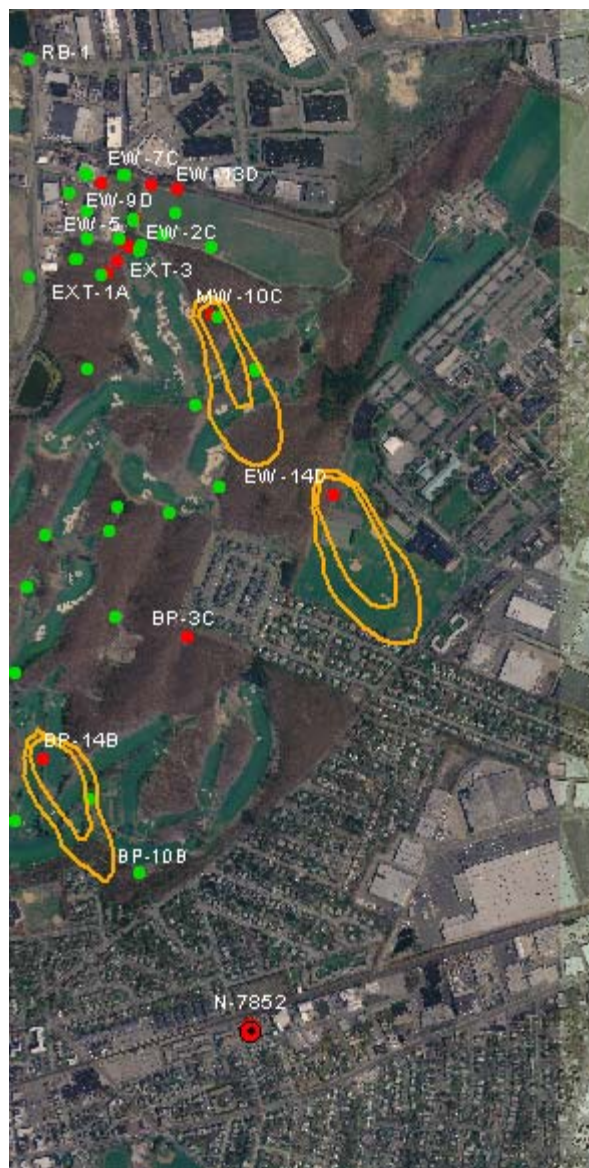
**Figure 3-15. USGS/MODFLOW/MT3D Predicted TCE Plumes in 10 Years for Zone C-Upper and Zone C-Middle**  
**Plume Map Contour Interval = 5, 10, 100, and 1000 ug/L**

*Predicted TCE concentration was below 5 ug/L in Zone C-Lower layer*





Zone A



Zone B



Zone C-Upper

**Figure 3-16. USGS/MODFLOW/MT3D Predicted 1,1-DCE Plumes in 5 Years for Zone A , Zone B, and Zone C-Upper**  
**Plume Map Contour Interval = 7 and 20 ug/L**

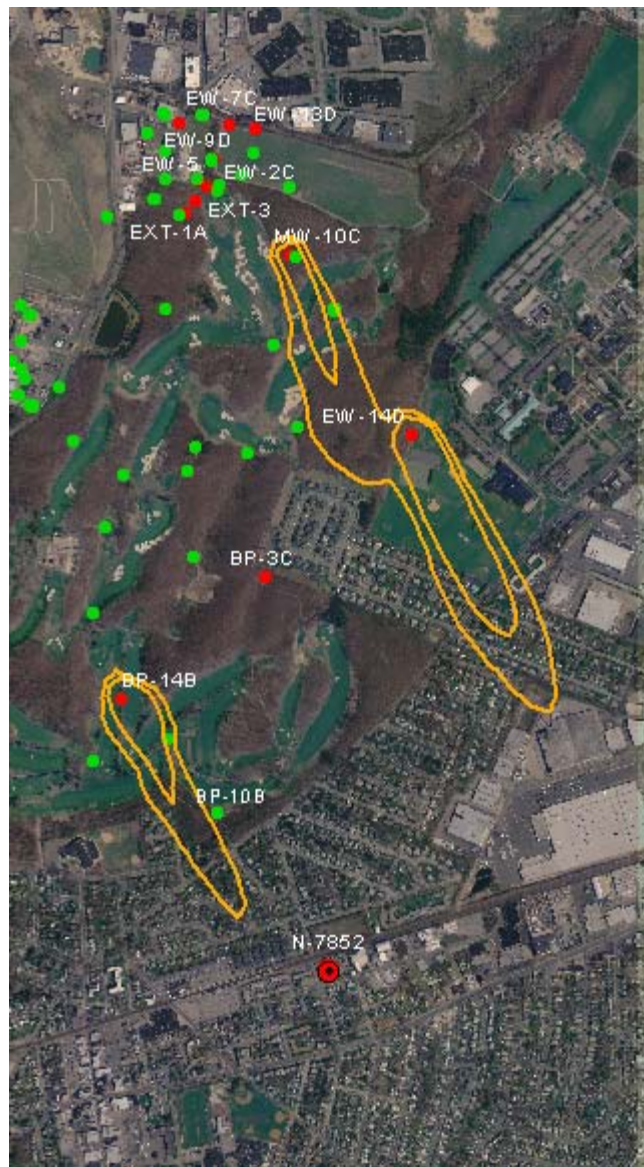
Scale: 1" = 1833 ft

*Predicted 1,1-DCE concentration was below 7 ug/L in Zone C-Middle, and Zone C-Lower layers*





Zone A



Zone B



Zone C-Upper

Scale: 1" = 1833 ft

**Figure 3-17. USGS/MODFLOW/MT3D Predicted 1,1- DCE Plumes in 10 Years for Zone A , Zone B, and Zone C-Upper**  
**Plume Map Contour Interval = 7 and 20 ug/L**

*Predicted 1,1-DCE concentration was below 7 ug/L in Zone C-Middle, and Zone C-Lower layers*

## APPENDIX A

**Table A-1 - Summary of Claremont Chemical Data**

Summarized Claremont Chemical Data (July 2006)								
Well	Date	1,1-Dichloroethylene (1,1-DCE) ug/l	Tetrachloroethylene (PCE) ug/l	Trichloroethylene (TCE) ug/l	Vinyl chloride ug/l	pH	Eh (ORP) (mV)	DO (mg/L)
Jul 2006								
BP-3A	7/27/2006	0.50	0.50	0.50	0.50	5.18	184.00	9.26
BP-3B	7/27/2006	0.50	13.00	0.64	0.50	5.46	177.00	9.78
BP-3C	7/27/2006	1.40	3.40	13.00	1.10	5.07	200.00	9.50
EW-2A	7/27/2006	BDL	1.00	0.20	BDL	6.14	-84.00	8.20
EW-2B	7/27/2006	BDL	1.20	0.60	BDL	5.60	152.00	8.14
EW-2C	7/27/2006	0.30	1.10	6.50	0.30	4.76	201.00	9.90
EW-2D	7/27/2006	BDL	0.30	1.80	BDL	4.90	235.00	8.30
EW-3A	7/25/2006	BDL	BDL	BDL	BDL	5.24	179.00	11.09
EW-3B	7/27/2006	BDL	BDL	0.20	BDL	5.12	189.00	8.66
EW-3C	7/25/2006	0.50	1.20	7.20	0.50	5.20	191.00	8.00
EW-4A	7/25/2006	0.50	30.00	0.32	0.50	4.90	204.00	8.16
EW-4B	7/25/2006	5.00	18.00	150.00	5.00	5.24	188.00	7.37
EW-4C	7/25/2006	31.00	34.00	640.00	31.00	5.85	167.00	9.63
EW-4D	7/24/2006	0.35	0.65	1.90	0.50	5.85	170.00	5.86
EW-7C	7/24/2006	31.00	46.00	1400.00	31.00	4.77	313.00	4.66
EW-7D	7/24/2006	1.80	3.60	38.00	2.10	4.52	352.00	9.80
EW-10C	7/24/2006	6.60	15.00	22.00	1.80	4.99	219.00	5.46
EW-14D	7/25/2006	42.00	5.90	400.00	0.50	5.67	134.00	1.80
Summarized Claremont Chemical Data (Jan/Feb 2006)								
Well	Date	1,1-Dichloroethylene (1,1-DCE) ug/l	Tetrachloroethylene (PCE) ug/l	Trichloroethylene (TCE) ug/l	Vinyl chloride ug/l	pH	Eh (ORP) (mV)	DO (mg/L)
BP-3A	2/3/2006	0.50	0.50	0.50	0.50	5.18	184.00	9.26
BP-3B	2/3/2006	0.50	19.00	2.60	0.50	5.29	246.00	10.56
BP-3C	2/3/2006	1.10	2.10	11.00	0.64	4.96	244.00	10.26
EW-2A	2/1/2006	0.50	1.60	0.50	0.50	5.63	-23.00	4.19
EW-2B	2/1/2006	0.50	1.30	3.10	0.50	6.22	137.00	6.41
EW-2C	2/1/2006	0.56	1.10	4.60	0.50	4.68	210.00	8.84
EW-2D	1/30/2006	ND	ND	ND	ND	6.21	-67.00	3.62
EW-3A	1/30/2006	0.50	0.50	0.50	0.50	5.36	250.00	11.21
EW-3B	1/30/2006	ND	ND	ND	ND	5.28	265.00	9.57
EW-3C	2/1/2006	0.36	1.10	8.60	0.50	5.19	265.00	7.80
EW-4A	2/1/2006	1.00	33.00	1.30	0.50	4.93	308.00	5.29
EW-4B	2/1/2006	5.20	13.00	100.00	1.00	5.27	293.00	5.53
EW-4C	2/1/2006	3.90	44.00	780.00	5.00	5.60	281.00	6.98
EW-4D			ND					
EW-7C	2/1/2006	10.00	44.00	1400.00	10.00	4.19	296.00	6.02
EW-7D	2/1/2006	0.79	6.00	36.00	0.50	4.11	295.00	7.82
EW-10C			ND					
EW-14D	1/10/2007	ND	ND	ND	ND	6.45	268.00	3.18
Summarized Claremont Chemical Data (July 2005)								
Well	Date	1,1-Dichloroethylene (1,1-DCE) ug/l	Tetrachloroethylene (PCE) ug/l	Trichloroethylene (TCE) ug/l	Vinyl chloride ug/l	pH	Eh (ORP) (mV)	DO (mg/L)
BP-3A	7/21/2005	0.50	0.50	0.50	0.50	5.37	234.00	10.81
BP-3B	7/21/2005	0.50	18.00	0.98	0.50	5.44	272.00	14.11
BP-3C	7/21/2005	1.30	3.30	16.00	1.60	4.75	314.00	9.01
EW-2A	7/20/2005	0.50	1.80	0.50	0.50	5.49	448.00	5.67
EW-2B	7/21/2005	0.50	1.70	1.80	0.50	6.58	360.00	2.94
EW-2C	7/21/2005	1.10	1.80	12.00	0.50	4.48	354.00	7.46
EW-2D			ND					
EW-3A	7/19/2005	0.50	0.50	0.50	0.50	5.07	334.00	11.60
EW-3B	7/19/2005	0.50	0.50	0.50	0.50	5.24	320.00	10.91
EW-3C	7/19/2005	4.00	5.80	45.00	4.00	5.14	295.00	8.87
EW-4A	7/18/2005	2.50	32.00	2.50	2.50	4.75	309.00	6.50
EW-4B	7/18/2005	1.60	7.80	160.00	0.50	5.25	293.00	7.52
EW-4C	7/18/2005	0.53	10.00	280.00	0.50	5.67	270.00	8.64
EW-4D			ND					
EW-7C	7/19/2005	2.20	40.00	1300.00	0.50	4.64	453.00	6.67
EW-7D	7/20/2005	0.50	4.40	35.00	0.50	4.35	473.00	8.21
EW-10C	ND							
EW-14D	ND							



**Table A-1 - Summary of Claremont Chemical Data**

Summarized Claremont Chemical Data (February 2005)								
Well	Date	1,1-Dichloroethylene (1,1-DCE) ug/l	Tetrachloroethylene (PCE) ug/l	Trichloroethylene (TCE) ug/l	Vinyl chloride ug/l	pH	Eh (ORP) (mV)	DO (mg/L)
BP-3A	2/24/2005	0.50	0.50	0.50	0.50	4.94	256.00	7.80
BP-3B	2/24/2005	2.00	36.00	2.50	2.00	5.15	244.00	8.38
BP-3C	2/24/2005	0.50	2.60	16.00	2.20	4.99	281.00	5.85
EW-2A	2/23/2005	0.50	0.77	5.00	0.50	5.79	-129.00	0.83
EW-2B	2/23/2005	0.50	2.10	2.00	0.50	6.39	148.00	5.81
EW-2C	2/23/2005	0.50	1.60	9.70	0.50	4.82	300.00	6.43
EW-2D								
EW-3A	2/22/2005	0.50	0.50	0.50	0.50	5.40	305.00	8.79
EW-3B	2/22/2005	0.50	0.50	0.50	0.50	5.40	314.00	7.52
EW-3C	2/22/2005	2.00	3.00	29.00	2.00	5.38	332.00	6.44
EW-4A	2/21/2005	0.50	62.00	0.66	0.50	5.07	334.00	4.91
EW-4B	2/21/2005	0.50	9.00	69.00	0.50	5.46	317.00	5.02
EW-4C	2/21/2005	1.70	23.00	490.00	0.50	5.89	299.00	5.49
EW-4D								
EW-7C	2/22/2005	0.50	18.00	900.00	0.50	4.89	248.00	5.76
EW-7D	2/22/2005	0.50	0.36	6.90	0.50	5.18	133.00	5.51
EW-10C								
EW-14D								
Summarized Claremont Chemical Data (July 2004)								
Well	Date	1,1-Dichloroethylene (1,1-DCE) ug/l	Tetrachloroethylene (PCE) ug/l	Trichloroethylene (TCE) ug/l	Vinyl chloride ug/l	pH	Eh (ORP) (mV)	DO (mg/L)
BP-3A	7/21/2004	0.50	0.50	0.50	0.50	4.36	365.00	7.52
BP-3B	7/21/2004	0.50	25.00	2.10	0.50	4.39	360.00	6.78
BP-3C	7/21/2004	1.60	3.10	15.00	2.50	4.30	368.00	1.38
EW-2A	7/22/2004	0.50	1.20	3.60	0.50	5.47	17.00	1.10
EW-2B	7/22/2004	0.50	2.40	1.20	0.50	6.06	278.00	5.75
EW-2C	7/22/2004	9.90	3.60	40.00	0.50	4.75	294.00	6.61
EW-2D								
EW-3A	7/20/2004	0.50	0.50	0.50	0.50	5.17	227.00	12.04
EW-3B	7/20/2004	0.50	0.50	0.50	0.50	5.22	245.00	9.33
EW-3C	7/22/2004	1.80	4.50	39.00	2.00	4.90	273.00	8.07
EW-4A	7/19/2004	0.51	110.00	2.20	0.50	4.26	466.00	3.43
EW-4B	7/19/2004	1.30	7.70	47.00	0.50	4.72	437.00	3.99
EW-4C	7/19/2004	1.90	22.00	490.00	2.50	5.36	398.00	5.74
EW-4D								
EW-7C								
EW-7D								
EW-10C								
EW-14D								
Summarized Claremont Chemical Data (2003)								
Well	Date	1,1-Dichloroethylene (1,1-DCE) ug/l	Tetrachloroethylene (PCE) ug/l	Trichloroethylene (TCE) ug/l	Vinyl chloride ug/l	pH	Eh (ORP) (mV)	DO (mg/L)
BP-3A	7/29/2003	0.50	0.50	0.50	0.50	5.22	302.00	10.73
BP-3B	7/29/2003	BDL	64.40	4.50	BDL	5.21	276.00	8.71
BP-3C	7/29/2003	1.50	3.00	14.60	5.10	4.85	322.00	1.72
EW-2A	10/23/2003	0.50	1.70	23.00	0.50	ND	ND	ND
EW-2B	7/30/2003	0.99	3.50	5.10	0.50		NA	
EW-2C	7/30/2003	17.00	7.50	68.00	0.50	4.75	300.00	3.62
EW-2D								
EW-3A								
EW-3B	7/30/2003	0.50	0.23	0.23	0.50	5.27	259.00	7.38
EW-3C	7/30/2003	6.60	24.00	160.00	0.50	5.06	273.00	4.57
EW-4A	7/29/2003	0.33	58.00	1.30	0.50	4.82	290.00	2.22
EW-4B	7/29/2003	1.30	7.70	47.00	0.50	5.42	189.00	0.74
EW-4C	7/29/2003	0.58	25.00	770.00	0.50	5.36	221.00	5.47
EW-4D								
EW-7C								
EW-7D								
EW-10C								
EW-14D								

**Table A-1 - Summary of Claremont Chemical Data**

Summarized Claremont Chemical Data (2002)								
Well	Date	1,1-Dichloroethylene (1,1-DCE) ug/l	Tetrachloroethylene (PCE) ug/l	Trichloroethylene (TCE) ug/l	Vinyl chloride ug/l	pH	Eh (ORP) (mV)	DO (mg/L)
BP-3A				DRY				
BP-3B	10/25/2002	BDL	BDL	6.60	20.00	5.62	204.00	8.05
BP-3C	10/25/2002	BDL	BDL	7.60	21.70	6.02	159.00	0.30
EW-2A	5/17/2002	0.50	73.00	0.98	0.50	ND	ND	ND
EW-2B	10/23/2002	0.50	6.00	3.50	0.50	5.26	275.00	3.21
EW-2C	10/23/2002	12.00	3.50	18.00	0.50	5.07	303.00	3.70
EW-2D				ND				
EW-3A				ND				
EW-3B	10/24/2002	0.50	0.24	0.23	0.50	5.46	261.00	8.89
EW-3C	10/24/2002	6.30	6.80	86.00	6.30	5.28	285.00	6.44
EW-4A	10/23/2002	3.10	84.00	2.60	3.10	5.04	308.00	2.70
EW-4B	10/23/2002	2.10	3.20	59.00	2.10	5.48	275.00	5.16
EW-4C	10/23/2002	25.00	14.00	890.00	25.00	5.80	253.00	6.51
EW-4D				ND				
EW-7C				ND				
EW-7D				ND				
EW-10C				ND				
EW-14D				ND				
Summarized Claremont Chemical Data (2001)								
Well	Date	1,1-Dichloroethylene (1,1-DCE) ug/l	Tetrachloroethylene (PCE) ug/l	Trichloroethylene (TCE) ug/l	Vinyl chloride ug/l	pH	Eh (ORP) (mV)	DO (mg/L)
BP-3A				ND				
BP-3B				ND				
BP-3C				ND				
EW-2A	8/23/2001	0.40	120.00	3.00	10.00		ND	
EW-2B	8/23/2001	7.00	26.00	10.00	10.00		ND	
EW-2C	8/23/2001	52.00	20.00	25.00	10.00		ND	
EW-2D				ND				
EW-3A				ND				
EW-3B				ND				
EW-3C				ND				
EW-4A	8/22/2001	5.00	29.00	1.00	10.00		ND	
EW-4B	8/22/2001	5.00	4.00	110.00	10.00		ND	
EW-4C	8/22/2001	25.00	21.00	840.00	50.00		ND	
EW-4D				ND				
EW-7C				ND				
EW-7D				ND				
EW-10C				ND				
EW-14D				ND				
Summarized Claremont Chemical Data (2000)								
Well	Date	1,1-Dichloroethylene (1,1-DCE) ug/l	Tetrachloroethylene (PCE) ug/l	Trichloroethylene (TCE) ug/l	Vinyl chloride ug/l	pH	Eh (ORP) (mV)	DO (mg/L)
BP-3A				ND				
BP-3B				ND				
BP-3C				ND				
EW-2A	6/8/2000	10.00	320.00	4.00	20.00		ND	
EW-2B	6/8/2000	5.00	110.00	34.00	10.00		ND	
EW-2C	6/7/2000	5.00	18.00	530.00	50.00		ND	
EW-2D				ND				
EW-3A				ND				
EW-3B				ND				
EW-3C				ND				
EW-4A	5/25/2000	5.00	180.00	31.00	10.00		ND	
EW-4B	5/24/2000	1.00	17.00	320.00	20.00		ND	
EW-4C	5/24/2000	25.00	15.00	660.00	50.00		ND	
EW-4D				ND				
EW-7C				ND				
EW-7D				ND				
EW-10C				ND				
EW-14D				ND				

**Table A-1 - Summary of Claremont Chemical Data**

Summarized Claremont Chemical Data (June 1996)								
Well	Date	1,1-Dichloroethylene (1,1-DCE) ug/l	Tetrachloroethylene (PCE) ug/l	Trichloroethylene (TCE) ug/l	Vinyl chloride ug/l	pH	Eh (ORP)	DO (mg/L)
BP-3A				ND				
BP-3B	6/1/1996	3.40	9.70	27.60	19.60		ND	
BP-3C	4/1/1996	BDL	BDL	1.70	BDL		ND	
EW-2A				ND				
EW-2B				ND				
EW-2C				ND				
EW-2D				ND				
EW-3A				ND				
EW-3B				ND				
EW-3C				ND				
EW-4A				ND				
EW-4B				ND				
EW-4C				ND				
EW-4D				ND				
EW-7C				ND				
EW-7D				ND				
EW-10C				ND				
EW-14D				ND				
Summarized Claremont Chemical Data (1993)								
Well	Date	1,1-Dichloroethylene (1,1-DCE) ug/l	Tetrachloroethylene (PCE) ug/l	Trichloroethylene (TCE) ug/l	Vinyl chloride ug/l	pH	Eh (ORP)	DO (mg/L)
BP-3A				ND				
BP-3B	12/1/1993	BDL	24.50	2.20	BDL		ND	
BP-3C	12/1/1993	BDL	BDL	BDL	BDL		ND	
EW-2A				ND				
EW-2B				ND				
EW-2C				ND				
EW-2D				ND				
EW-3A				ND				
EW-3B				ND				
EW-3C				ND				
EW-4A				ND				
EW-4B				ND				
EW-4C				ND				
EW-4D				ND				
EW-7C				ND				
EW-7D				ND				
EW-10C				ND				
EW-14D				ND				
Summarized Claremont Chemical Data (1992)								
Well	Date	1,1-Dichloroethylene (1,1-DCE) ug/l	Tetrachloroethylene (PCE) ug/l	Trichloroethylene (TCE) ug/l	Vinyl chloride ug/l	pH	Eh (ORP)	DO (mg/L)
BP-3A				ND				
BP-3B				ND				
BP-3C				ND				
EW-2A	7/1/1992	1800.00	2200.00	400.00	ND		ND	
EW-2B	7/1/1992	96.00	210.00	23.00	ND		ND	
EW-2C	7/1/1992	ND	24.00	210.00	ND		ND	
EW-2D				ND				
EW-3A				ND				
EW-3B				ND				
EW-3C				ND				
EW-4A	7/1/1992	110.00	290.00	58.00	ND		ND	
EW-4B	7/1/1992	11.00	43.00	48.00	ND		ND	
EW-4C	7/1/1992	ND	N	5000.00	ND		ND	
EW-4D				ND				
EW-7C				ND				
EW-7D				ND				
EW-10C				ND				
EW-14D				ND				



### Table A-1 - Summary of Claremont Chemical Data

Summarized Claremont Chemical Data (1990)								
Well	Date	1,1-Dichloroethylene (1,1-DCE) ug/l	Tetrachloroethylene (PCE) ug/l	Trichloroethylene (TCE) ug/l	Vinyl chloride ug/l	pH	Eh (ORP)	DO (mg/L)
BP-3A				ND				
BP-3B	11/1/1990	BDL	BDL	1.70	BDL	5.03	ND	
BP-3C	11/1/1990	BDL	12.00	3.00	BDL	5.64	ND	
EW-2A				ND				
EW-2B				ND				
EW-2C				ND				
EW-2D				ND				
EW-3A				ND				
EW-3B				ND				
EW-3C				ND				
EW-4A				ND				
EW-4B				ND				
EW-4C				ND				
EW-4D				ND				
EW-7C				ND				
EW-7D				ND				
EW-10C				ND				
EW-14D				ND				
Summarized Claremont Chemical Data (1989)								
Well	Date	1,1-Dichloroethylene (1,1-DCE) ug/l	Tetrachloroethylene (PCE) ug/l	Trichloroethylene (TCE) ug/l	Vinyl chloride ug/l	pH	Eh (ORP)	DO (mg/L)
BP-3A				ND				
BP-3B				ND				
BP-3C				ND				
EW-2A	6/1/1989	1.00	170.00	8.00	ND		ND	
EW-2B	6/1/1989	170.00	6.00	ND	ND		ND	
EW-2C	6/1/1989	ND	2.00	ND	ND		ND	
EW-2D				ND				
EW-3A				ND				
EW-3B				ND				
EW-3C				ND				
EW-4A	6/1/1989	160.00	190.00	31.00	ND		ND	
EW-4B	6/1/1989	8.00	7.00	2.00	ND		ND	
EW-4C	6/1/1989	ND	1.00	ND	ND		ND	
EW-4D				ND				
EW-7C				ND				
EW-7D				ND				
EW-10C				ND				
EW-14D				ND				
Data References:								
<a href="#">montpolychemical.com/filter.aspx?results_2007_03_07_1700.xls</a>								
<a href="#">WQ Master - 06_18_07.xls</a>								

**Table A-2 - Claremont Transmissivity and Screen Depth Intervals**

Well No.	Diameter (in)	Radius (ft)	Time (hours)	Time (days)	Yield (gpm)	Drawdown (ft)	Screen Depth Interval (ft)	T'	log value'	Transmissivity' (gpd/ft)	T''	log value''	Transmissivity'' (gpd/ft)
N-7438	12	0.50	8	0.333	992	19	495 - 563	90000	7.556	104,152.892	104,152.892	7.620	105,027.168
N-8668	10	0.42	8	0.333	743	30	434 - 484	90000	7.715	50,441.566	50,441.566	7.463	48,797.459
N-5705	12	0.50	4	0.167	500	35	450 - 492	90000	7.255	27,362.742	27,362.742	6.738	25,412.601
N-617	12	0.50	48	2.000	1,017	22	145 - 175	90000	8.334	101,713.674	101,713.674	8.388	102,362.155
N-8205	10	0.42	4	0.167	495	28	300 - 330	90000	7.414	34,600.494	34,600.494	6.998	32,662.882
N-5890	6	0.25	3	0.125	120	16	126 - 132	90000	7.732	15,804.015	15,804.015	6.977	14,259.922
N-7124	6	0.25	2	0.083	305	35	118 - 138	90000	7.556	17,383.814	17,383.814	6.842	15,740.981
N-4010	8	0.33	4	0.167	1,010	32	231 - 261	90000	7.607	63,389.119	63,389.119	7.455	62,120.681
N-7421	12	0.50	6	0.250	1,471	36	482 - 527	90000	7.431	80,164.598	80,164.598	7.381	79,622.428
N-6956	12	0.50	6	0.250	1,438	35	514 -	90000	7.431	81,773.434	81,773.434	7.390	81,315.342
S-20041	12	0.50	8	0.333	1,500	20	190.5 - 268	90000	7.556	149,614.790	149,614.790	7.777	153,985.283
N-1937	12	0.50	24	1.000	845	28	116 - 154.5	90000	8.033	65,167.134	65,167.134	7.893	64,029.718
N-9591	12	0.50	8	0.333	1,370	33	606 - 682	90000	7.556	82,817.075	82,817.075	7.520	82,421.171
S-6656	12	0.50	8	0.333	1,387	42	637 - 697	90000	7.556	66,035.231	66,035.231	7.422	64,860.113
N-6644	12	0.50	8	0.333	1,212	28	175 - 221	90000	7.556	86,349.107	86,349.107	7.538	86,143.589
N-7852	12	0.50	5.5	0.229	1,248	30	299 - 356	90000	7.394	81,199.200	81,199.200	7.349	80,708.389
S-20042	12	0.50	5	0.208	1,450	36	524 - 585	90000	7.352	78,178.207	78,178.207	7.291	77,527.907

Transmissivity Estimates - Explanation of Calculations  
 Claremont Polychemical Superfund Site  
 Old Bethpage, NY

Historical well data was used to generate estimates of transmissivity . The historical data was acquired from the USGS office in Coram, Long Island, NY on June 27, 2007 by Richard Cronic and Shannon Sellers. Jack Monti of USGS provided the pertinent well files. Well logs and associated pumping test information ranged in date from 1938 to 1966.

The empirical equation used to estimate transmissivity was based on the Theis equation (Driscoll, 1986 pg 219 and supporting Appendix 16D). The equation used to estimate T is as follows:

$$T = [(264*Q)/d]*[\log (0.3*T*t / r^2*S)]$$

Where:

d = drawdown in ft  
 Q = yield in gpm  
 T = transmissivity in gpm/ft  
 t = time in days  
 r = well radius in ft  
 S = aquifer storage coefficient

Assume: S = 0.001

Due to the organization of the equation, the T factor contained in the independent side of the equation could not be calculated directly. Therefore, based on the general characteristics of the aquifer as indicated by the drilling logs, a value of 90,000 gpm/ft was used as a first approximation of T in the independent side of the equation. An aquifer storage coefficient of 0.001 was also assumed based on the physical characteristics of the aquifer. Based on these assumptions an initial approximation of transmissivity was calculated. Subsequently the calculated transmissivity value was substituted for T and re-calculated as a second approximation.

Example Calculation for Well number N-617

First Calculation using first approximation value of T

d = 22  
 Q = 1017  
 T = 90000  
 t = 2  
 r = 0.5  
 S = 0.001



$$T' = [(264 * Q) / d] * [\log (0.3 * T * t / r^2 * S)]$$

$$T' = [(264 * 1017) / 22] * [\log (0.3 * 90000 * 2 / (0.5)^2 * 0.001)]$$

$$8.334 = [\log (0.3 * 90000 * 2 / (0.5)^2 * 0.001)]$$

$$T' = [(264 * 1017) / 22] * 8.334$$

$$T' = 101,713.674 \text{ gpd/ft}$$

Second Calculation using solved value of T

$$d = 22$$

$$Q = 1017$$

$$T' = 101,713.674$$

$$t = 2$$

$$r = 0.5$$

$$S = 0.001$$

$$T'' = [(264 * Q) / d] * [\log (0.3 * T' * t / r^2 * S)]$$

$$T'' = [(264 * 1017) / 22] * [\log (0.3 * 101,713.674 * 2 / (0.5)^2 * 0.001)]$$

$$8.388 = [\log (0.3 * 101,713.674 * 2 / (0.5)^2 * 0.001)]$$

$$T'' = [(264 * 1017) / 22] * 8.388$$

$$T'' = 102,362.155$$

## APPENDIX B